THE UNIVERSITY OF SYDNEY

ARC CENTRE OF EXCELLENCE FOR DARK MATTER

Axions

Ciaran O'Hare
U. Sydney

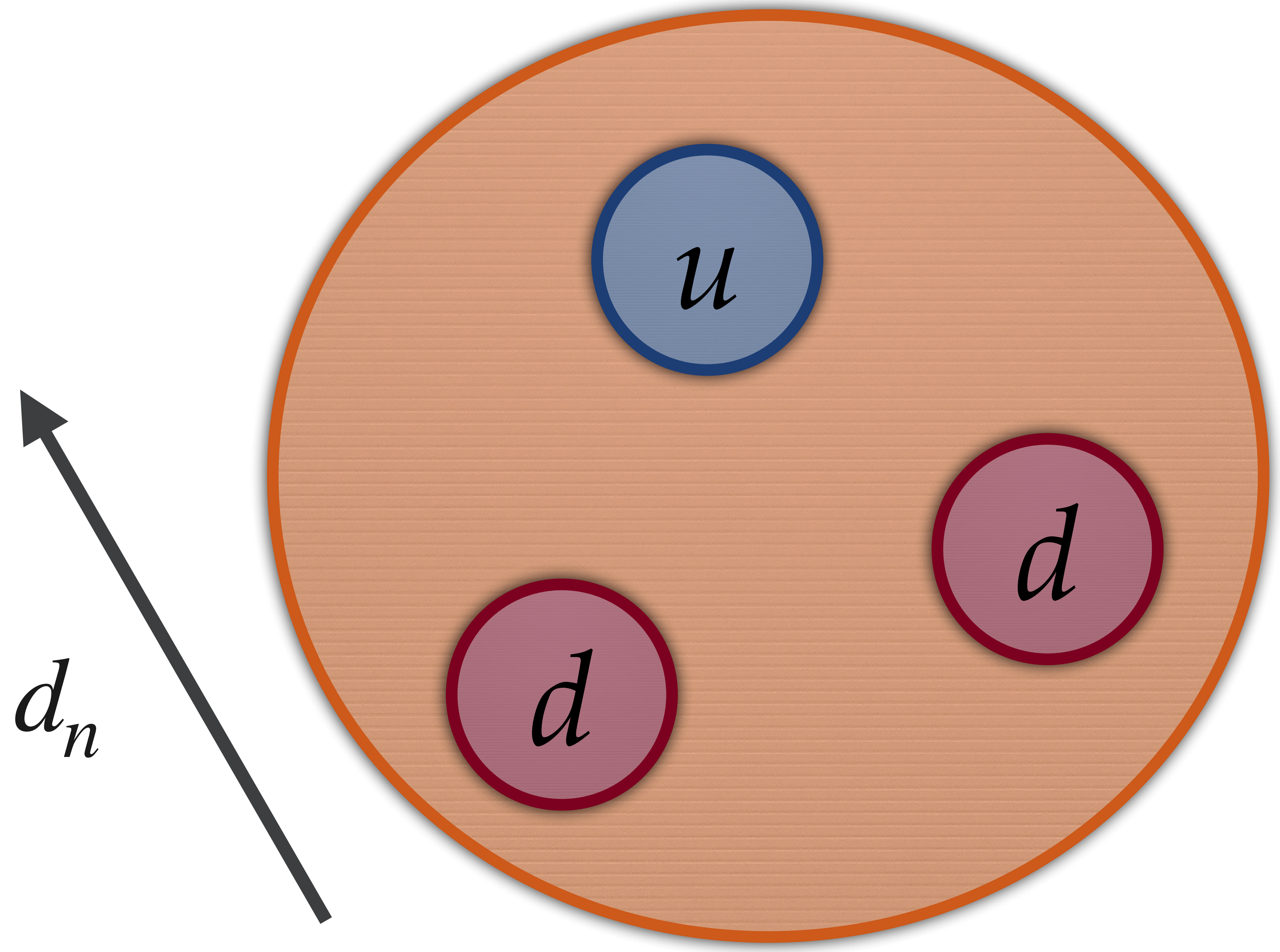

$$d_n \approx e \cdot \mathrm{fm}\,?$$

$$d_n = (2.4 \pm 1.0)\bar{\theta} \times 10^{-3}\, e\,\mathrm{fm}$$

$$\bar{\theta} = \theta_{\mathrm{QCD}} + \theta_q$$

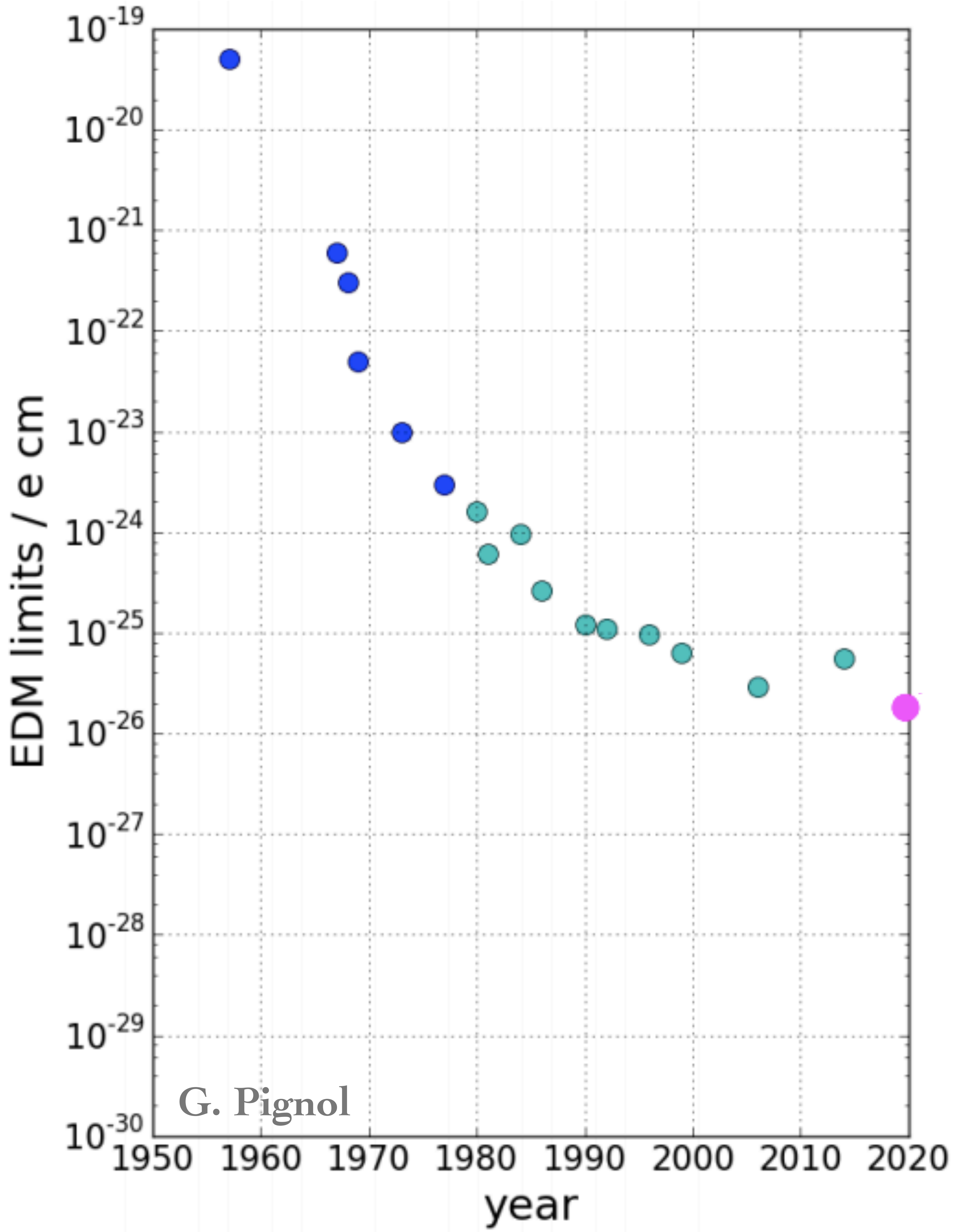

$$|d_n| < 1.8 \times 10^{-26}\, e\,\mathrm{cm} \quad \text{(90\% CL)}$$

$$\Rightarrow \theta \lesssim 10^{-10}$$

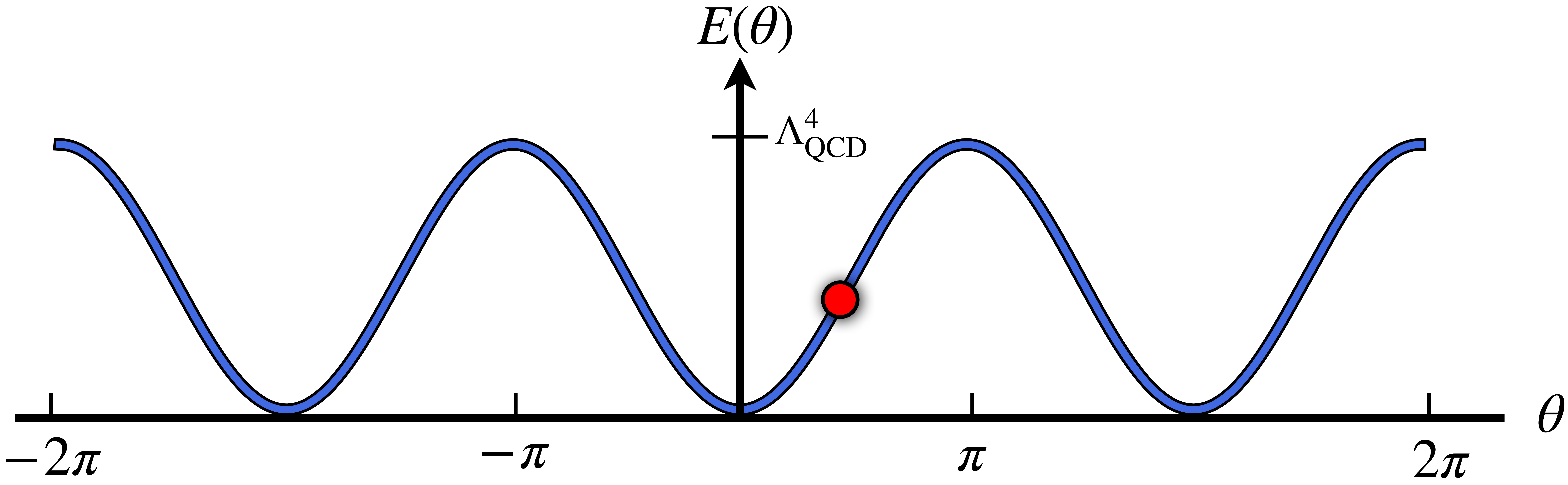

$E(\theta)$
$\Lambda_{\rm QCD}^4$
θ
-2π
$-\pi$
π
2π

The axion

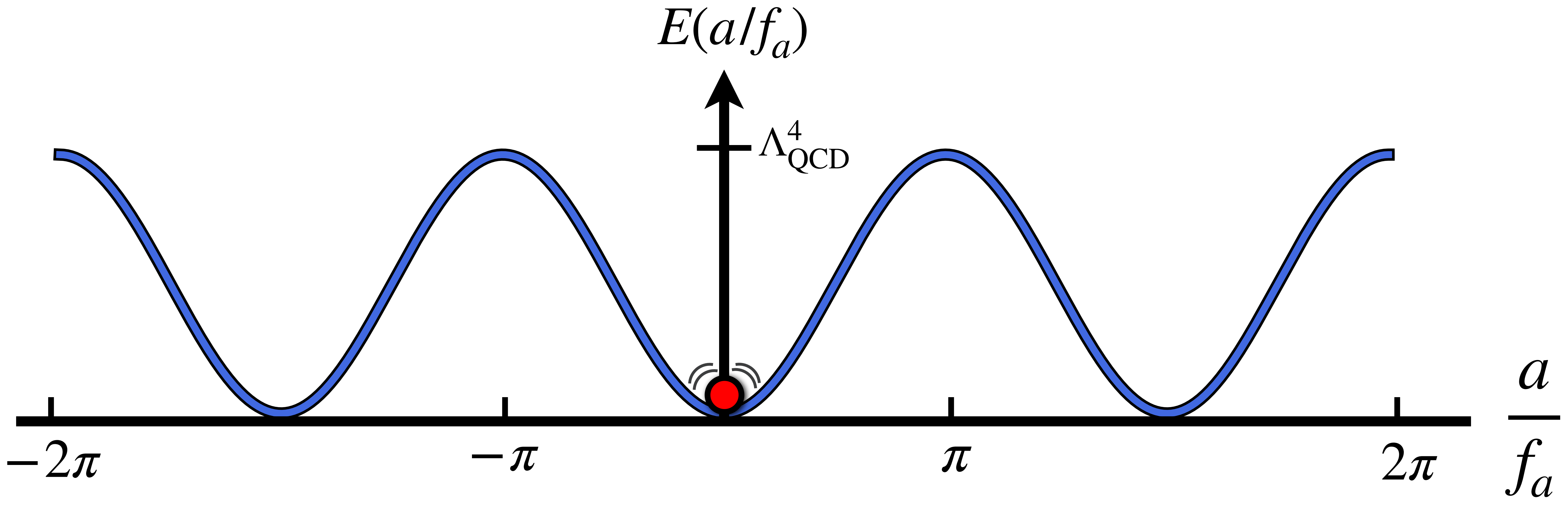

$$V(a) \approx \Lambda_{\rm QCD}^4 \left[1 - \cos\left(\bar{\theta} + \frac{a}{f_a}\right)\right]$$

$$m_a \simeq \frac{\Lambda_{\rm QCD}^2}{f_a}$$

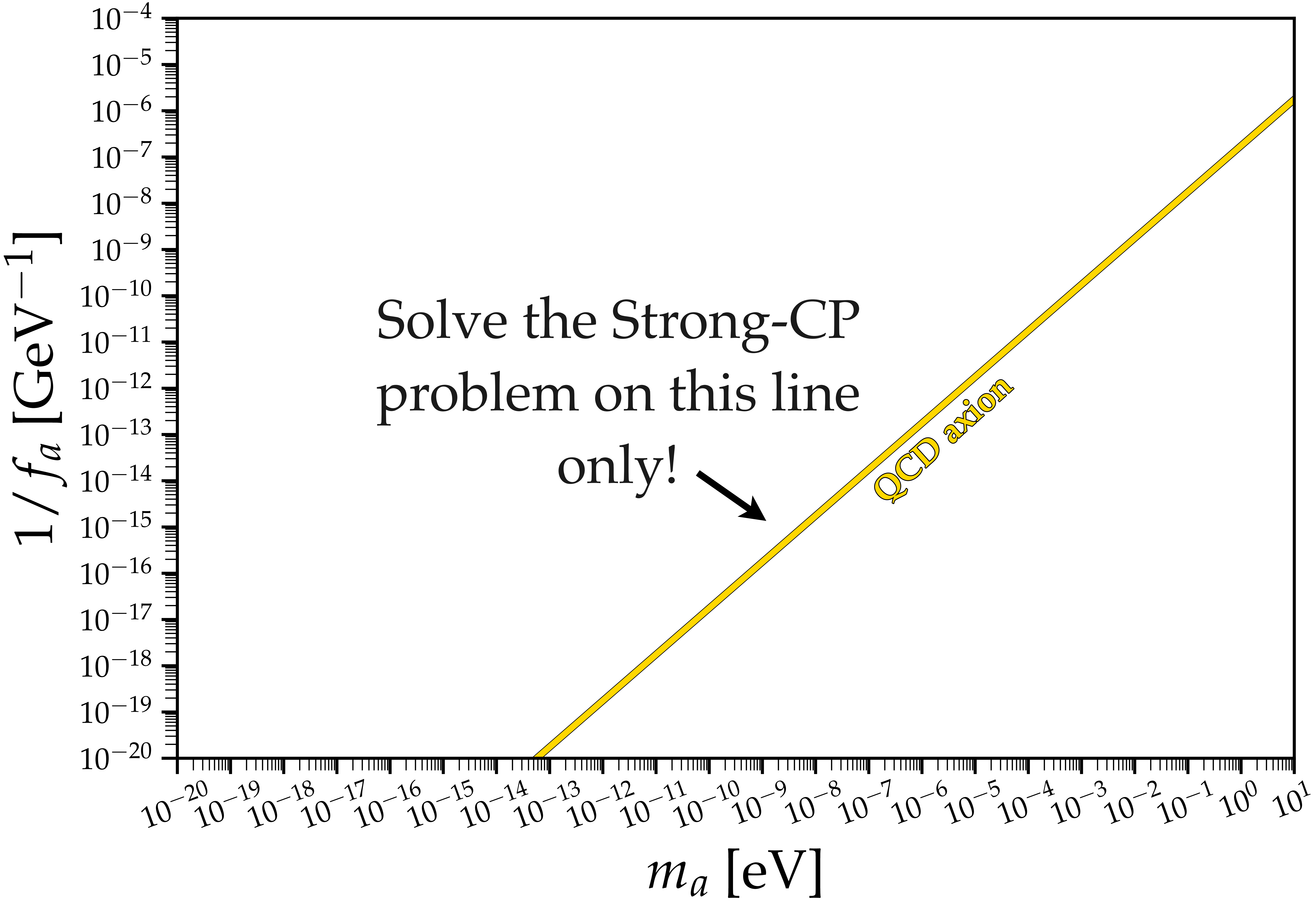

Solve the Strong-CP problem on this line only!
QCD axion
$1/f_a$ [GeV^{-1}]
m_a [eV]
10^{-4}
10^{-5}
10^{-6}
10^{-7}
10^{-8}
10^{-9}
10^{-10}
10^{-11}
10^{-12}
10^{-13}
10^{-14}
10^{-15}
10^{-16}
10^{-17}
10^{-18}
10^{-19}
10^{-20}
10^{-20} 10^{-19} 10^{-18} 10^{-17} 10^{-16} 10^{-15} 10^{-14} 10^{-13} 10^{-12} 10^{-11} 10^{-10} 10^{-9} 10^{-8} 10^{-7} 10^{-6} 10^{-5} 10^{-4} 10^{-3} 10^{-2} 10^{-1} 10^{0} 10^{1}

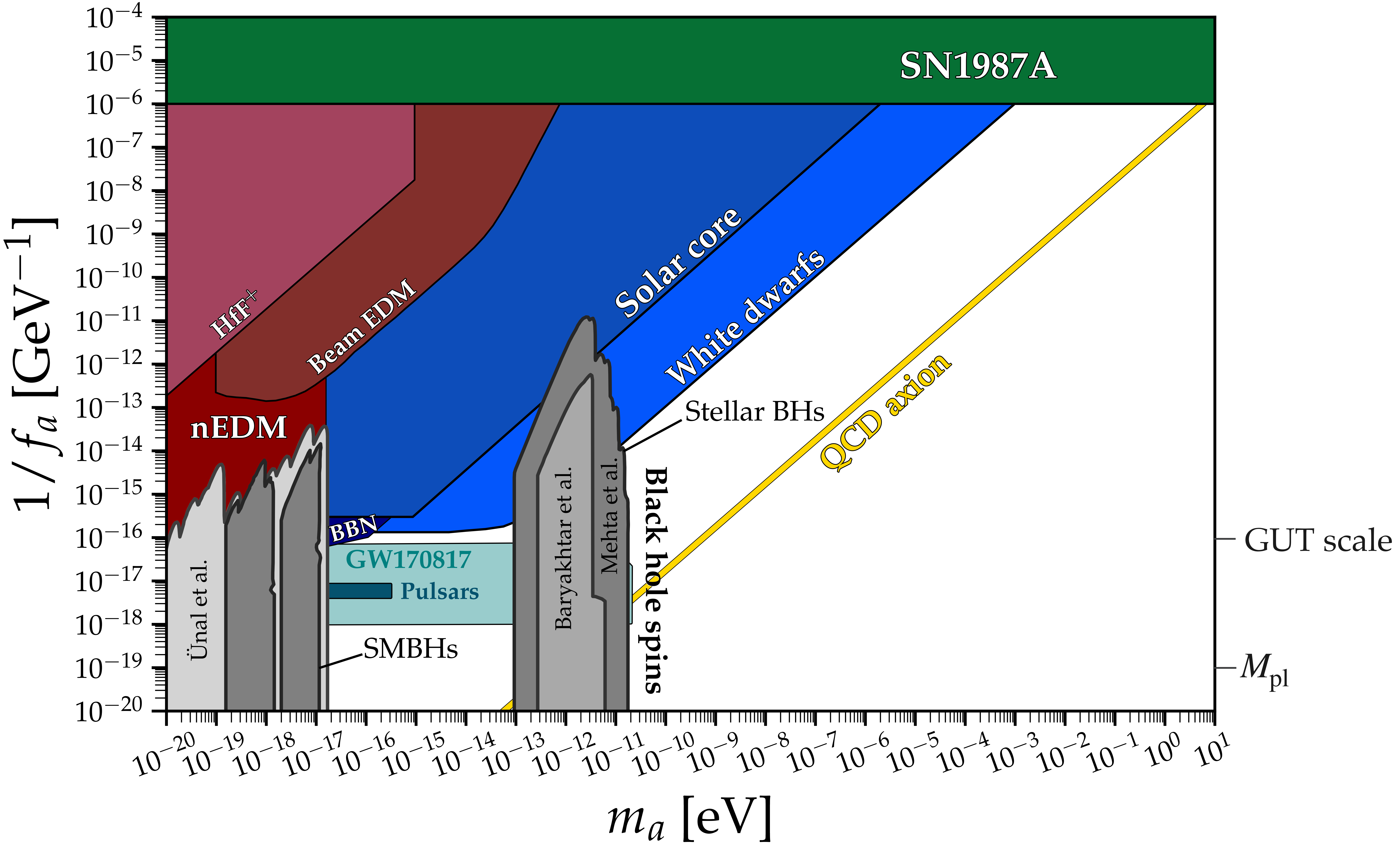

SN1987A
Solar core
White dwarfs
HfF+
Beam EDM
nEDM
BBN
GW170817
Pulsars
SMBHs
Ünal et al.
Baryakhtar et al.
Mehta et al.
Stellar BHs
Black hole spins
QCD axion
GUT scale
M_{pl}
$1/f_a$ [GeV^{-1}]
m_a [eV]

Axion-photon

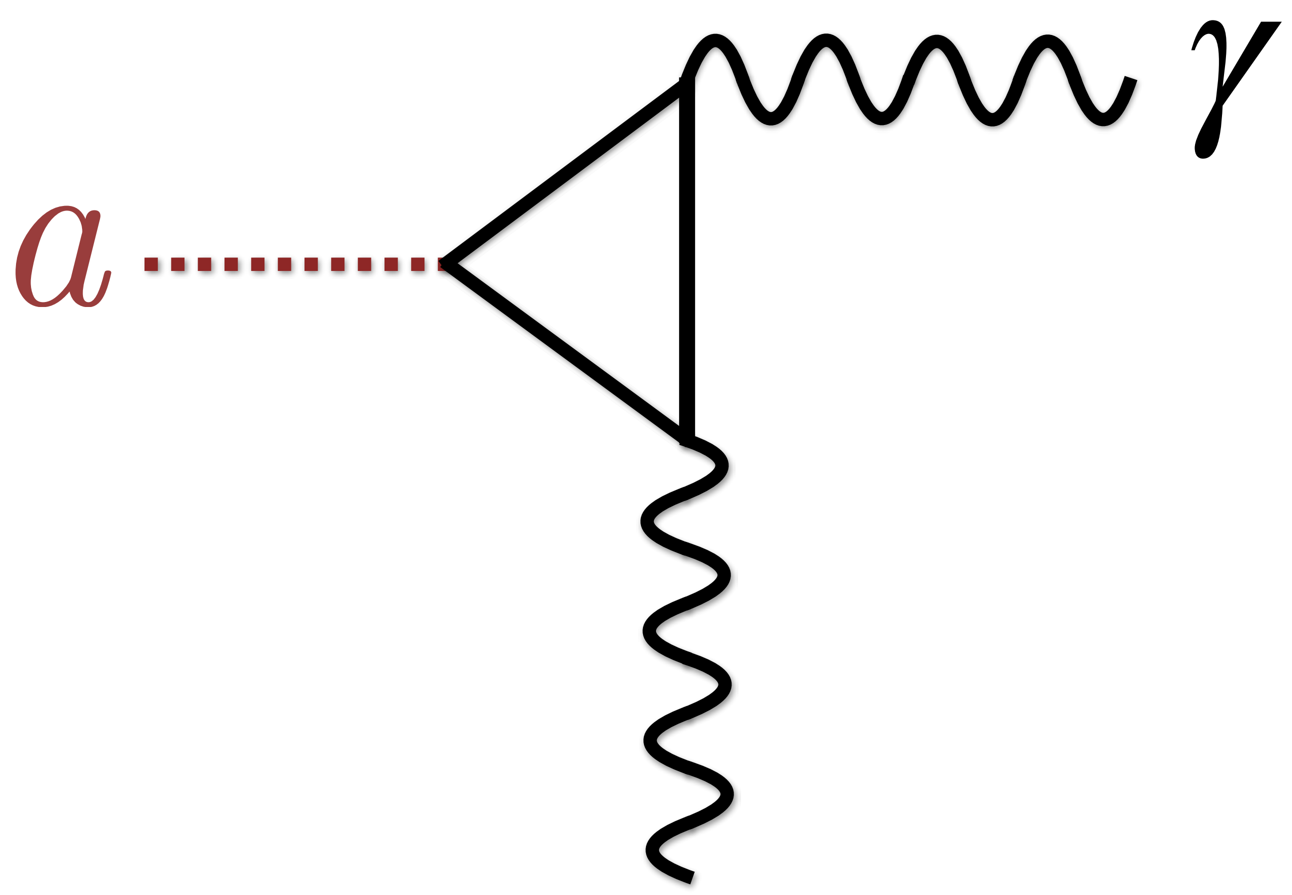

Axion-fermion

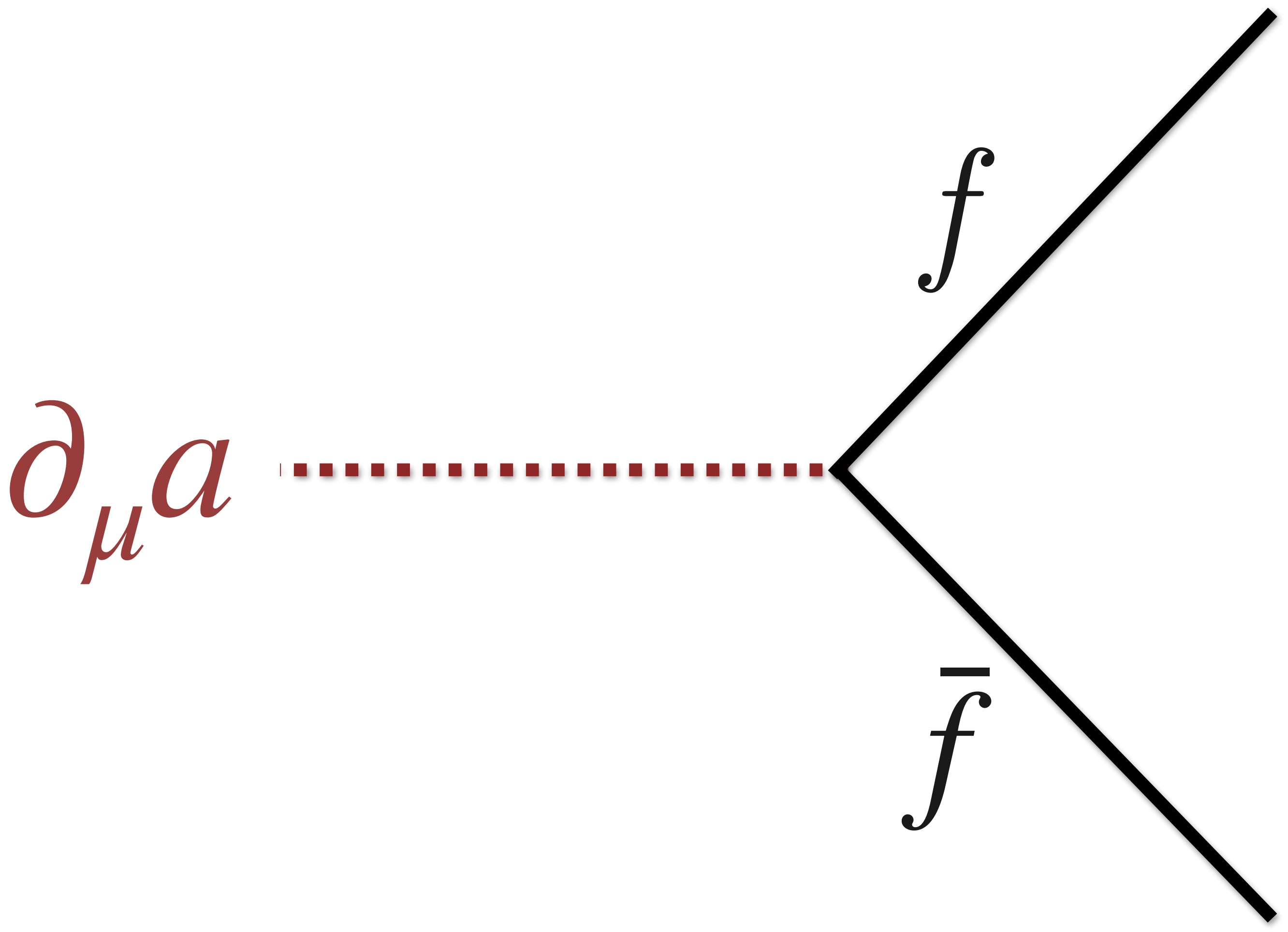

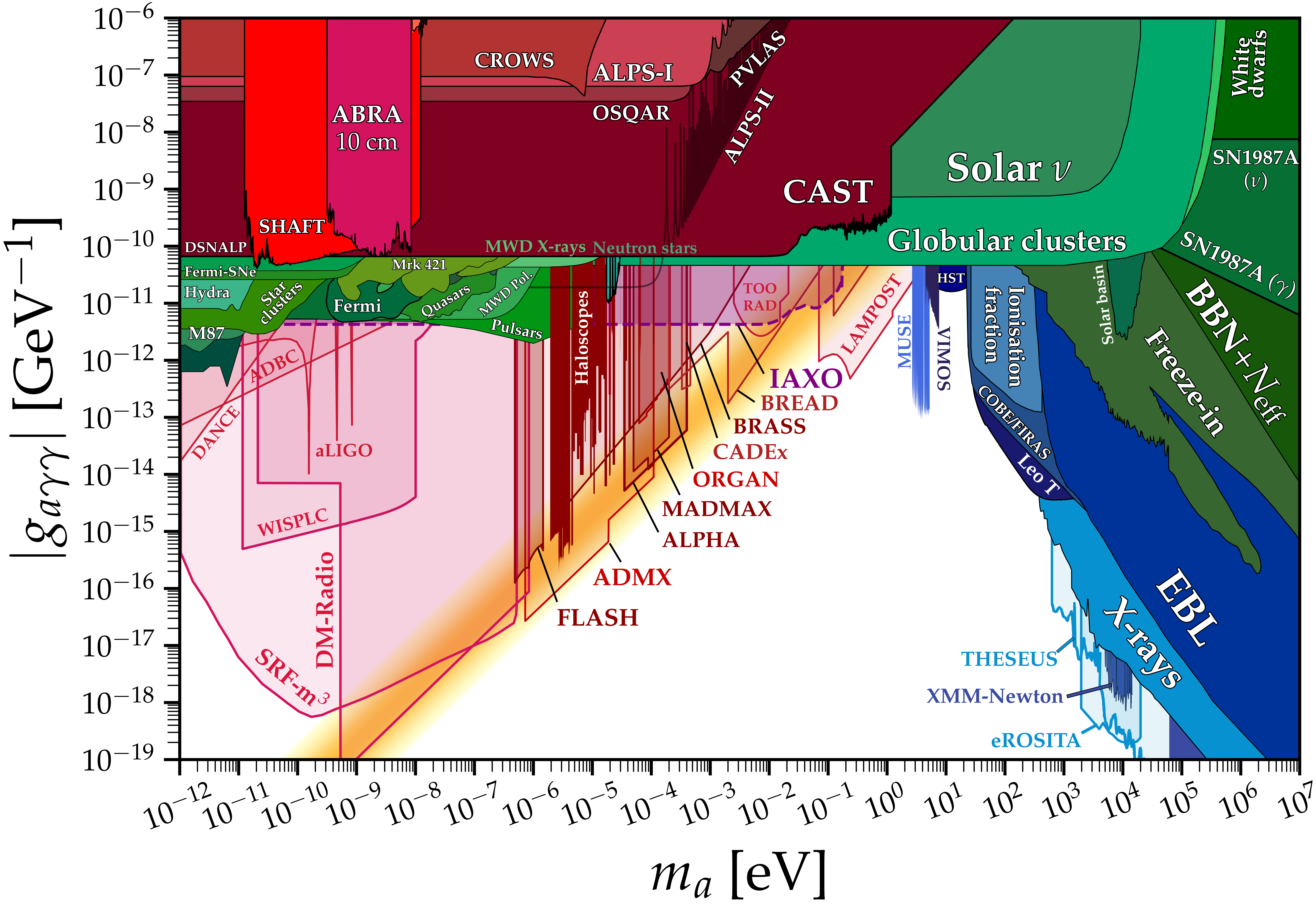

CROWS
ALPS-I
OSQAR
PVLAS
ALPS-II
ABRA
10 cm
SHAFT
CAST
Solar ν
Globular clusters
White dwarfs
SN1987A (ν)
SN1987A (γ)
BBN+N_eff
Freeze-in
DSNALP
MWD X-rays
Neutron stars
Fermi-SNe
Mrk 421
Hydra
Star clusters
Fermi
Quasars
MWD Pol.
Pulsars
M87
Haloscopes
TOO RAD
LAMPOST
MUSE
HST
VIMOS
Ionisation fraction
Solar basin
COBE/FIRAS
Leo T
EBL
X-rays
THESEUS
XMM-Newton
eROSITA
IAXO
BREAD
BRASS
CADEx
ORGAN
MADMAX
ALPHA
ADMX
FLASH
ADBC
DANCE
aLIGO
WISPLC
DM-Radio
SRF-m³
$|g_{a\gamma\gamma}|$ [GeV^{-1}]
m_a [eV]

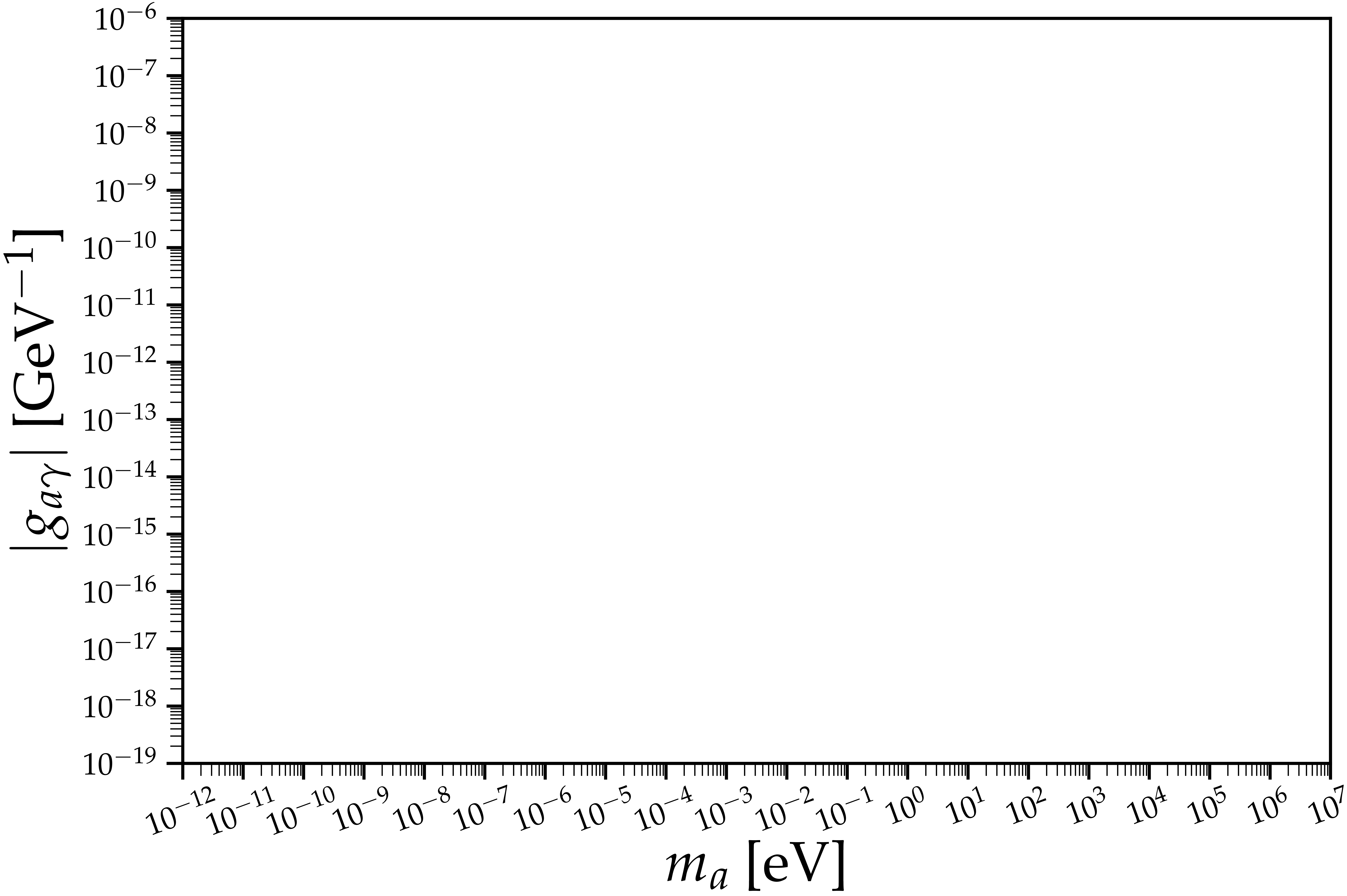
$|g_{a\gamma}|$ [GeV^{-1}]
10^{-6}
10^{-7}
10^{-8}
10^{-9}
10^{-10}
10^{-11}
10^{-12}
10^{-13}
10^{-14}
10^{-15}
10^{-16}
10^{-17}
10^{-18}
10^{-19}
10^{-12} 10^{-11} 10^{-10} 10^{-9} 10^{-8} 10^{-7} 10^{-6} 10^{-5} 10^{-4} 10^{-3} 10^{-2} 10^{-1} 10^{0} 10^{1} 10^{2} 10^{3} 10^{4} 10^{5} 10^{6} 10^{7}
m_a [eV]

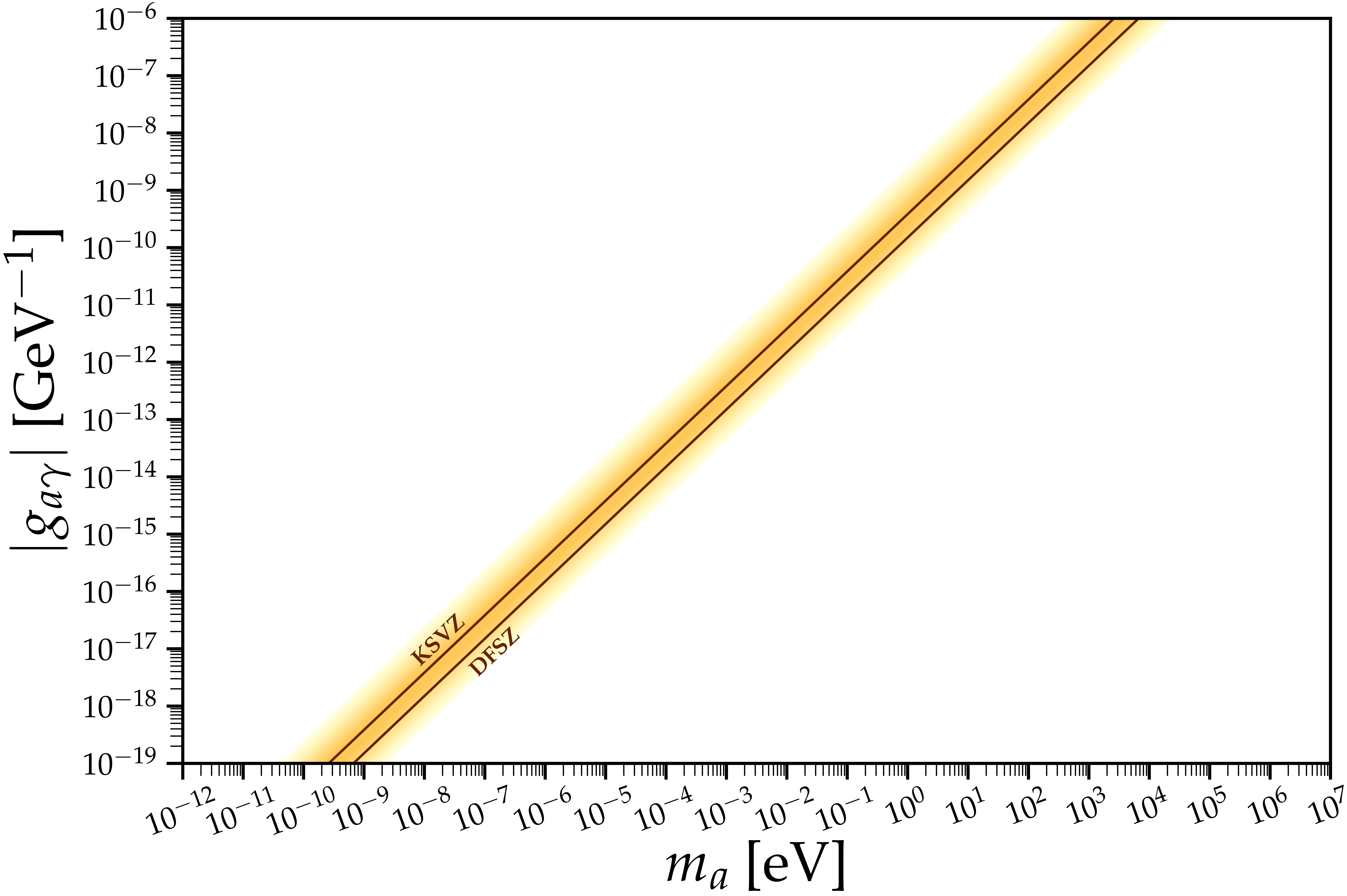

KSVZ
DFSZ
$|g_{a\gamma}|$ [GeV^{-1}]
m_a [eV]
10^{-6}
10^{-7}
10^{-8}
10^{-9}
10^{-10}
10^{-11}
10^{-12}
10^{-13}
10^{-14}
10^{-15}
10^{-16}
10^{-17}
10^{-18}
10^{-19}
10^{-12} 10^{-11} 10^{-10} 10^{-9} 10^{-8} 10^{-7} 10^{-6} 10^{-5} 10^{-4} 10^{-3} 10^{-2} 10^{-1} 10^{0} 10^{1} 10^{2} 10^{3} 10^{4} 10^{5} 10^{6} 10^{7}

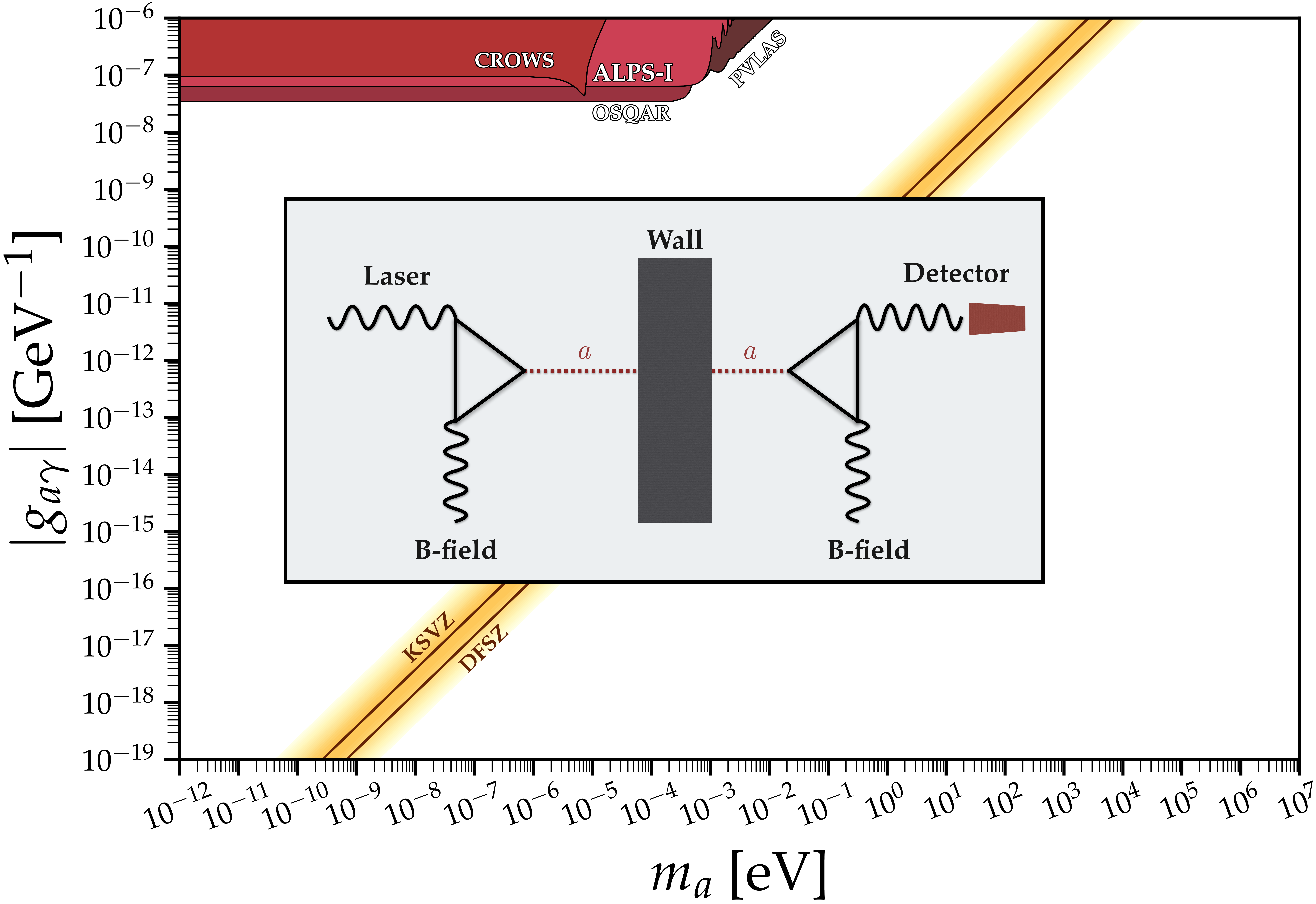

CROWS
ALPS-I
OSQAR
PVLAS
KSVZ
DFSZ
Wall
Laser
Detector
a
a
B-field
B-field
$|g_{a\gamma}|$ [GeV^{-1}]
m_a [eV]

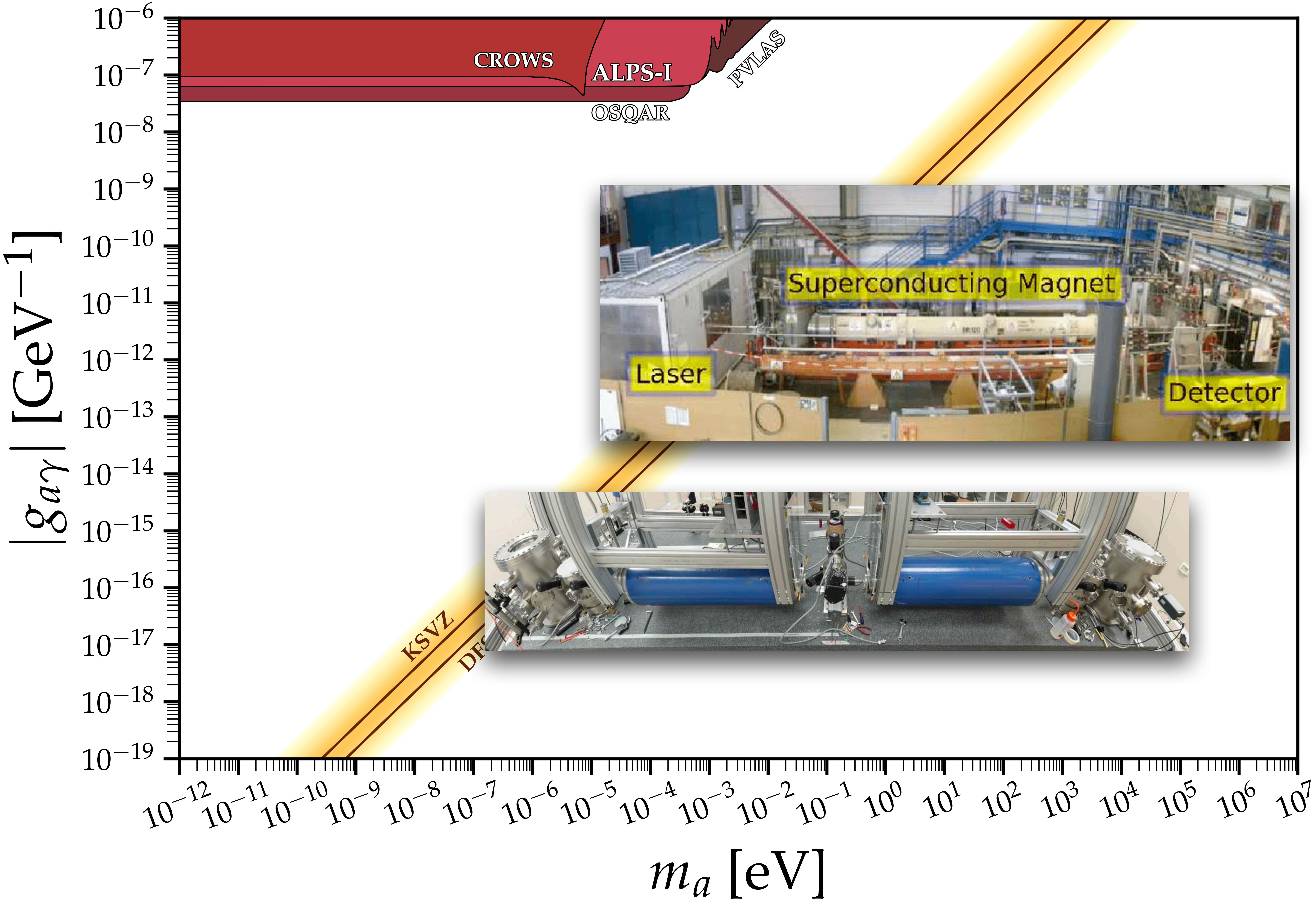
CROWS
ALPS-I
OSQAR
PVLAS
Superconducting Magnet
Laser
Detector
KSVZ
$|g_{a\gamma}|$ [GeV^{-1}]
m_a [eV]

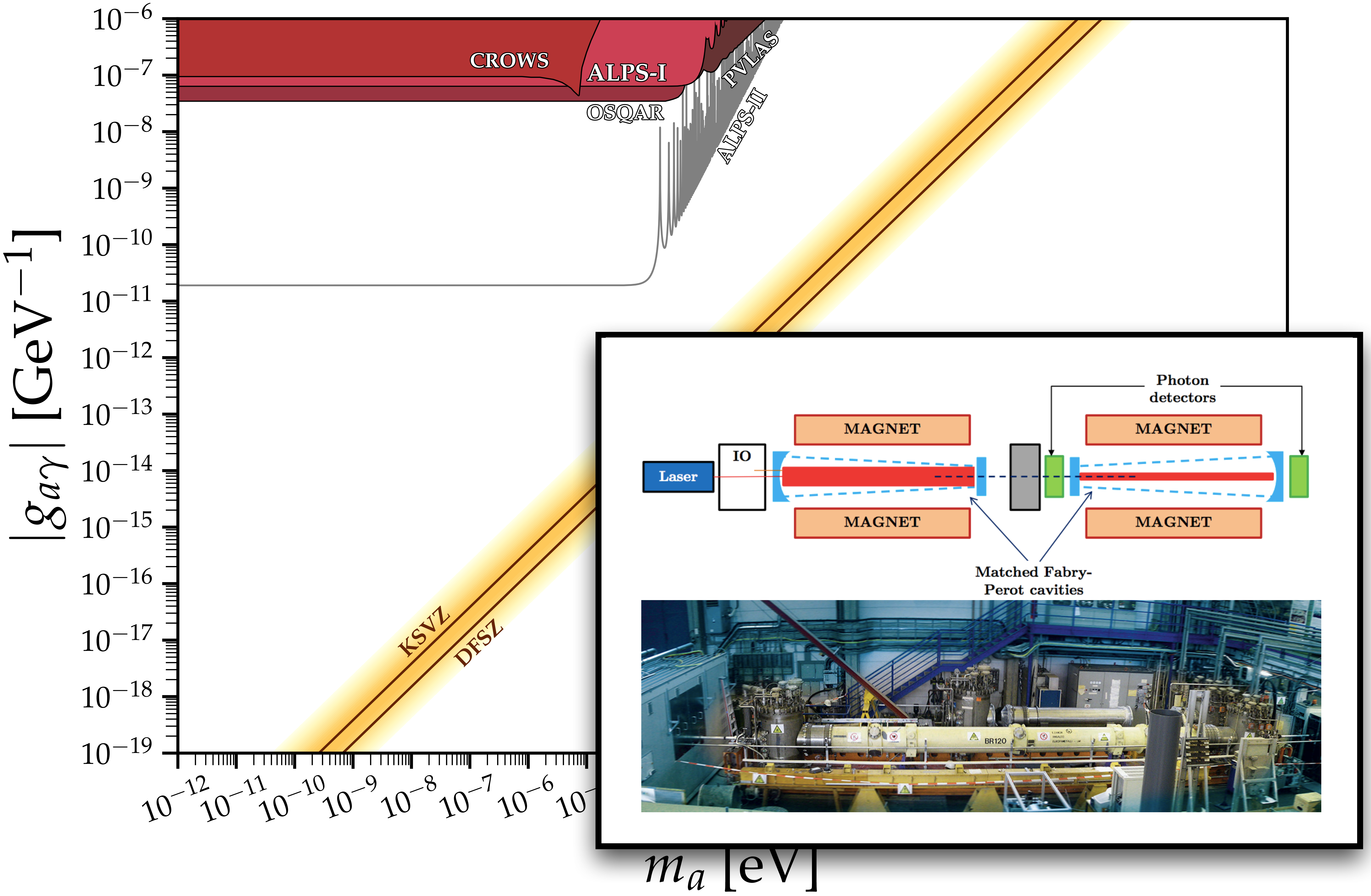

CROWS
ALPS-I
OSQAR
PVLAS
ALPS-II
KSVZ
DFSZ
$|g_{a\gamma}|$ [GeV^{-1}]
m_a [eV]
Photon detectors
MAGNET
MAGNET
MAGNET
MAGNET
IO
Laser
Matched Fabry-Perot cavities
BR120

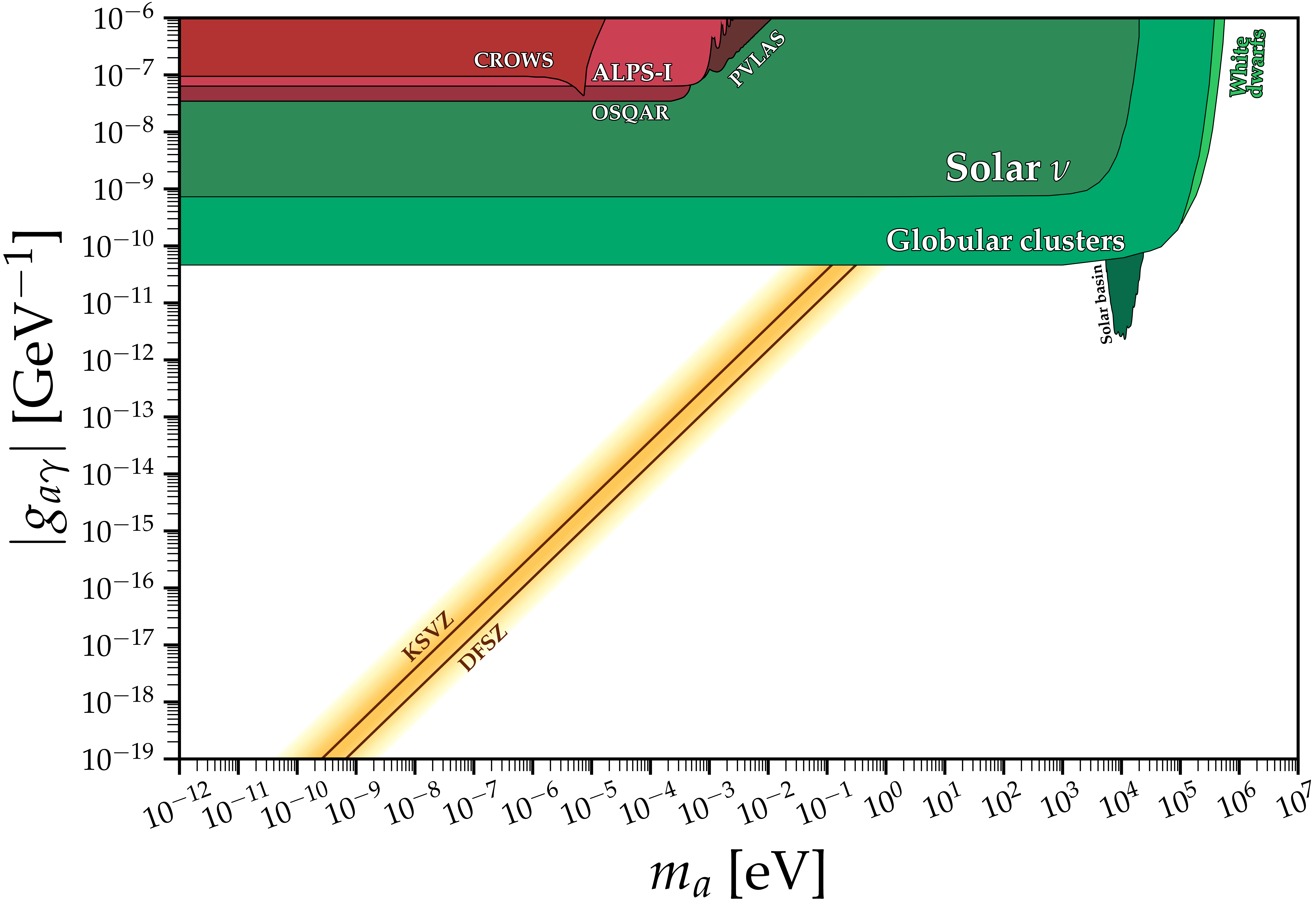
CROWS
ALPS-I
OSQAR
PVLAS
Solar ν
Globular clusters
White dwarfs
Solar basin
KSVZ
DFSZ
$|g_{a\gamma}|$ [GeV^{-1}]
m_a [eV]

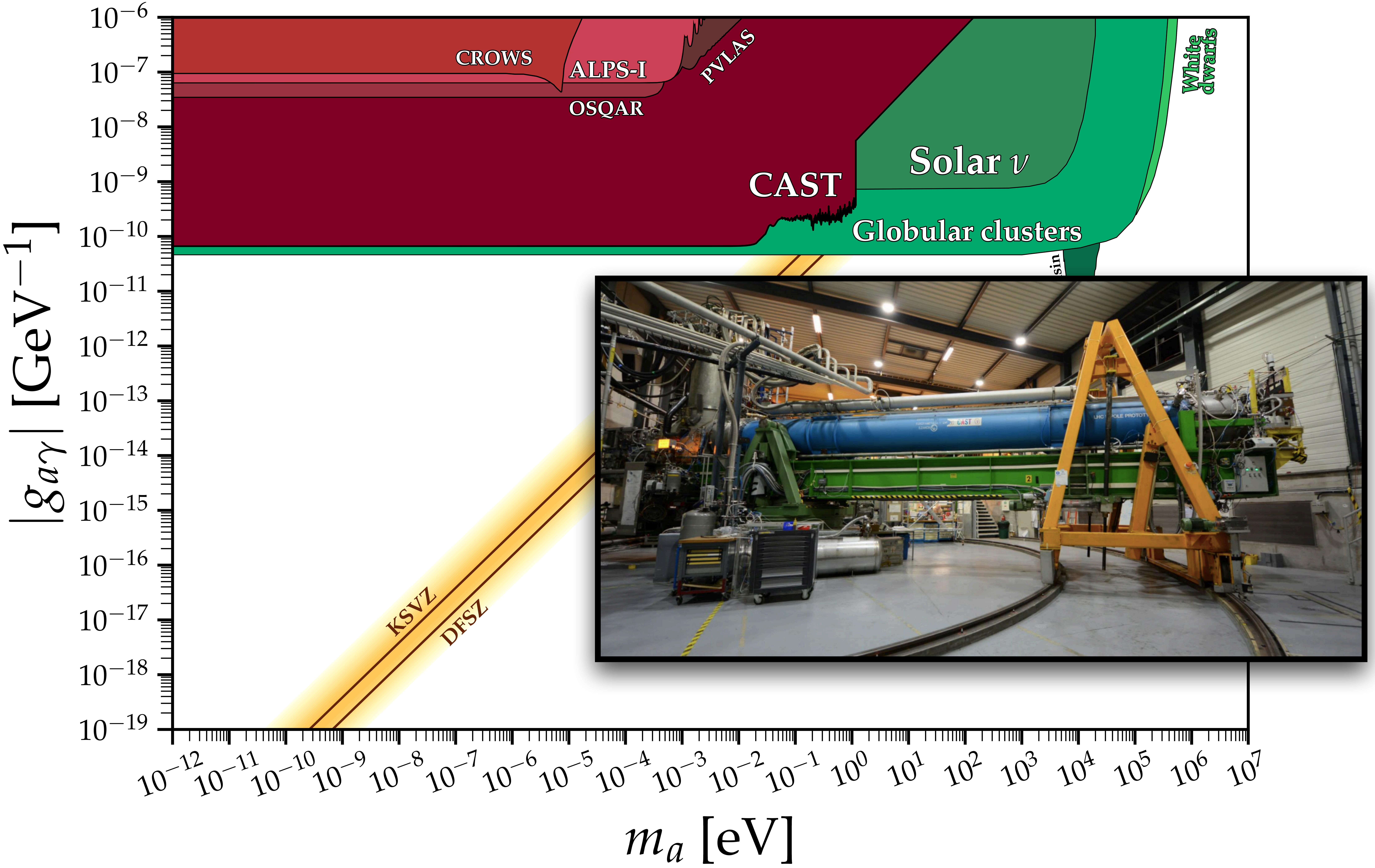
CROWS
ALPS-I
OSQAR
PVLAS
CAST
Solar ν
Globular clusters
White dwarfs
KSVZ
DFSZ
10^{-6}
10^{-7}
10^{-8}
10^{-9}
10^{-10}
10^{-11}
10^{-12}
10^{-13}
10^{-14}
10^{-15}
10^{-16}
10^{-17}
10^{-18}
10^{-19}
$|g_{a\gamma}|$ [GeV^{-1}]
10^{-12} 10^{-11} 10^{-10} 10^{-9} 10^{-8} 10^{-7} 10^{-6} 10^{-5} 10^{-4} 10^{-3} 10^{-2} 10^{-1} 10^{0} 10^{1} 10^{2} 10^{3} 10^{4} 10^{5} 10^{6} 10^{7}
m_a [eV]

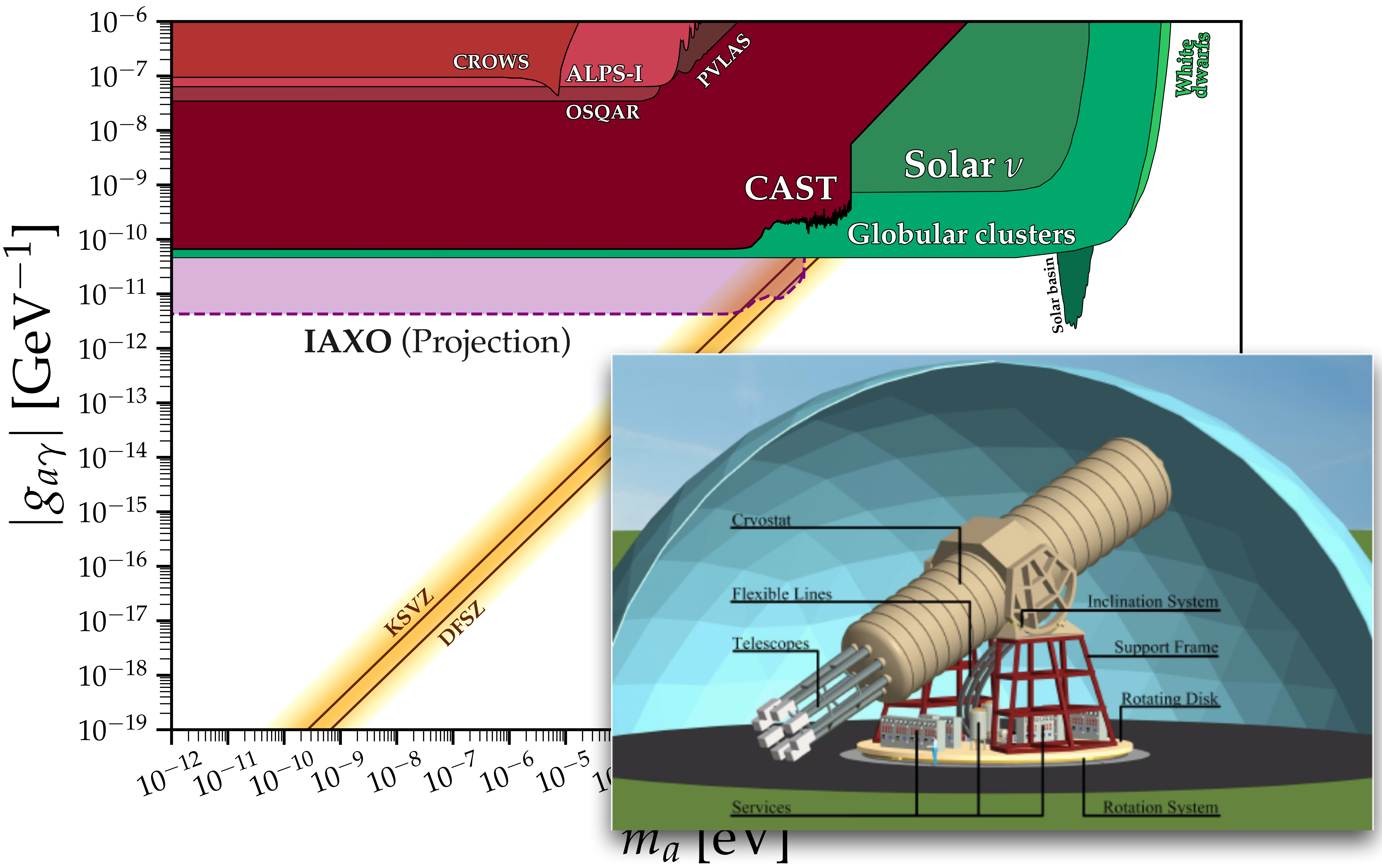

CROWS
ALPS-I
PVLAS
OSQAR
CAST
Solar ν
Globular clusters
White dwarfs
Solar basin
IAXO (Projection)
KSVZ
DFSZ
$|g_{a\gamma}|$ [GeV^{-1}]
m_a [eV]
Cryostat
Flexible Lines
Inclination System
Telescopes
Support Frame
Rotating Disk
Services
Rotation System

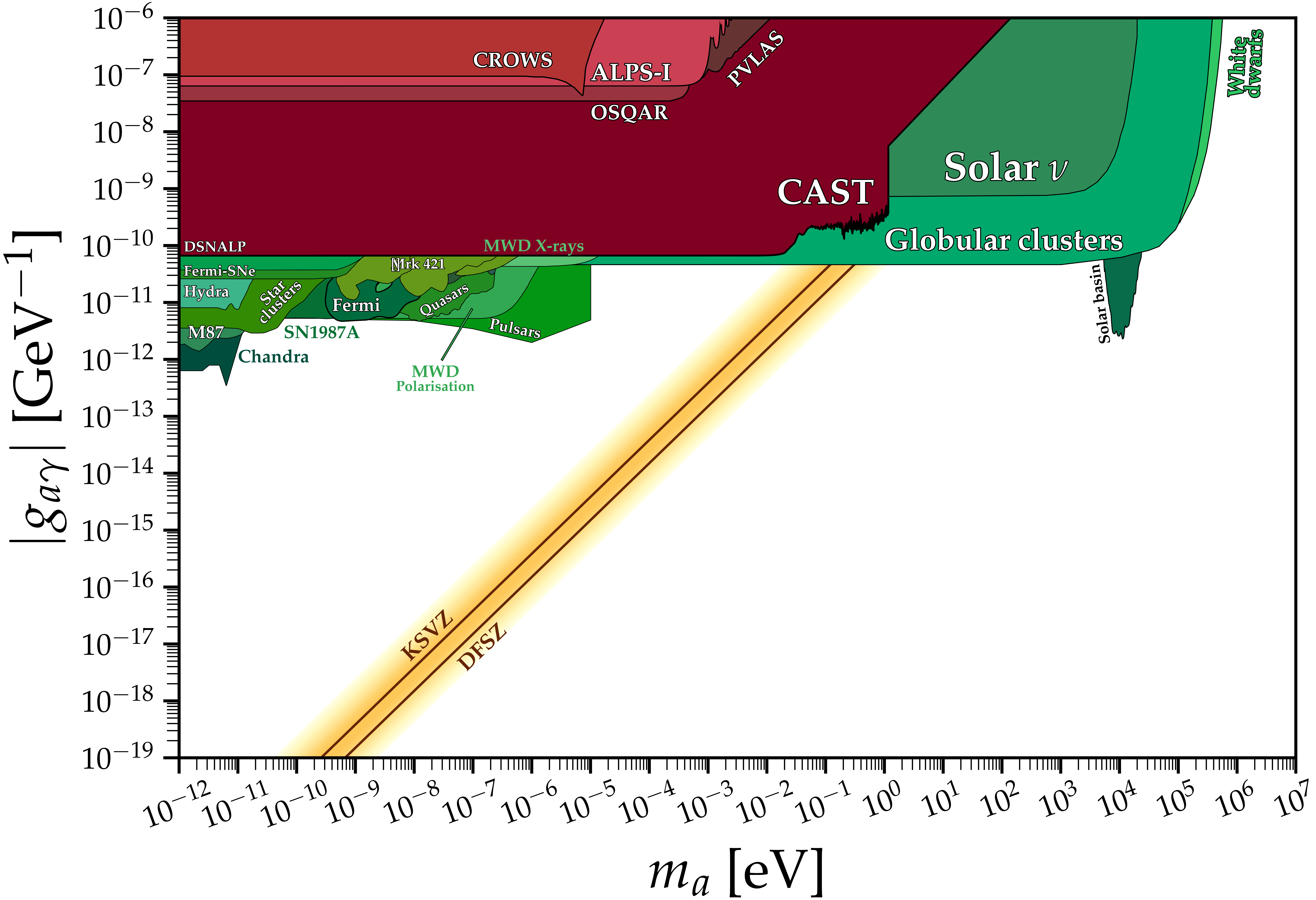

CROWS
ALPS-I
PVLAS
OSQAR
CAST
Solar ν
White dwarfs
Globular clusters
DSNALP
MWD X-rays
Fermi-SNe
Mrk 421
Hydra
Star clusters
Fermi
Quasars
SN1987A
Pulsars
M87
Chandra
MWD Polarisation
Solar basin
KSVZ
DFSZ
$|g_{a\gamma}|$ [GeV^{-1}]
m_a [eV]

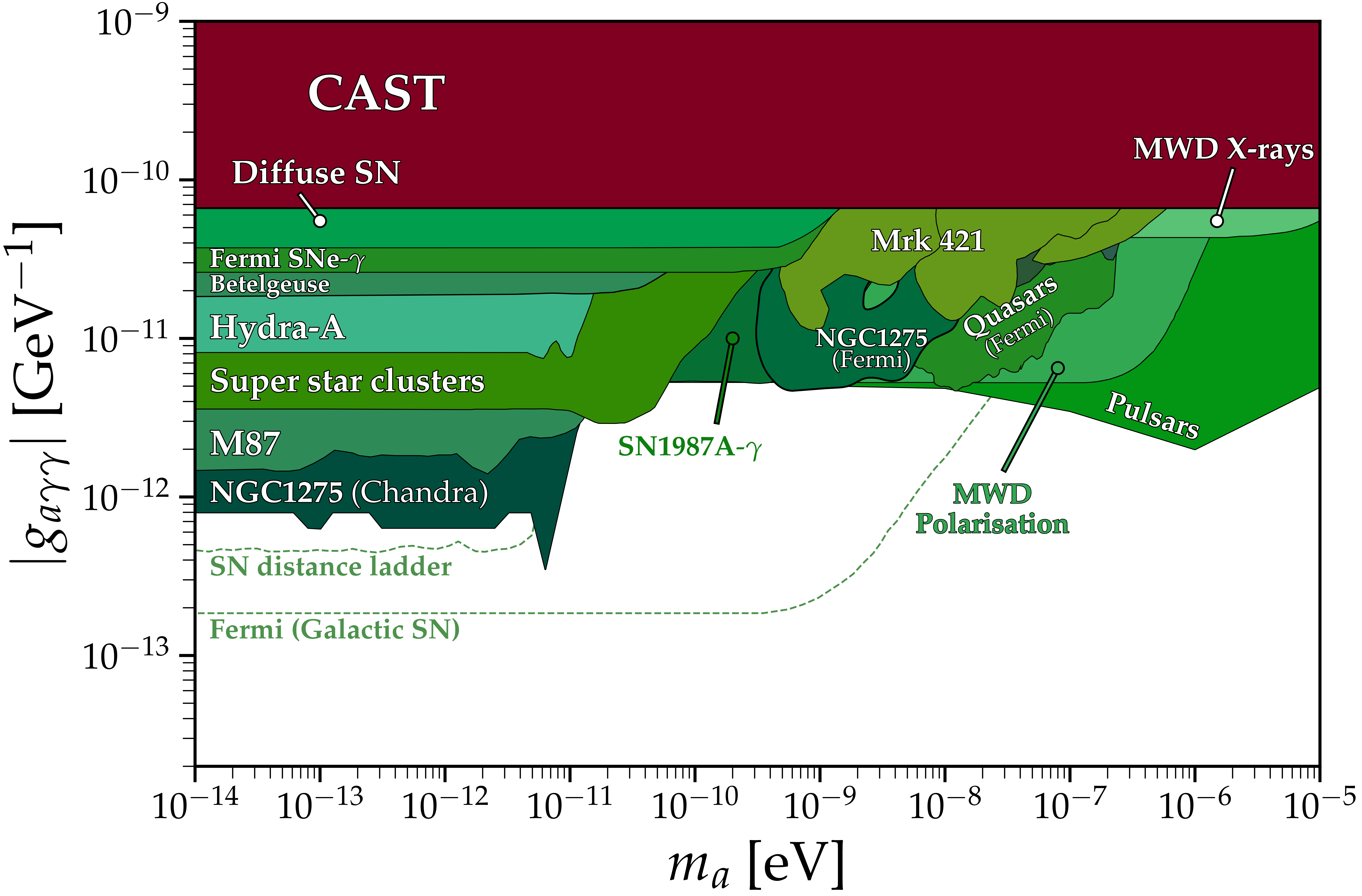

CAST
Diffuse SN
MWD X-rays
Fermi SNe-γ
Betelgeuse
Hydra-A
Super star clusters
M87
NGC1275 (Chandra)
SN distance ladder
Fermi (Galactic SN)
Mrk 421
NGC1275 (Fermi)
Quasars (Fermi)
SN1987A-γ
MWD Polarisation
Pulsars
$|g_{a\gamma\gamma}|$ [GeV^{-1}]
m_a [eV]
10^{-9}
10^{-10}
10^{-11}
10^{-12}
10^{-13}
10^{-14}
10^{-13}
10^{-12}
10^{-11}
10^{-10}
10^{-9}
10^{-8}
10^{-7}
10^{-6}
10^{-5}

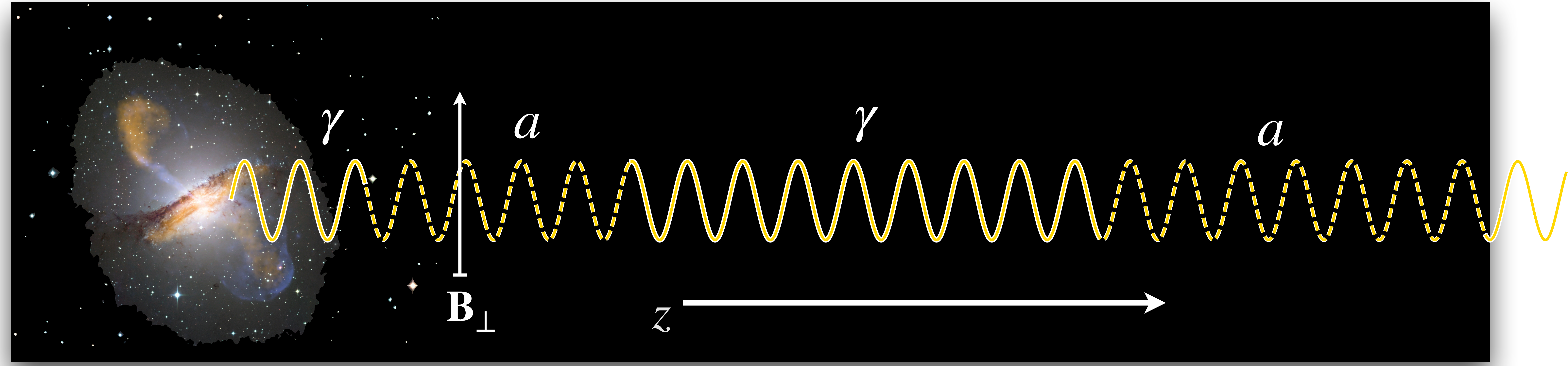

γ
a
γ
a
$\mathbf{B}_\perp$
z

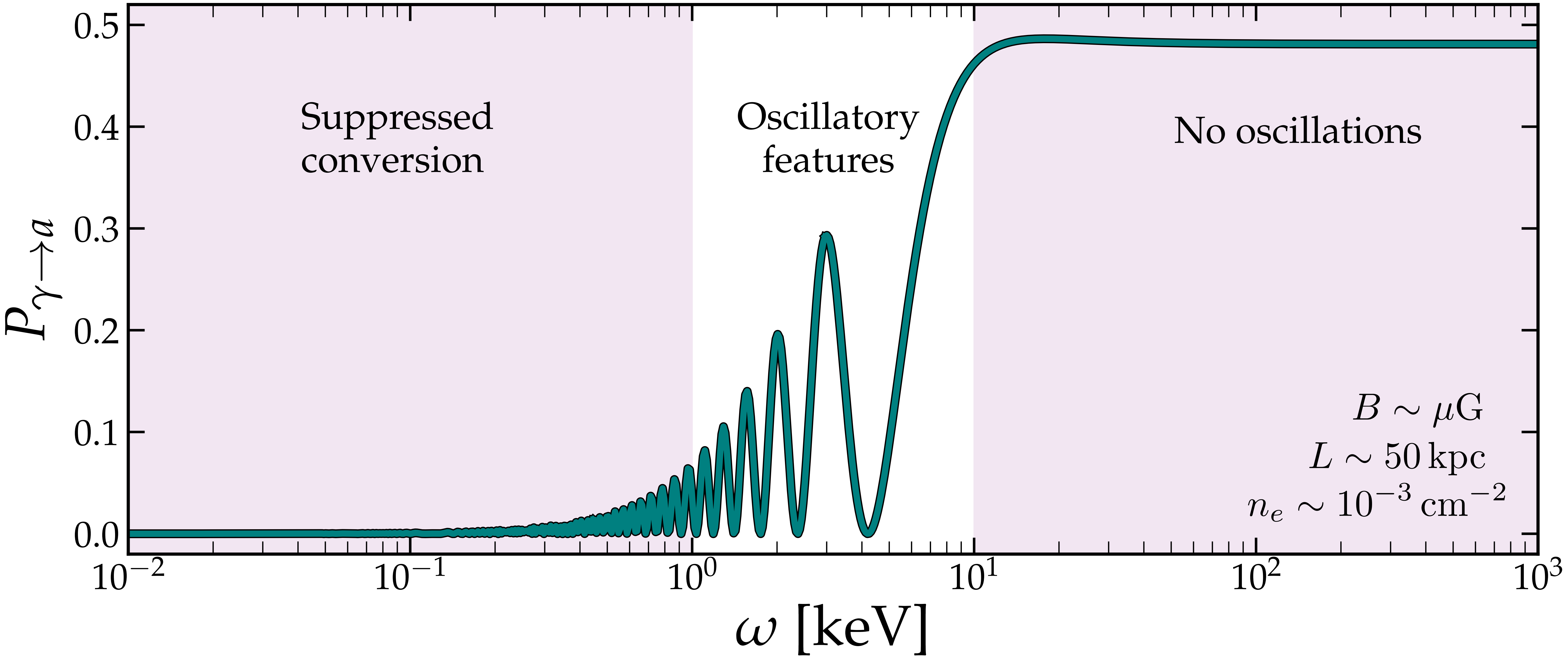

Suppressed conversion
Oscillatory features
No oscillations
$B \sim \mu$G
$L \sim 50\,$kpc
$n_e \sim 10^{-3}\,$cm^{-2}
$P_{\gamma\to a}$
0.5
0.4
0.3
0.2
0.1
0.0
10^{-2}
10^{-1}
10^{0}
10^{1}
10^{2}
10^{3}
ω [keV]

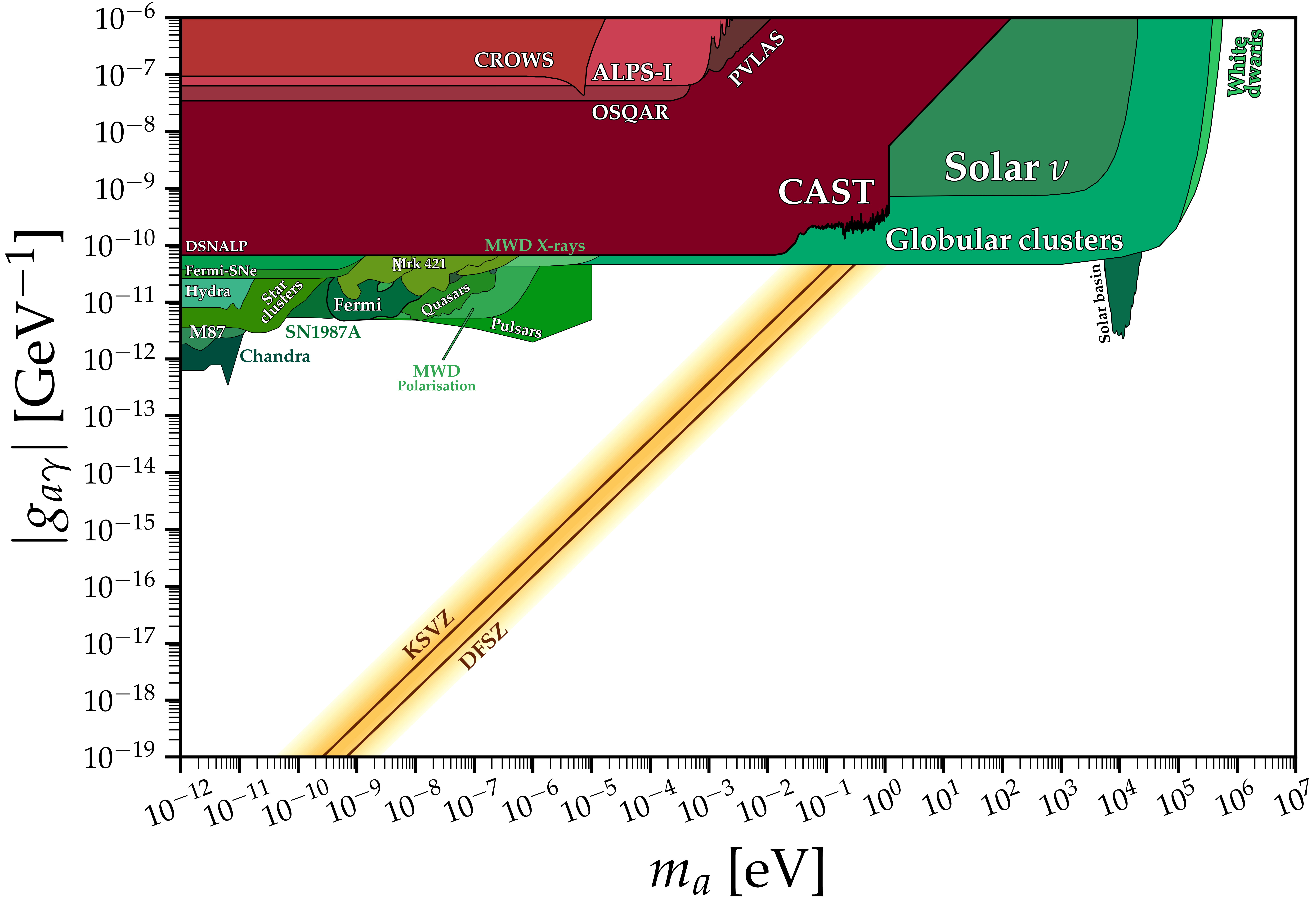
CROWS
ALPS-I
PVLAS
OSQAR
CAST
Solar ν
Globular clusters
White dwarfs
DSNALP
MWD X-rays
Fermi-SNe
Mrk 421
Hydra
Star clusters
Fermi
Quasars
SN1987A
Pulsars
M87
Chandra
MWD Polarisation
Solar basin
KSVZ
DFSZ
$|g_{a\gamma}|$ [GeV^{-1}]
m_a [eV]

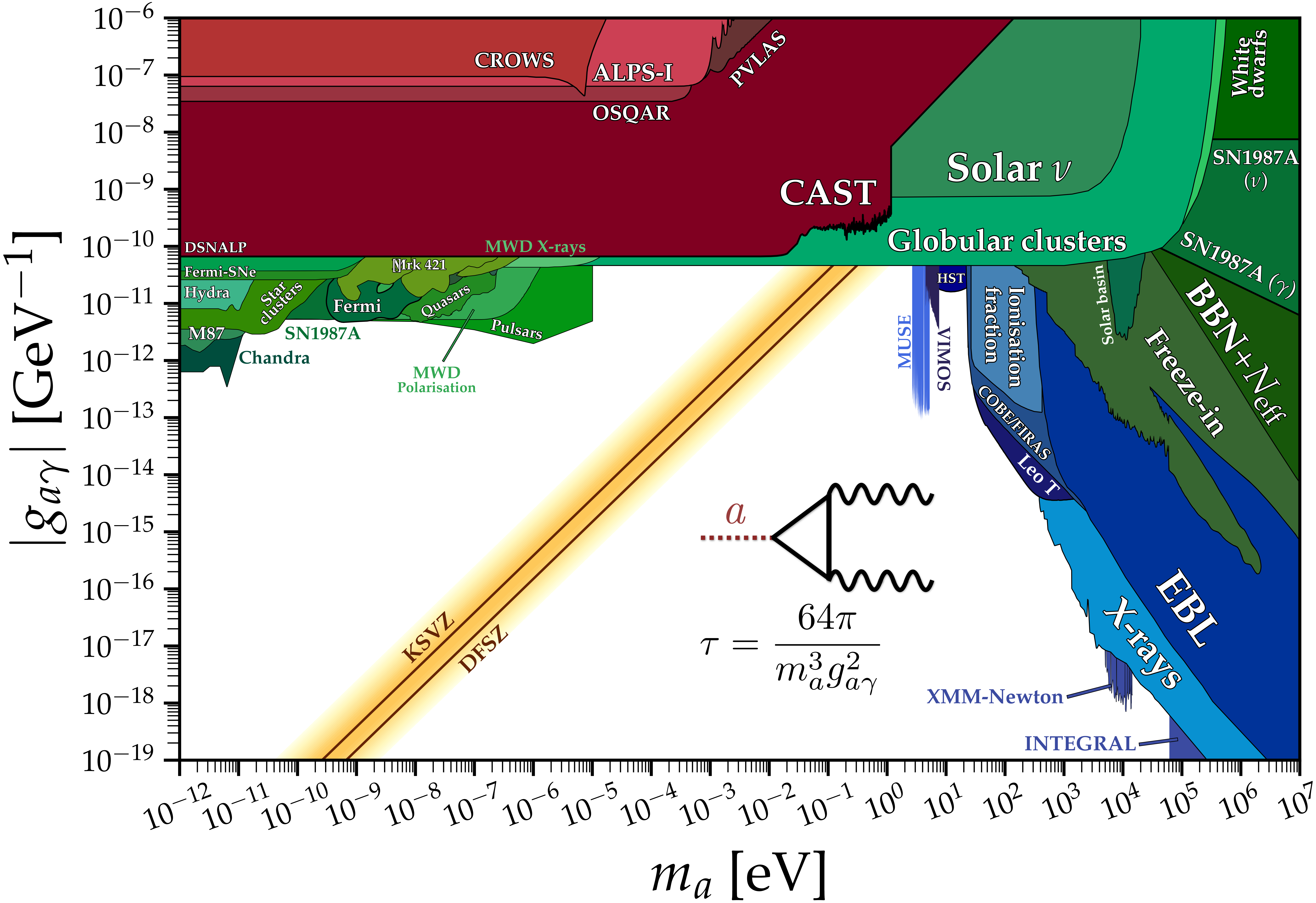

CROWS
ALPS-I
PVLAS
OSQAR
CAST
Solar ν
White dwarfs
SN1987A (ν)
Globular clusters
DSNALP
MWD X-rays
Fermi-SNe
Mrk 421
Hydra
Star clusters
Fermi
Quasars
Pulsars
M87
SN1987A
Chandra
MWD Polarisation
HST
MUSE
VIMOS
Ionisation fraction
COBE/FIRAS
Leo T
Solar basin
SN1987A (γ)
BBN+Neff
Freeze-in
EBL
X-rays
XMM-Newton
INTEGRAL
KSVZ
DFSZ
a
$\tau = \frac{64\pi}{m_a^3 g_{a\gamma}^2}$
$|g_{a\gamma}|$ [GeV^{-1}]
m_a [eV]

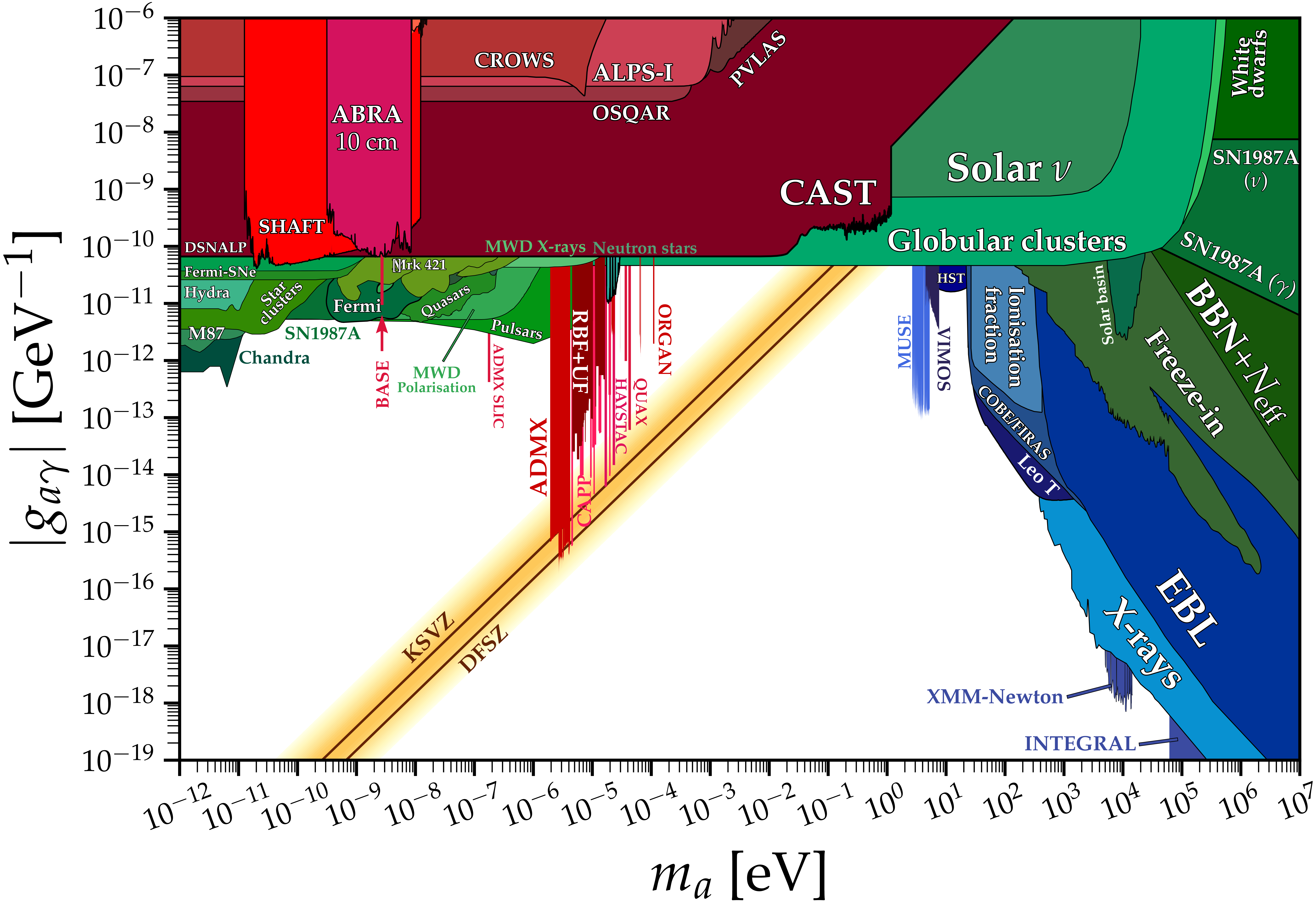

CROWS
ALPS-I
PVLAS
OSQAR
ABRA
10 cm
White dwarfs
SN1987A (ν)
Solar ν
CAST
SHAFT
DSNALP
Globular clusters
MWD X-rays
Neutron stars
Fermi-SNe
Mrk 421
Hydra
Star clusters
Fermi
Quasars
SN1987A (γ)
BBN+Neff
M87
SN1987A
Pulsars
Chandra
BASE
MWD
Polarisation
ADMX SLIC
ADMX
RBF+UF
CAPP
HAYSTAC
QUAX
ORGAN
MUSE
VIMOS
HST
Ionisation fraction
Solar basin
Freeze-in
COBE/FIRAS
Leo T
KSVZ
DFSZ
EBL
X-rays
XMM-Newton
INTEGRAL
$|g_{a\gamma}|$ [GeV^{-1}]
m_a [eV]
10^{-6}
10^{-7}
10^{-8}
10^{-9}
10^{-10}
10^{-11}
10^{-12}
10^{-13}
10^{-14}
10^{-15}
10^{-16}
10^{-17}
10^{-18}
10^{-19}
10^{-12} 10^{-11} 10^{-10} 10^{-9} 10^{-8} 10^{-7} 10^{-6} 10^{-5} 10^{-4} 10^{-3} 10^{-2} 10^{-1} 10^{0} 10^{1} 10^{2} 10^{3} 10^{4} 10^{5} 10^{6} 10^{7}

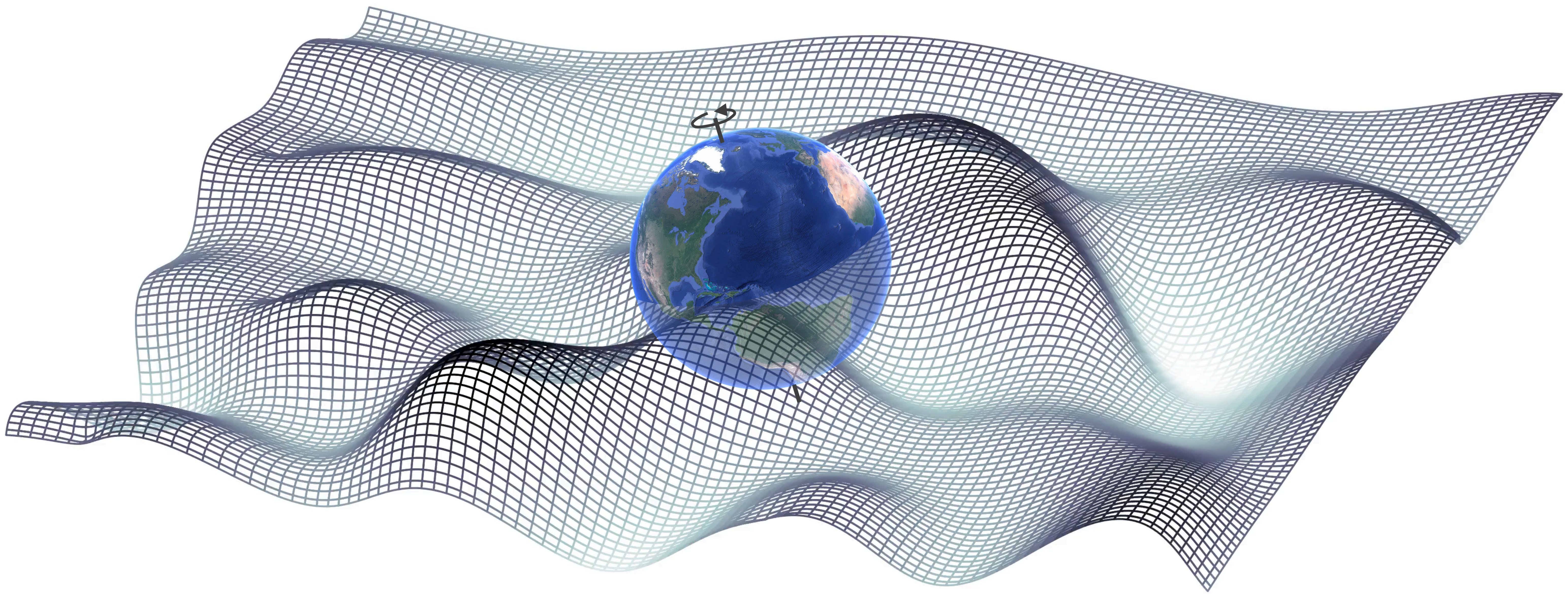

Amplitude: $A = \frac{\sqrt{2\rho_a}}{m_a}$

Frequency: $\omega = m_a + \frac{1}{2} m_a v^2$

$\approx m_a (1 + 10^{-6})$

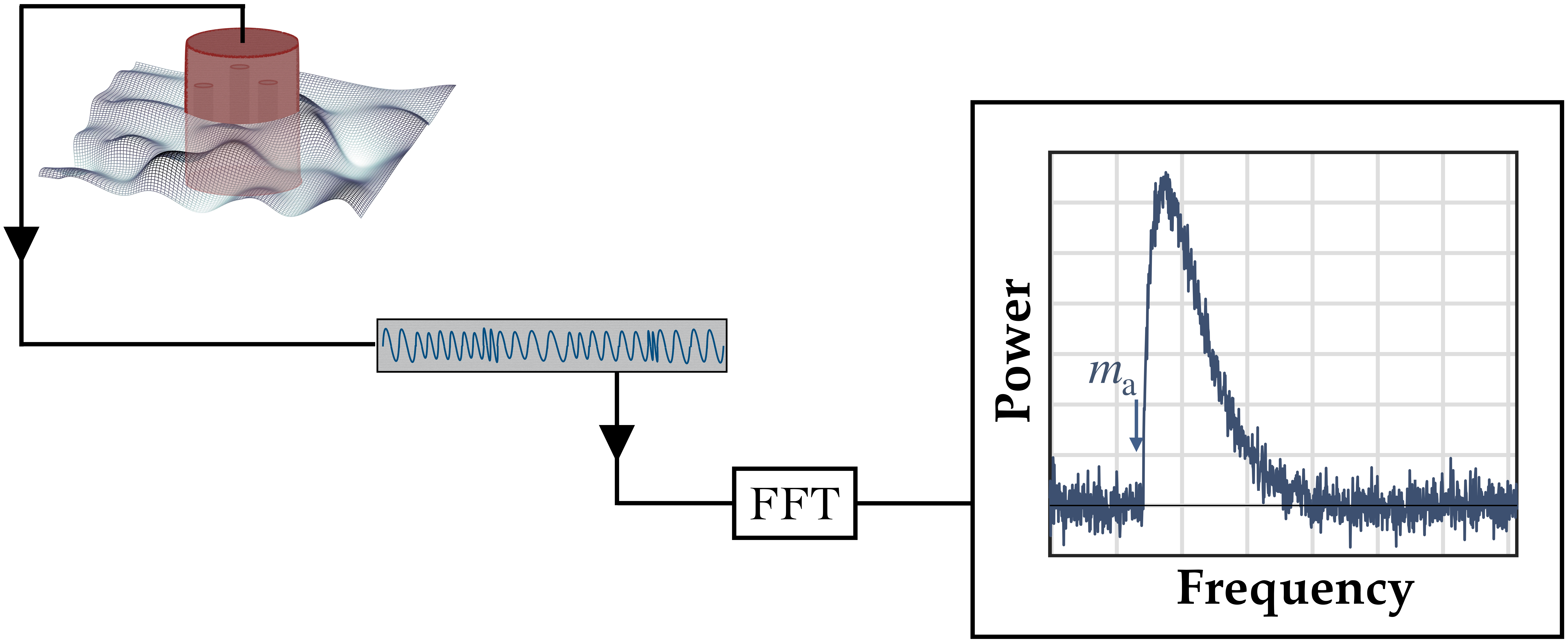
FFT
Power
m_a
Frequency

Frequency [MHz]
10^3
10^4
10^{-9}
10^{-10}
10^{-11}
10^{-12}
10^{-13}
10^{-14}
10^{-15}
$|g_{a\gamma\gamma}|$ [GeV^{-1}]
CAST
ADMX
RBF
UF
KSVZ
DFSZ
10^{-6}
10^{-5}
10^{-4}
m_a [eV]
FFT
Power
Frequency

Frequency [MHz]
10^3
10^4
10^{-9}
10^{-10}
10^{-11}
10^{-12}
10^{-13}
10^{-14}
10^{-15}
$|g_{a\gamma\gamma}|$ [GeV^{-1}]
10^{-6}
10^{-5}
10^{-4}
m_a [eV]
CAST
Neutron Stars
Globular clusters
Pulsars
ADMX
RBF
UF
CAPP
HAYSTAC
TASEH
CAST-CAPP
GrAHal
RADES
QUAX-$a\gamma$
ORGAN
KSVZ
DFSZ
RADES (CERN)
Co-axial ports
150 mm
25.1 mm
34 mm
Mode 1
Mode 2
Mode 3
Mode 4
Mode 5
ORGAN (UWA)
Cryogenic low-noise amplifier
Cryogenic circulator
1K temperature stage
100mK temperature stage
50mK temperature stage
Antenna
Microwave resonant cavity
QUAX (Legnaro)
CAPP (IBS)
HAYSTAC (Yale)
GrAHal (Grenoble)
2 m

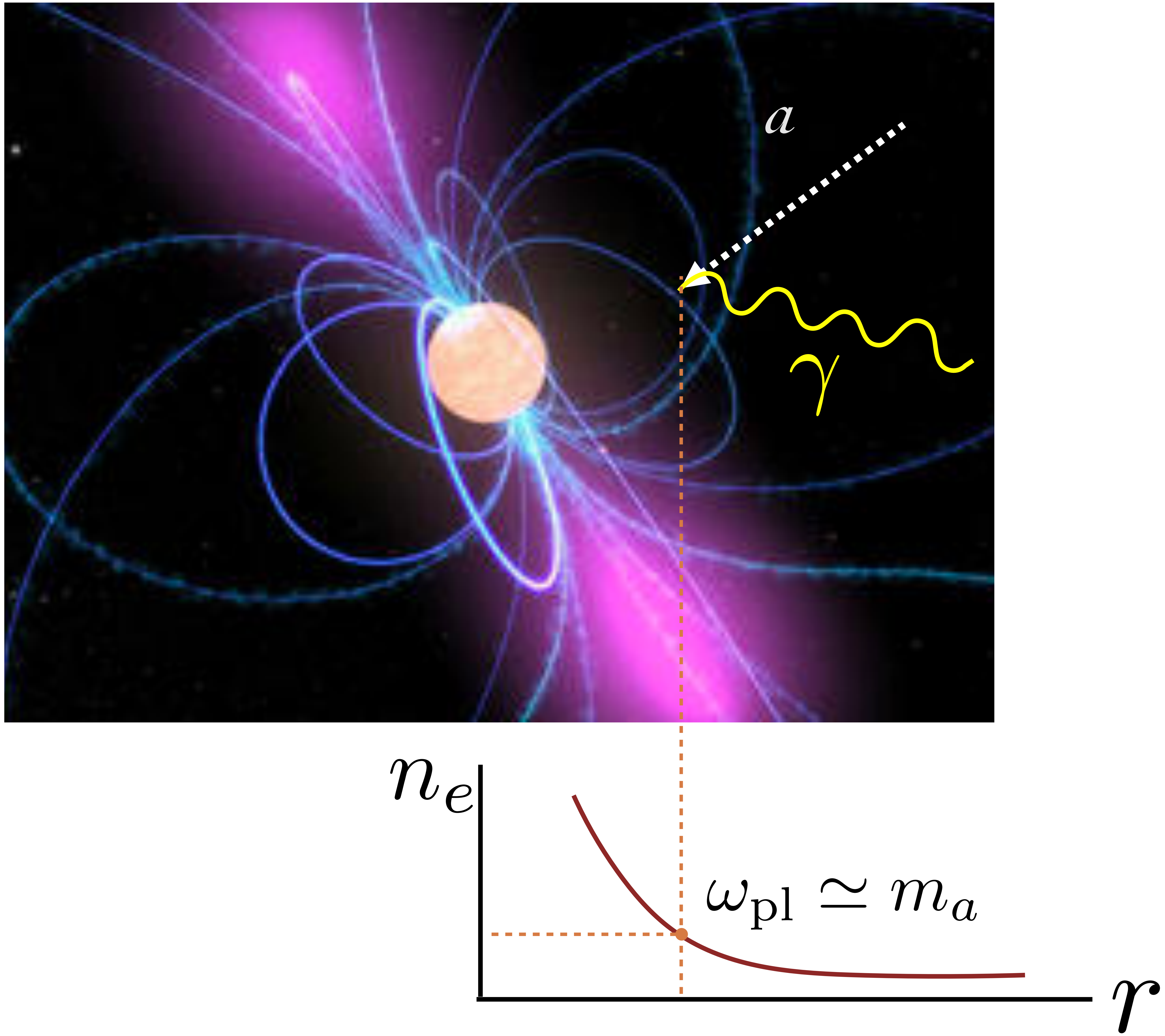

a
γ
n_e
$\omega_{\rm pl} \simeq m_a$
r

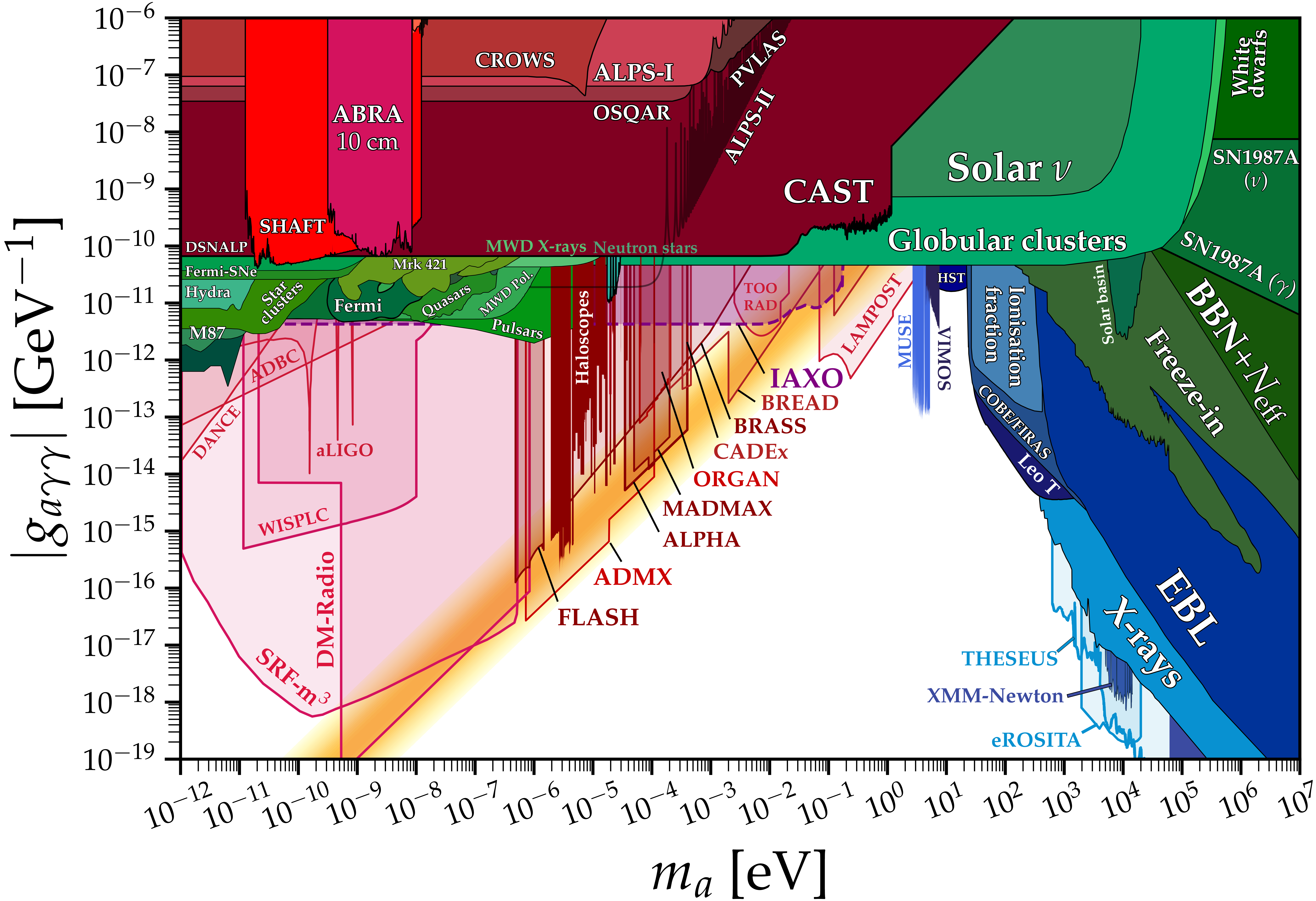

CROWS
ALPS-I
PVLAS
OSQAR
ALPS-II
ABRA
10 cm
SHAFT
CAST
Solar ν
Globular clusters
White dwarfs
SN1987A (ν)
SN1987A (γ)
DSNALP
MWD X-rays
Neutron stars
Fermi-SNe
Mrk 421
Hydra
Star clusters
Fermi
Quasars
MWD Pol.
Pulsars
M87
Haloscopes
TOO RAD
LAMPOST
MUSE
HST
VIMOS
Ionisation fraction
Solar basin
BBN+Neff
Freeze-in
ADBC
DANCE
aLIGO
IAXO
BREAD
BRASS
CADEx
ORGAN
MADMAX
ALPHA
ADMX
FLASH
WISPLC
DM-Radio
SRF-m3
COBE/FIRAS
Leo T
EBL
X-rays
THESEUS
XMM-Newton
eROSITA
$|g_{a\gamma\gamma}|$ [GeV^{-1}]
m_a [eV]

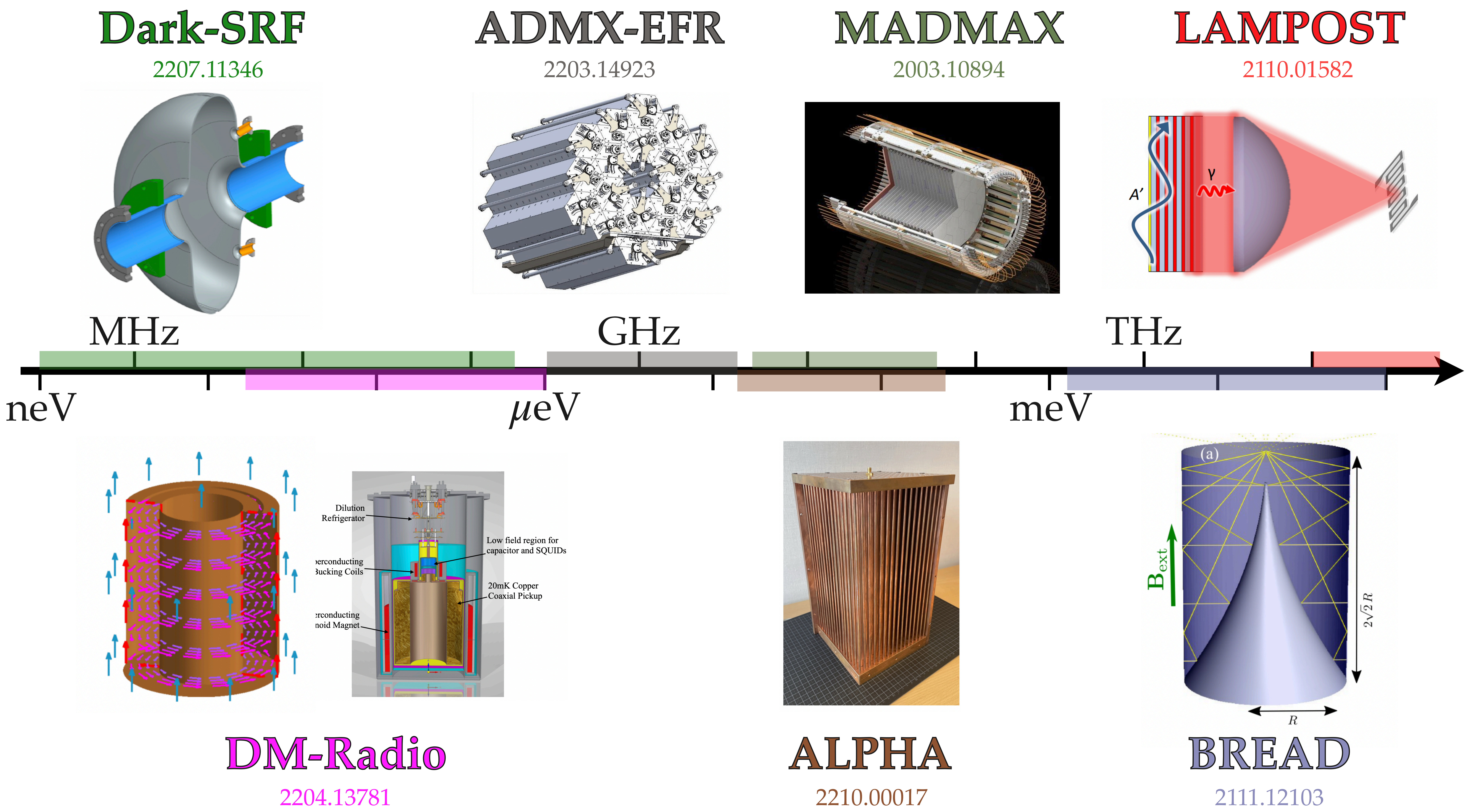
Dark-SRF
2207.11346
ADMX-EFR
2203.14923
MADMAX
2003.10894
LAMPOST
2110.01582
A′
γ
MHz
GHz
THz
neV
μeV
meV
Dilution Refrigerator
Low field region for capacitor and SQUIDs
Bucking Coils
20mK Copper Coaxial Pickup
(a)
B_{ext}
$2\sqrt{2}R$
R
DM-Radio
2204.13781
ALPHA
2210.00017
BREAD
2111.12103

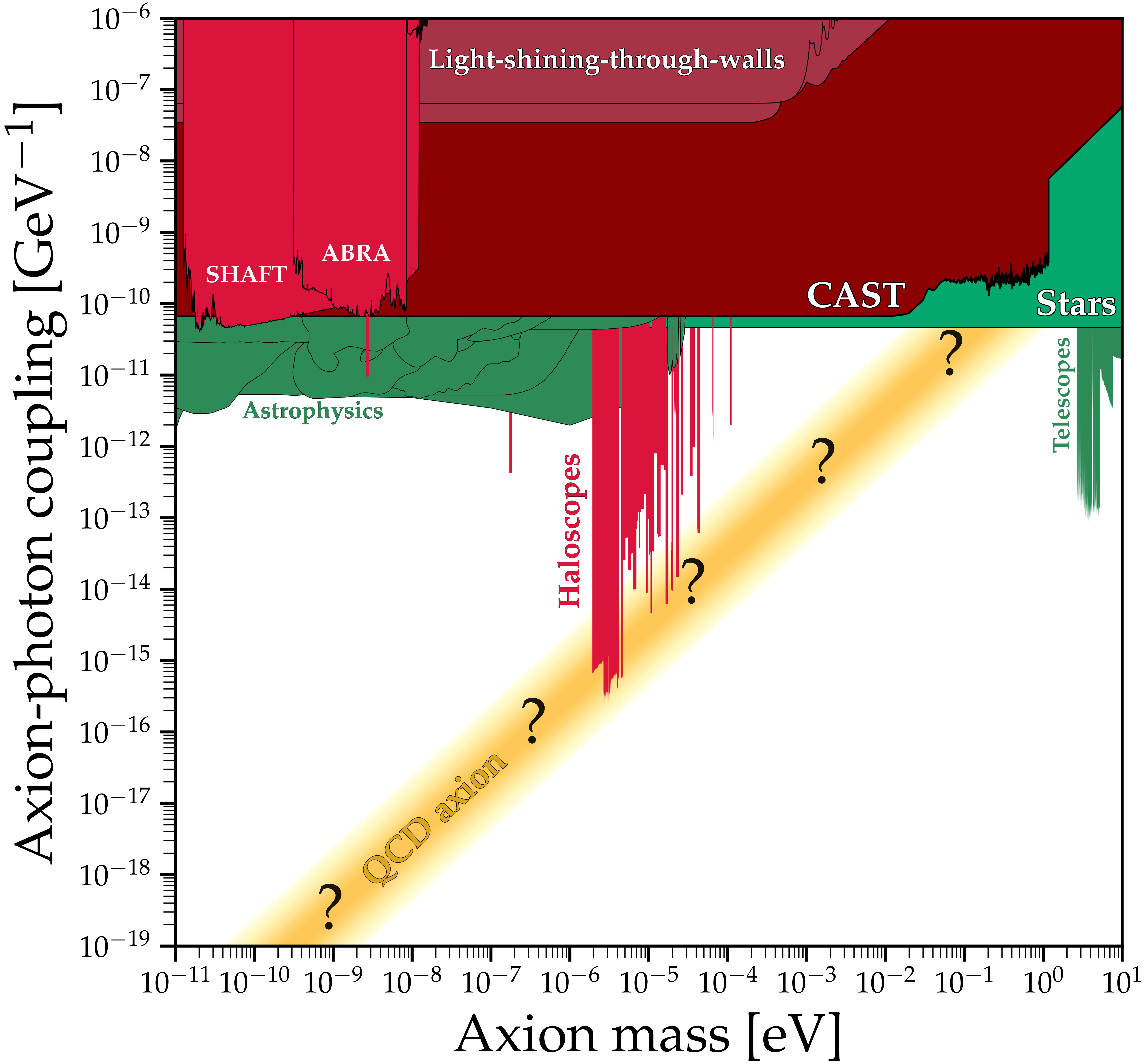

Light-shining-through-walls
SHAFT
ABRA
CAST
Stars
Astrophysics
Haloscopes
Telescopes
QCD axion
?
Axion-photon coupling [GeV^{-1}]
Axion mass [eV]
10^{-6}
10^{-7}
10^{-8}
10^{-9}
10^{-10}
10^{-11}
10^{-12}
10^{-13}
10^{-14}
10^{-15}
10^{-16}
10^{-17}
10^{-18}
10^{-19}
10^{-11} 10^{-10} 10^{-9} 10^{-8} 10^{-7} 10^{-6} 10^{-5} 10^{-4} 10^{-3} 10^{-2} 10^{-1} 10^{0} 10^{1}

Axion cosmology: the misalignment mechanism

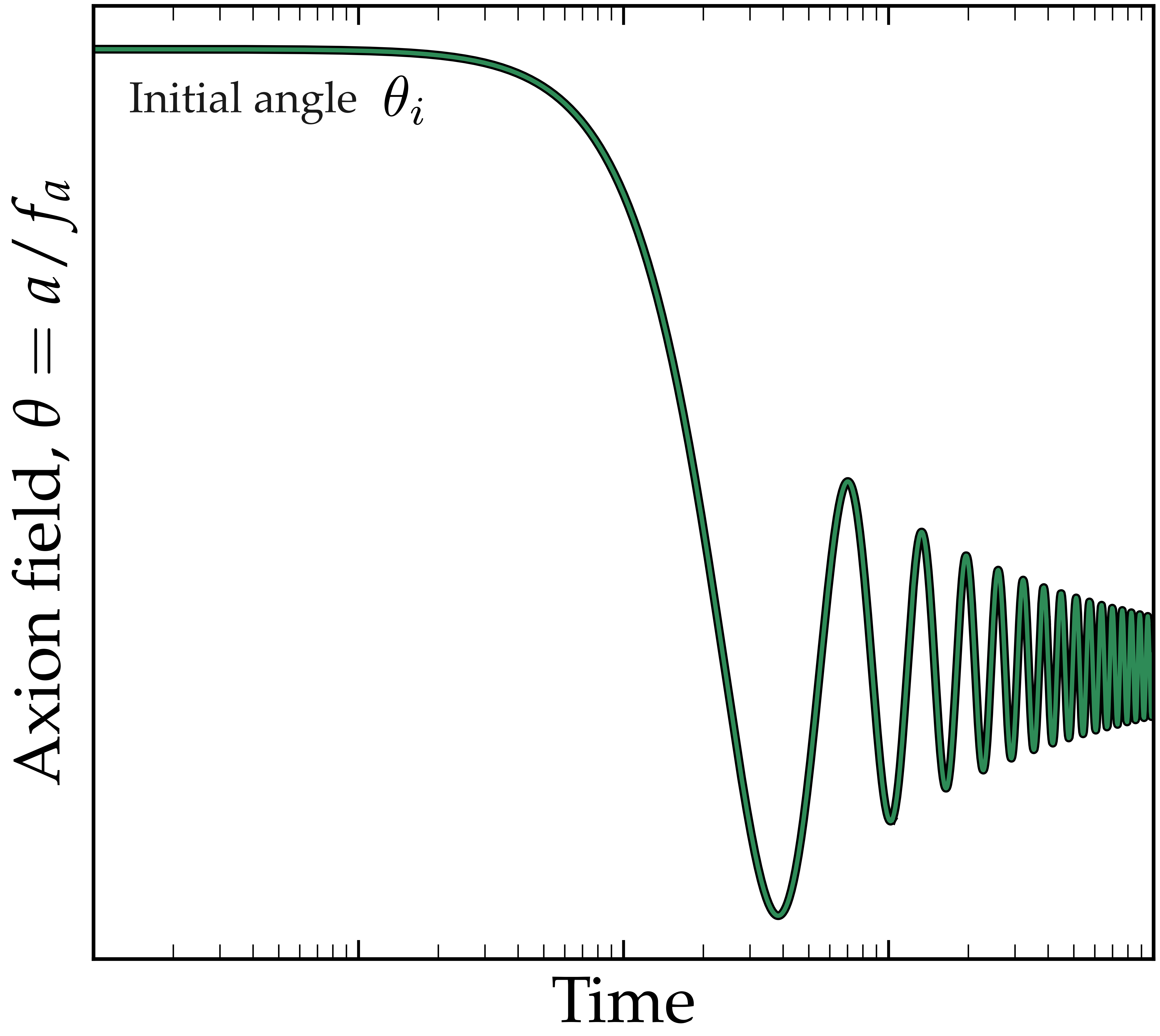

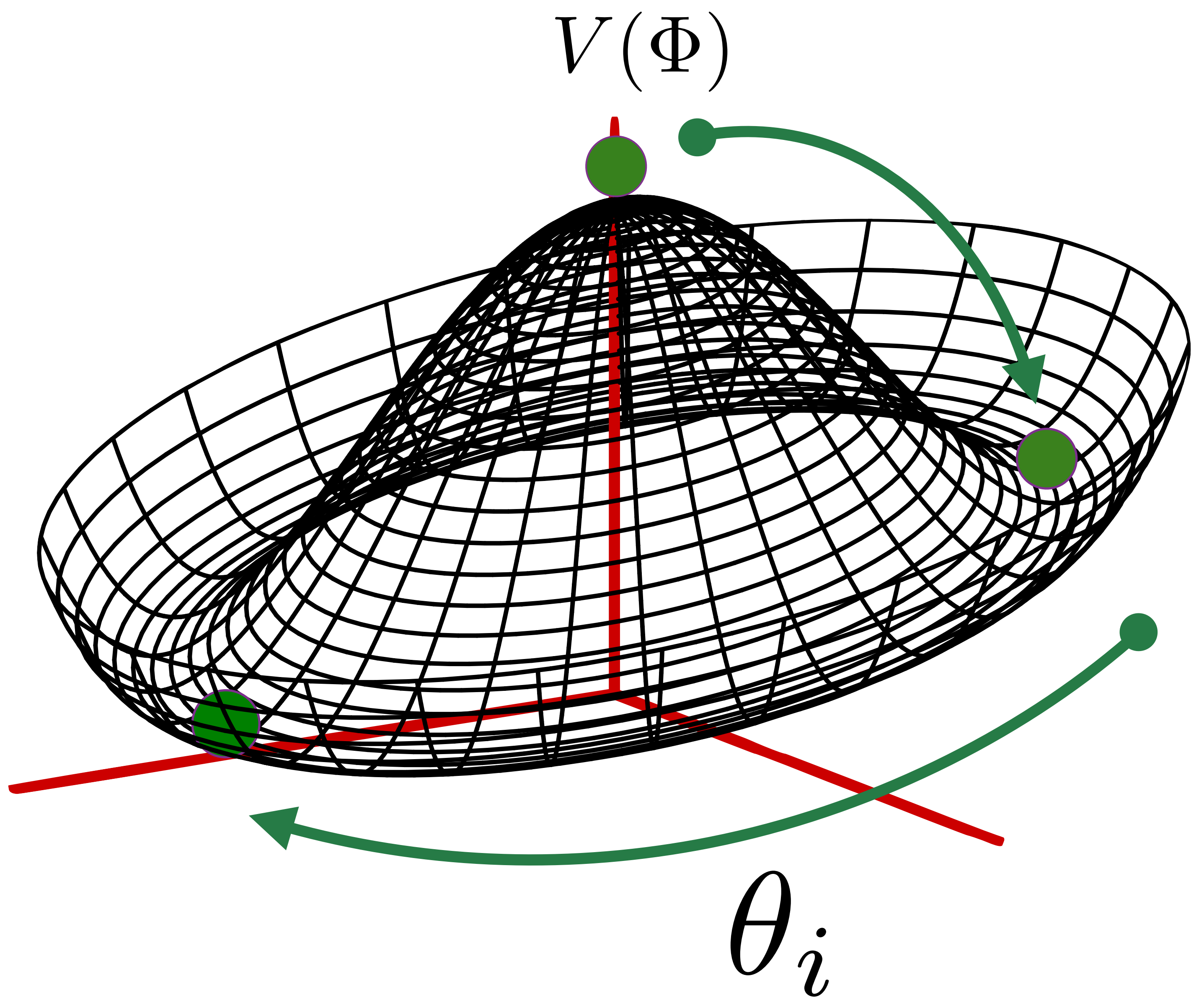

Amount of DM $\propto \theta_i^2 \, m_a^{-7/6}$

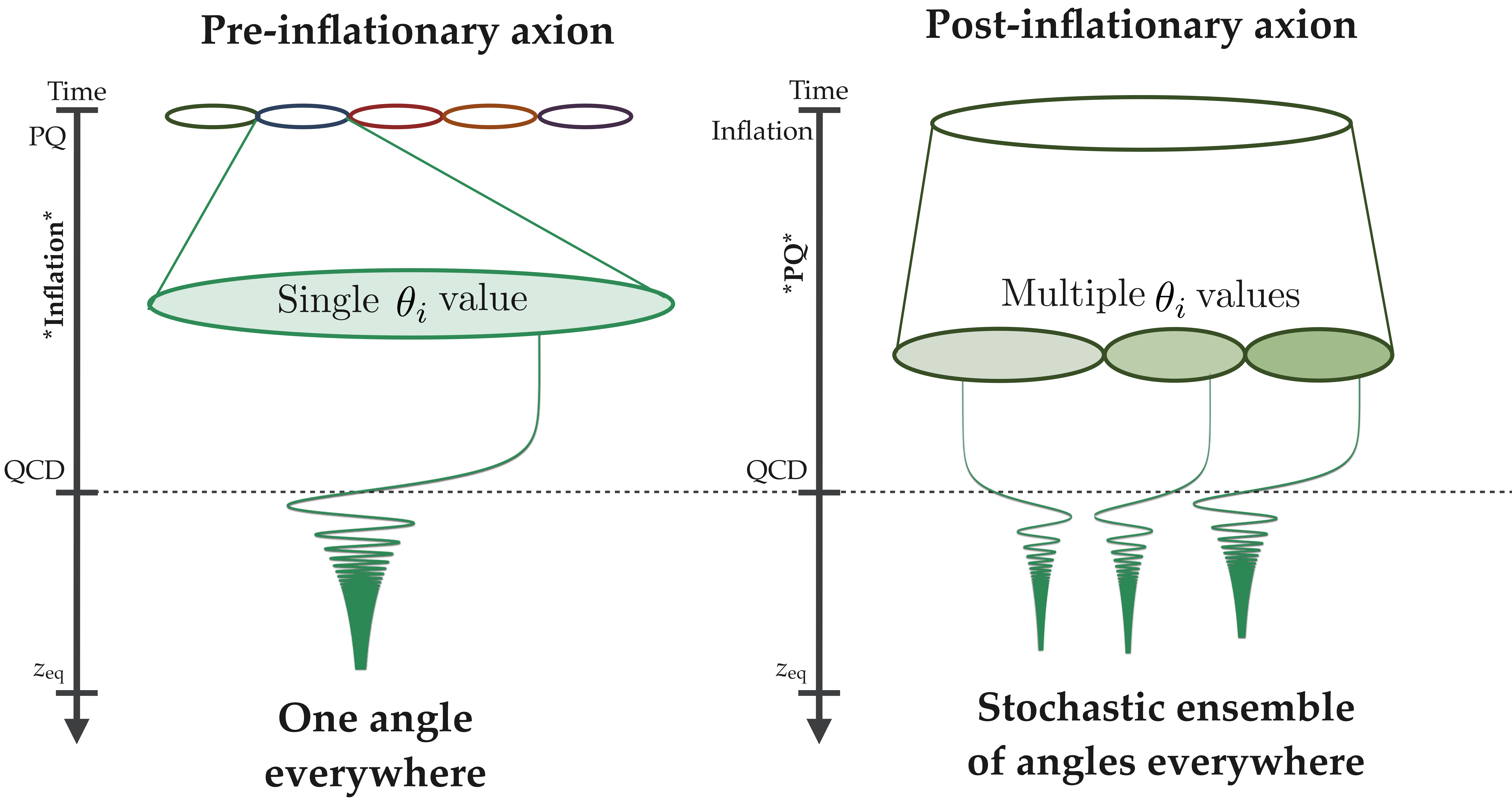
Pre-inflationary axion
Time
PQ
Inflation
Single θ_i value
QCD
$z_{\rm eq}$
One angle everywhere
Post-inflationary axion
Time
Inflation
PQ
Multiple θ_i values
QCD
$z_{\rm eq}$
Stochastic ensemble of angles everywhere

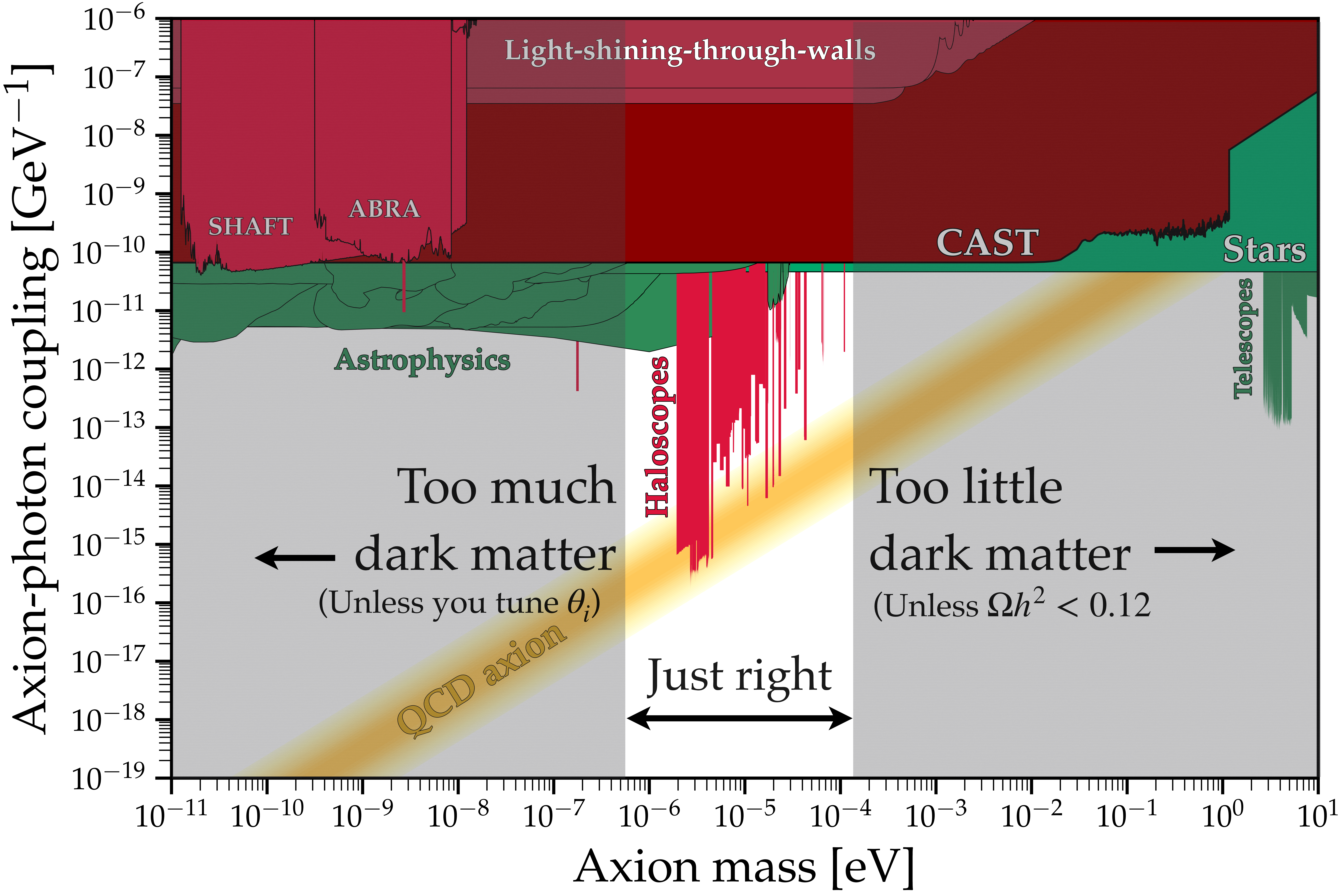

Light-shining-through-walls
SHAFT
ABRA
CAST
Stars
Astrophysics
Haloscopes
Telescopes
Too much
dark matter
(Unless you tune θ_i)
Too little
dark matter
(Unless $\Omega h^2 < 0.12$
Just right
QCD axion
Axion-photon coupling [GeV^{-1}]
Axion mass [eV]
10^{-6}
10^{-7}
10^{-8}
10^{-9}
10^{-10}
10^{-11}
10^{-12}
10^{-13}
10^{-14}
10^{-15}
10^{-16}
10^{-17}
10^{-18}
10^{-19}
10^{-11} 10^{-10} 10^{-9} 10^{-8} 10^{-7} 10^{-6} 10^{-5} 10^{-4} 10^{-3} 10^{-2} 10^{-1} 10^{0} 10^{1}

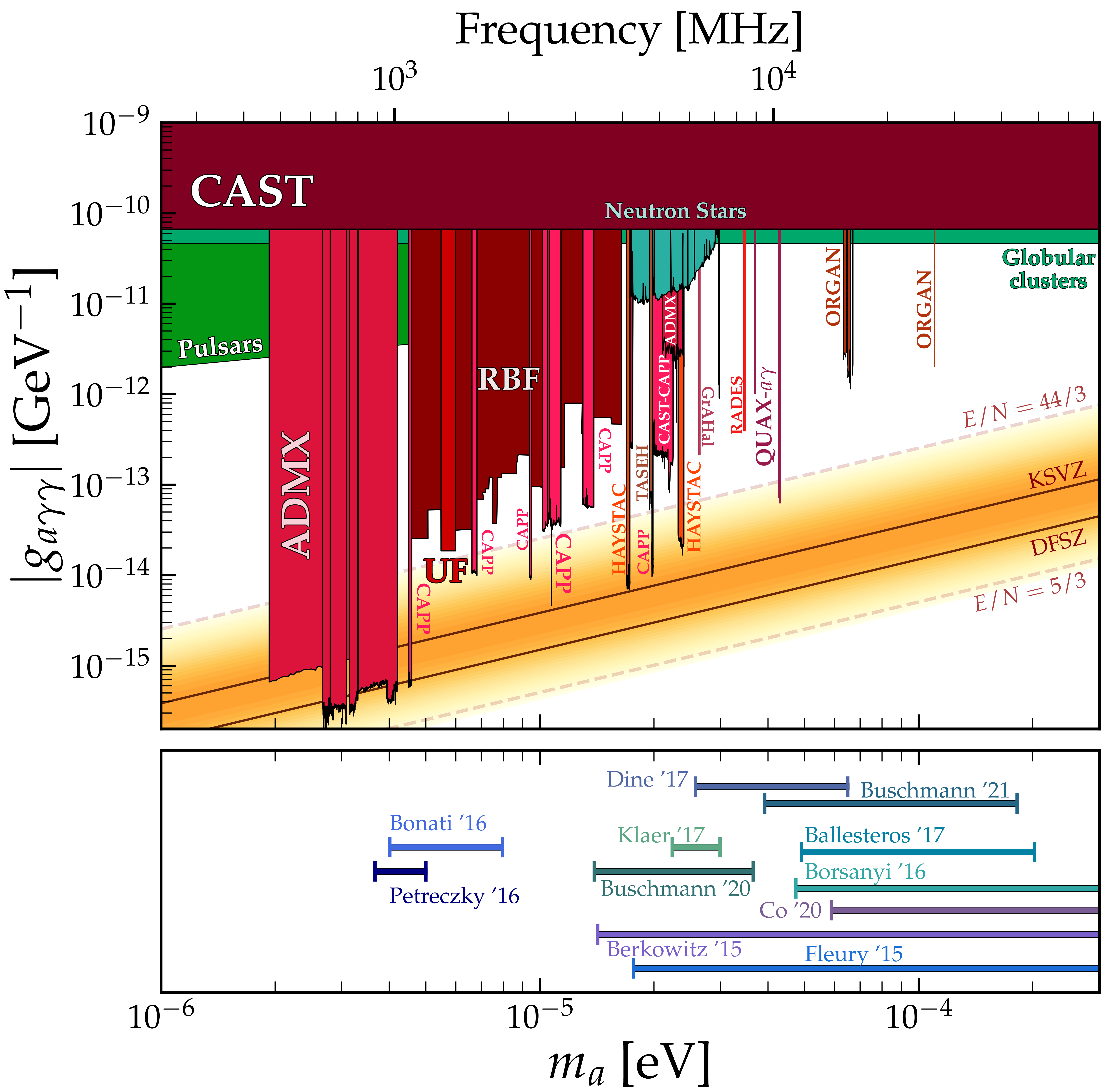

Frequency [MHz]
CAST
Neutron Stars
Globular clusters
Pulsars
ADMX
RBF
UF
CAPP
HAYSTAC
TASEH
CAST-CAPP
GrAHal
RADES
QUAX-$a\gamma$
ORGAN
E/N = 44/3
KSVZ
DFSZ
E/N = 5/3
$|g_{a\gamma\gamma}|$ [GeV^{-1}]
Dine '17
Buschmann '21
Bonati '16
Klaer '17
Ballesteros '17
Petreczky '16
Buschmann '20
Borsanyi '16
Co '20
Berkowitz '15
Fleury '15
m_a [eV]

Pre-inflation: calculation is easy… but there is a free parameter θ_i that we have no a priori knowledge of

Post-inflation: no free parameters… but things get complicated

Topological defects in the axion field in the post-inflationary scenario

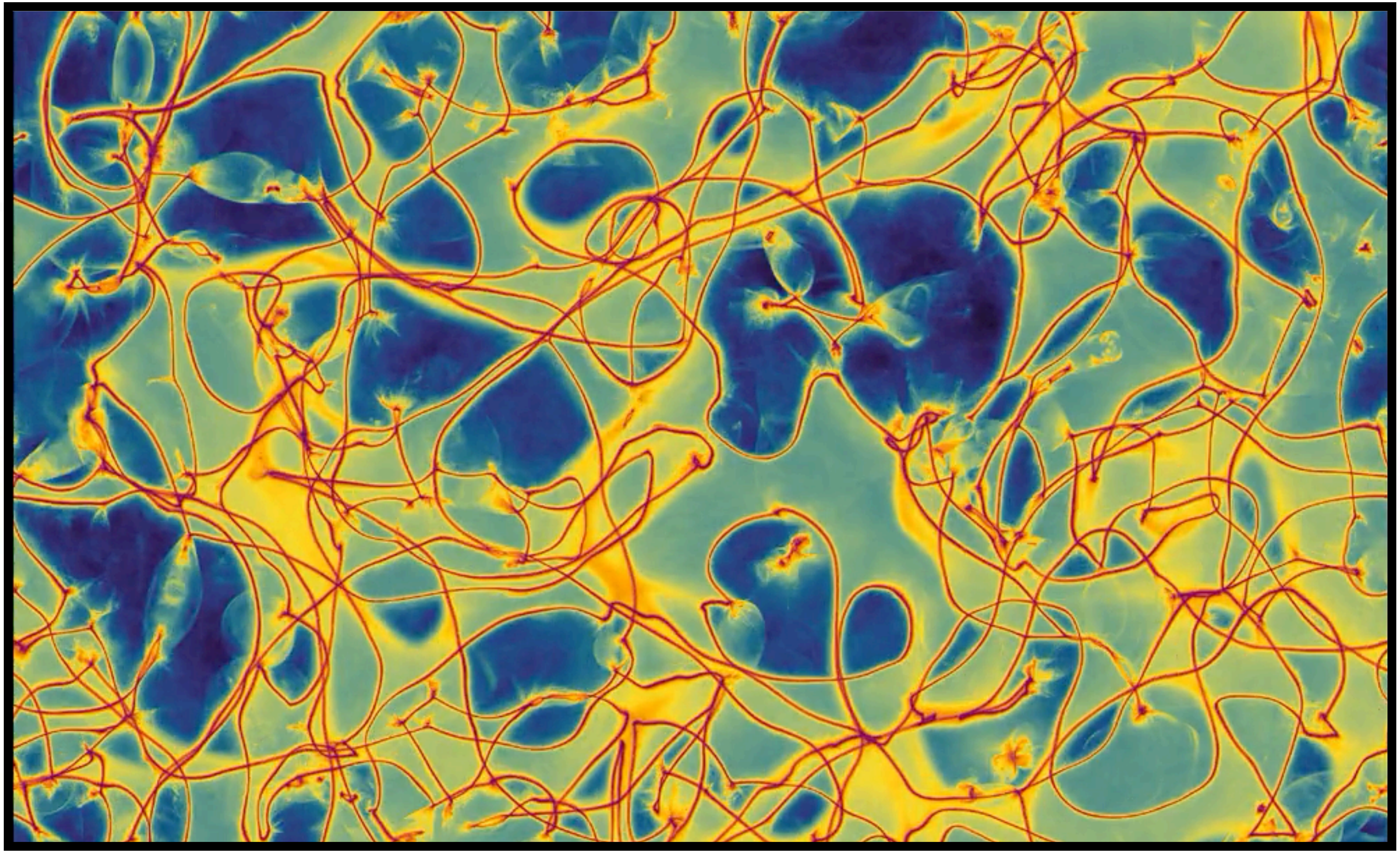

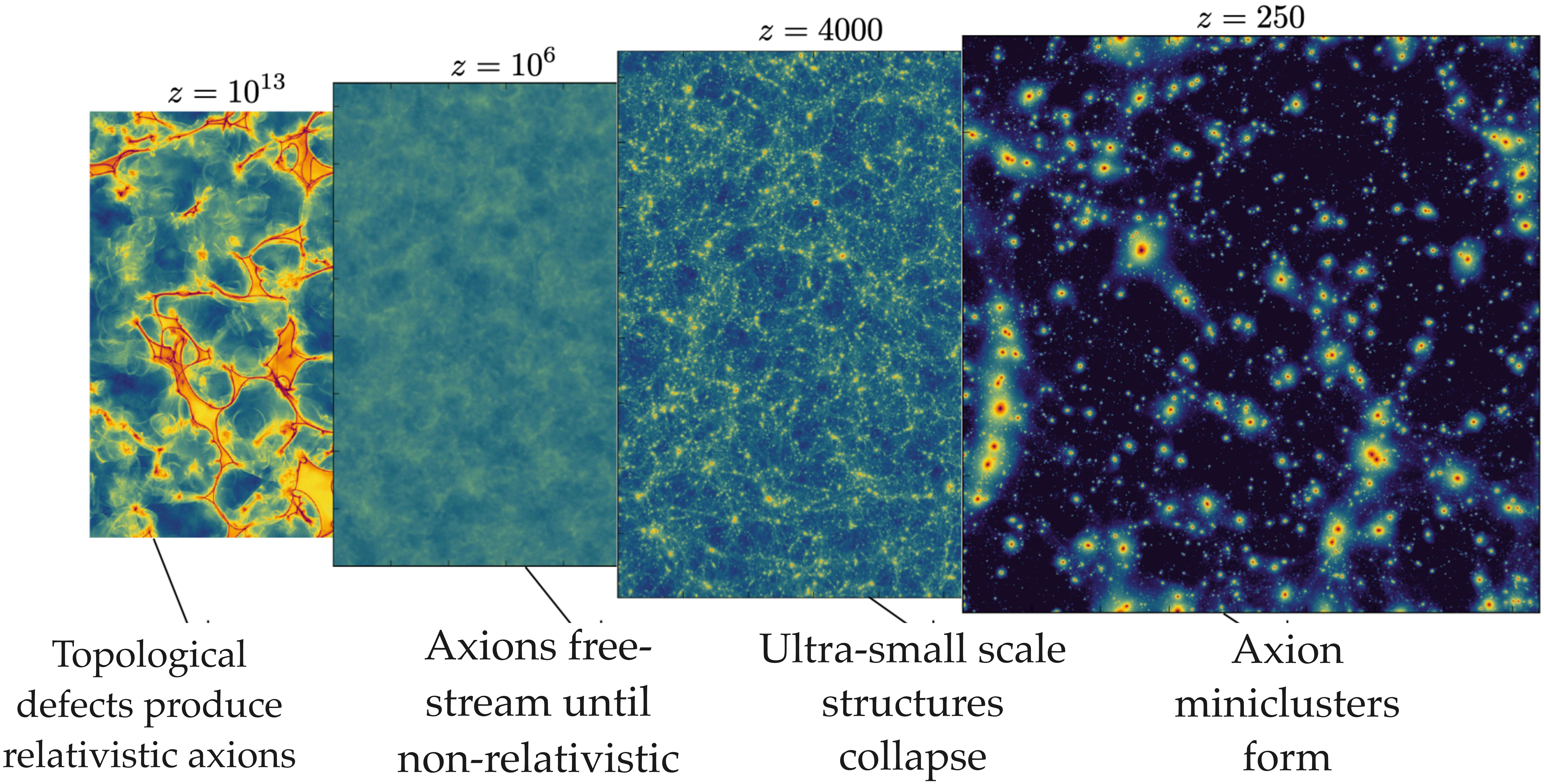

$z = 10^{13}$
$z = 10^6$
$z = 4000$
$z = 250$
Topological defects produce relativistic axions
Axions free-stream until non-relativistic
Ultra-small scale structures collapse
Axion miniclusters form

Not the end of the story…

Tidal disruption?

→ About ~60% of the miniclusters should be disrupted at the solar position (big uncertainty on density profile)

→ Disruption should re-fill phase space distribution, but by how much?

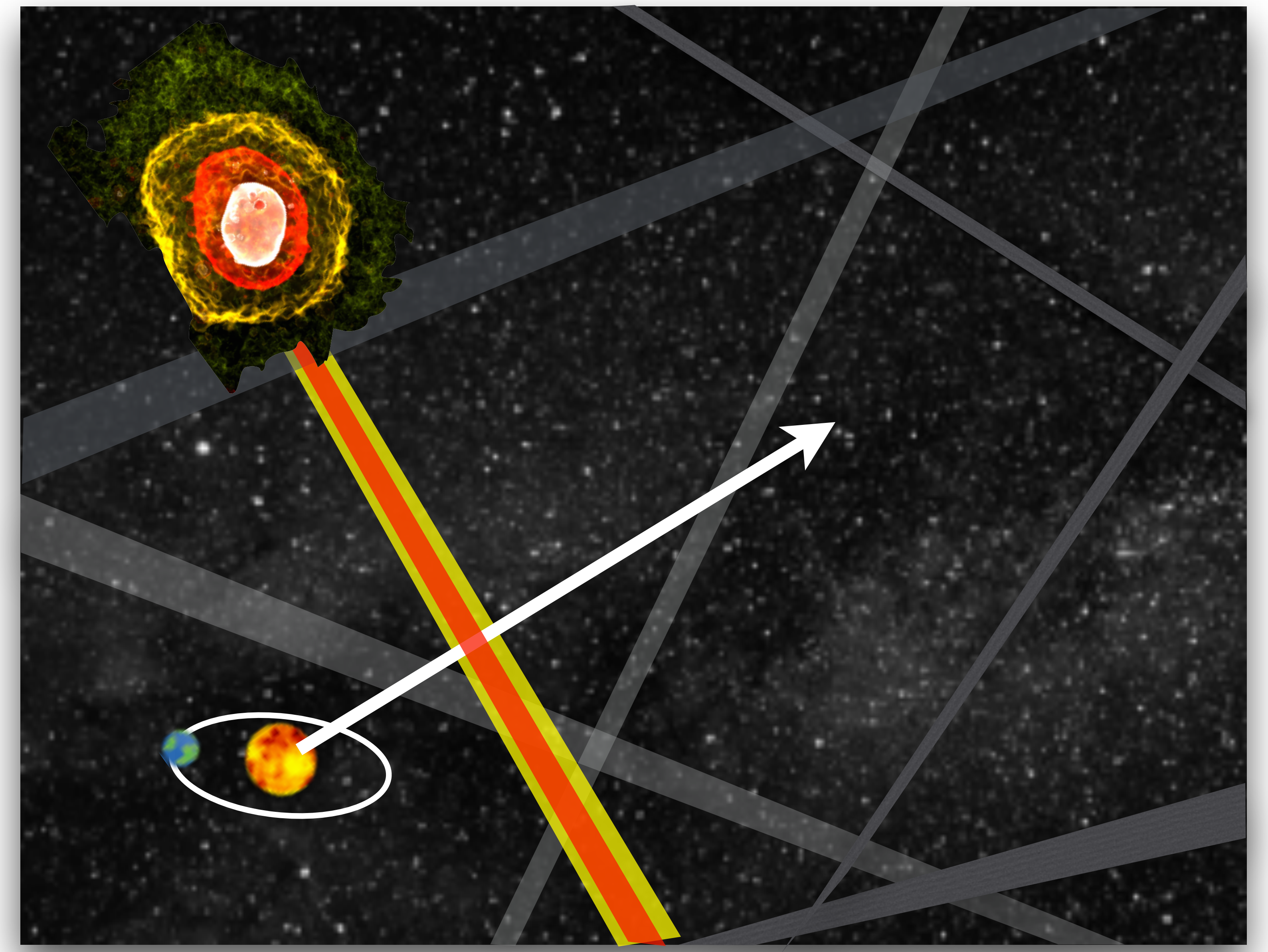

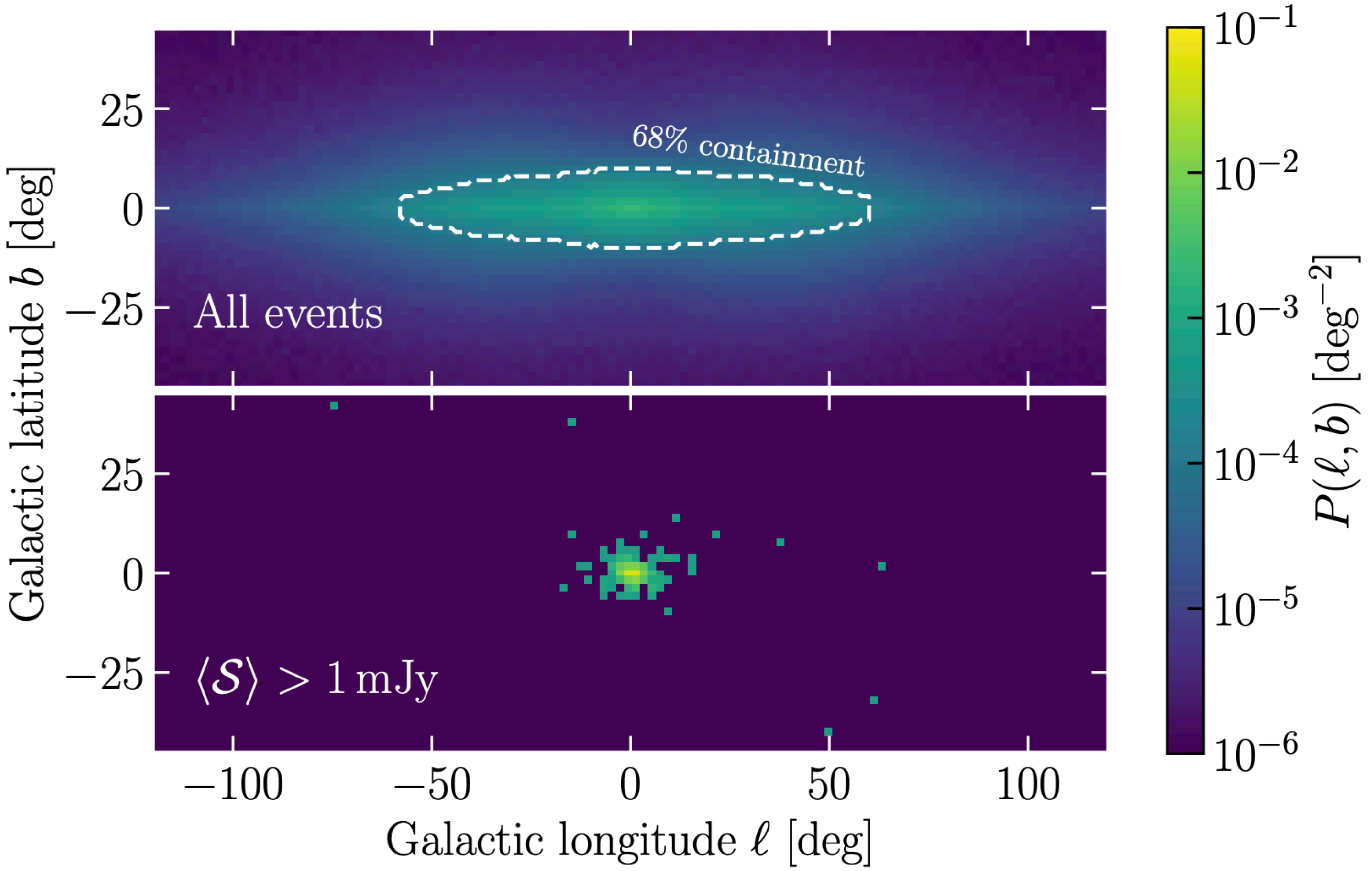

Indirect signals?

→ Collision of miniclusters with neutron stars, observe in radio [2011.05378]

→ Some miniclusters may be concentrated enough to microlense [2204.13187]

Axions

THE UNIVERSITY OF SYDNEY

ARC CENTRE OF EXCELLENCE FOR DARK MATTER

Back to axions… fermion couplings, e.g. neutron

→ Hard to beat astrophysical bounds

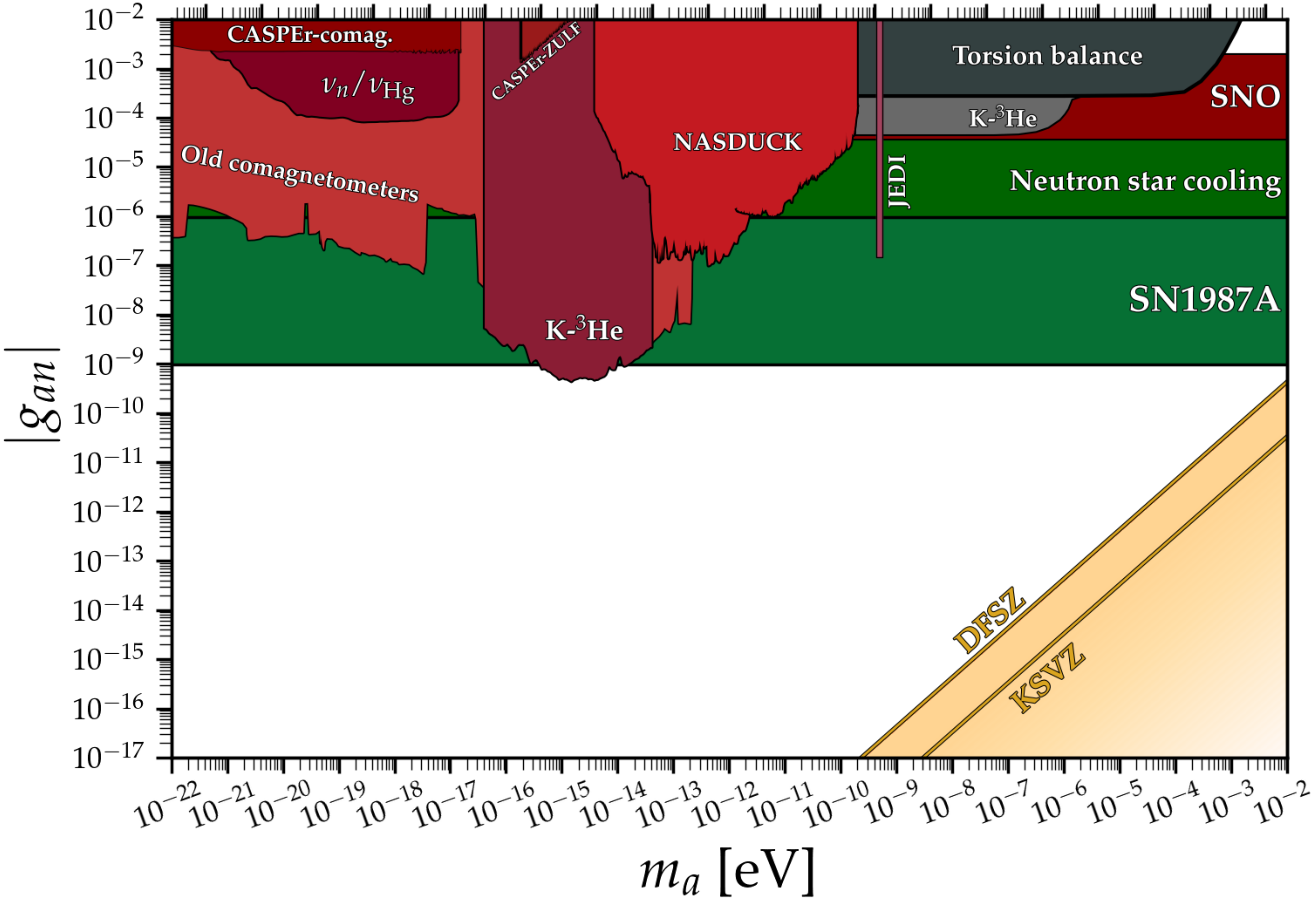

Why?

$$\mathcal{L} = -\frac{g_{an}}{2m_n}\partial_\mu a \underbrace{\bar{n}\gamma^5\gamma^\mu n}_{\text{Spin-dependent}}$$

Hard to get large-enough samples of spin-polarised materials to compete with a star

Back to axions… fermion couplings, e.g. neutron
→ Hard to beat astrophysical bounds

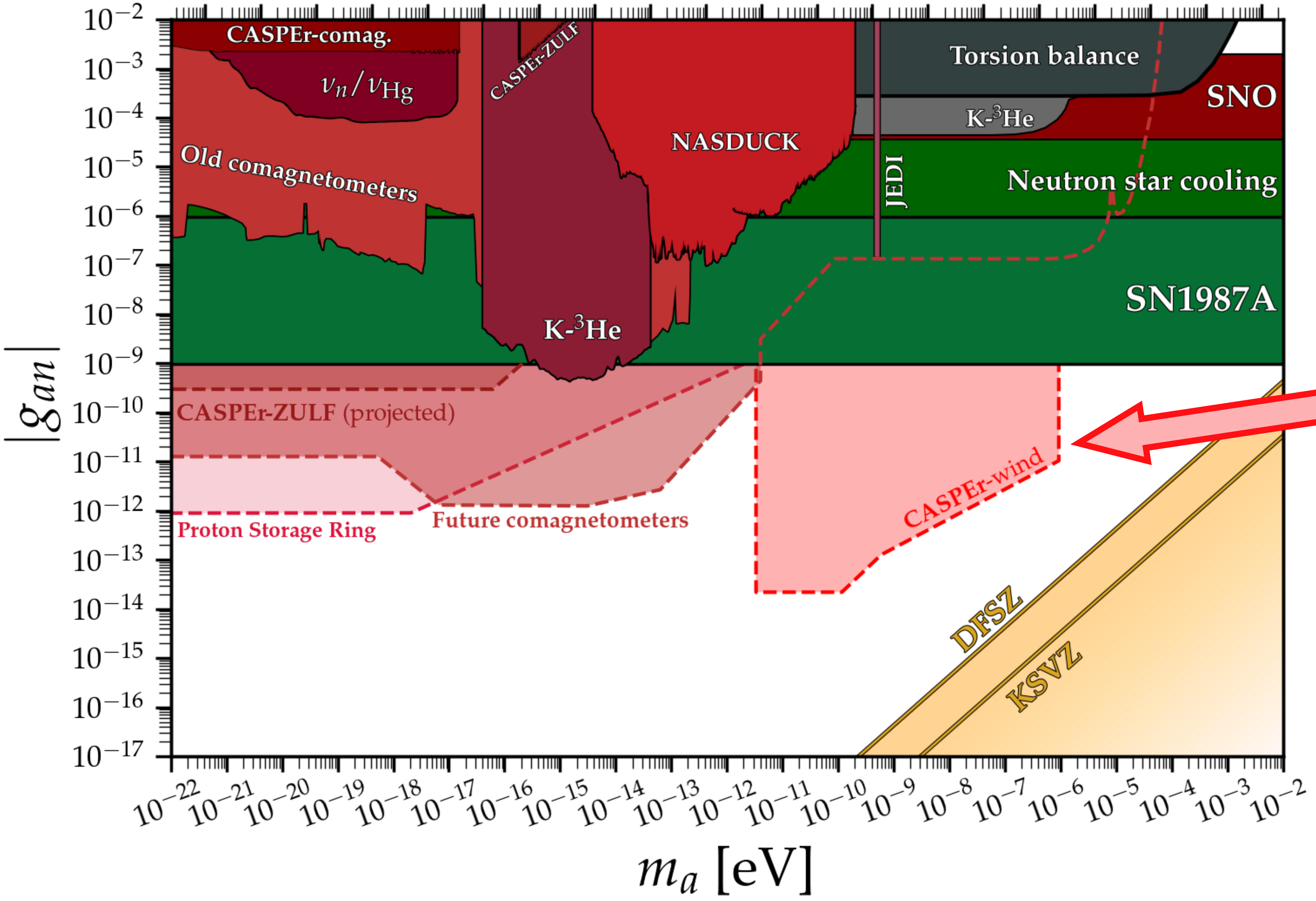

CASPEr-wind

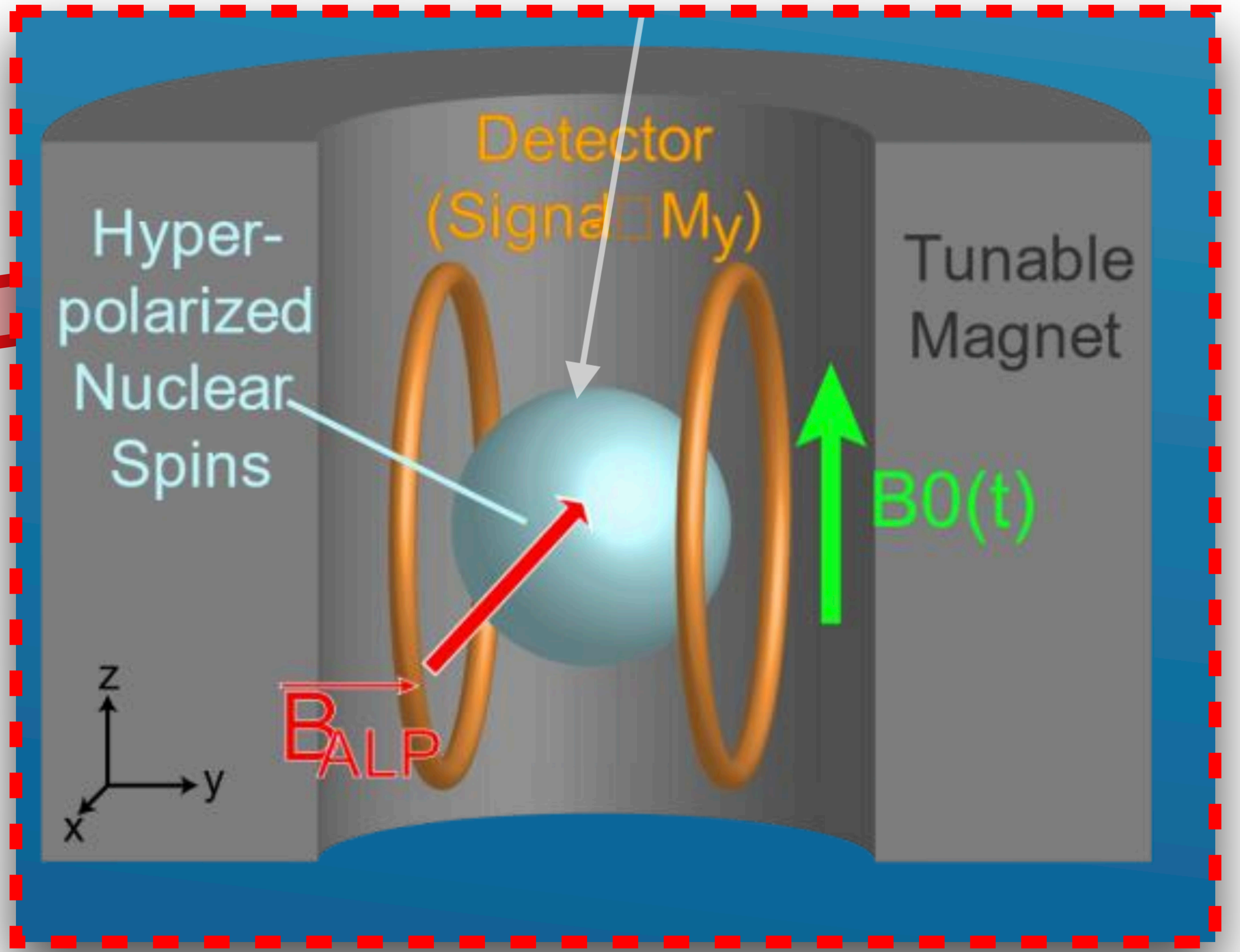

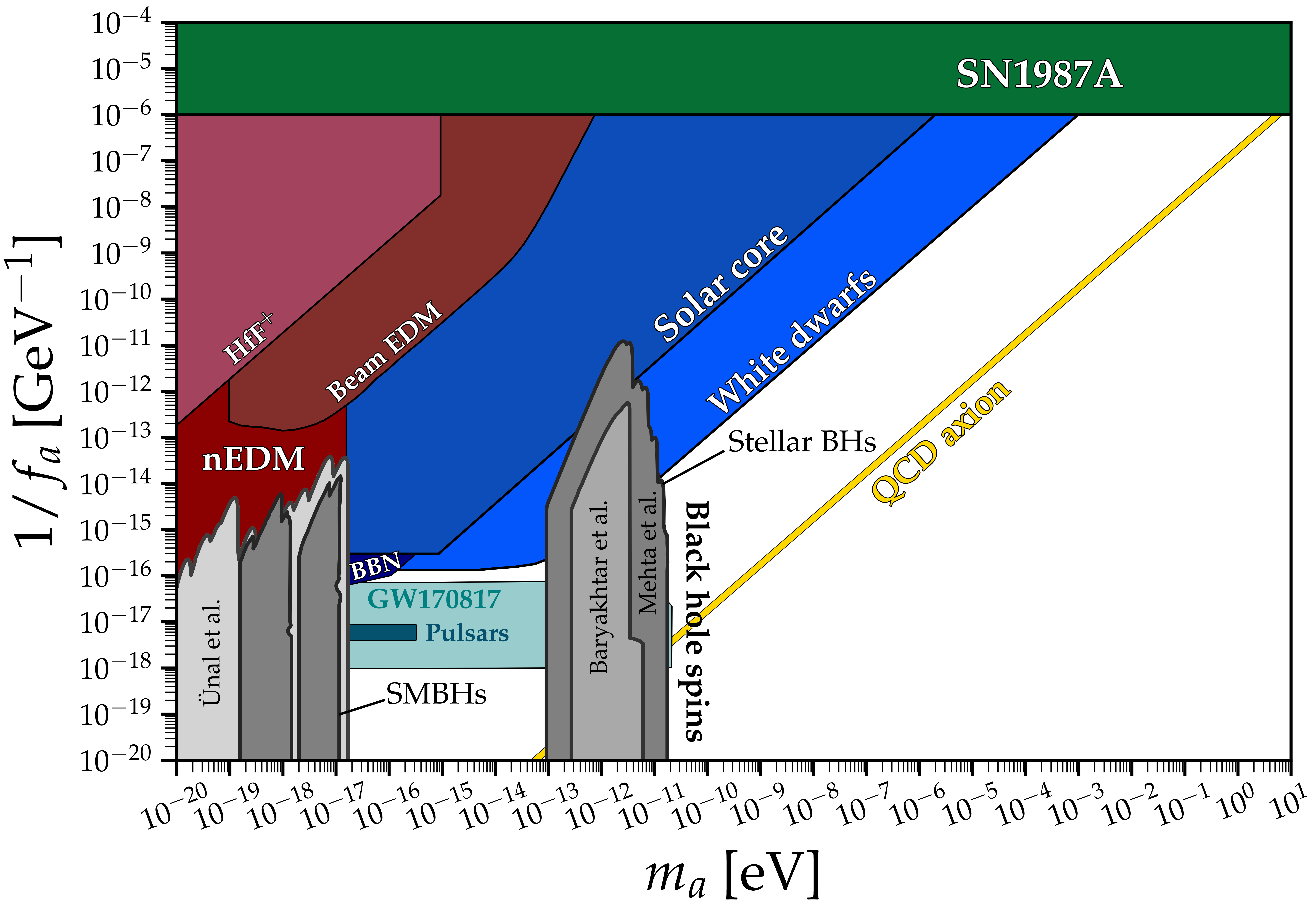

SN1987A
HfF+
Beam EDM
Solar core
White dwarfs
nEDM
Stellar BHs
QCD axion
BBN
GW170817
Pulsars
SMBHs
Ünal et al.
Baryakhtar et al.
Mehta et al.
Black hole spins
$1/f_a$ [GeV^{-1}]
m_a [eV]

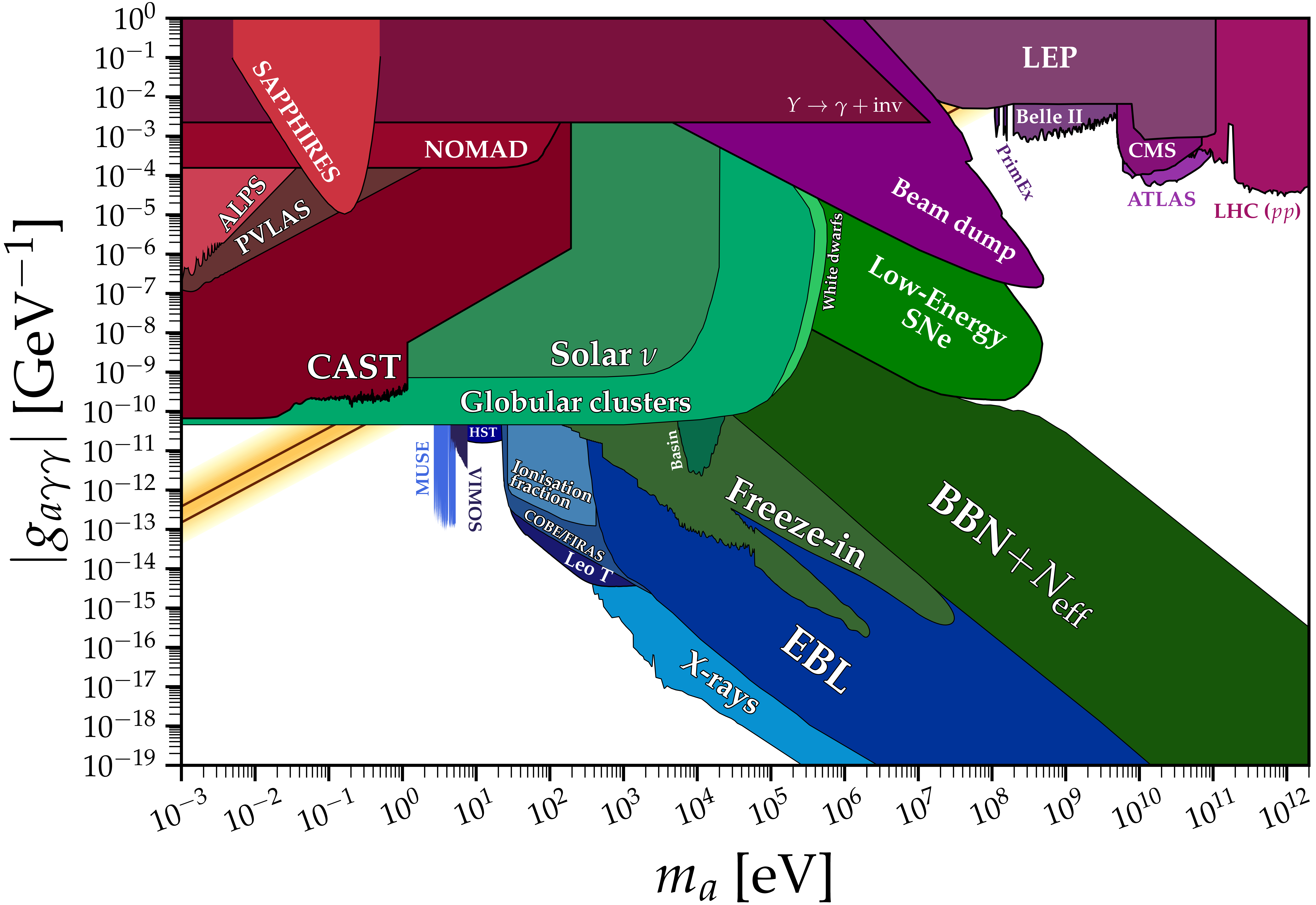

LEP
Belle II
CMS
ATLAS
LHC (pp)
PrimEx
Υ → γ + inv
SAPPHIRES
NOMAD
ALPS
PVLAS
CAST
Solar ν
Globular clusters
Beam dump
White dwarfs
Low-Energy SNe
HST
MUSE
VIMOS
Ionisation fraction
COBE/FIRAS
Leo T
Basin
Freeze-in
BBN+N_eff
EBL
X-rays
$|g_{a\gamma\gamma}|$ [GeV^{-1}]
m_a [eV]

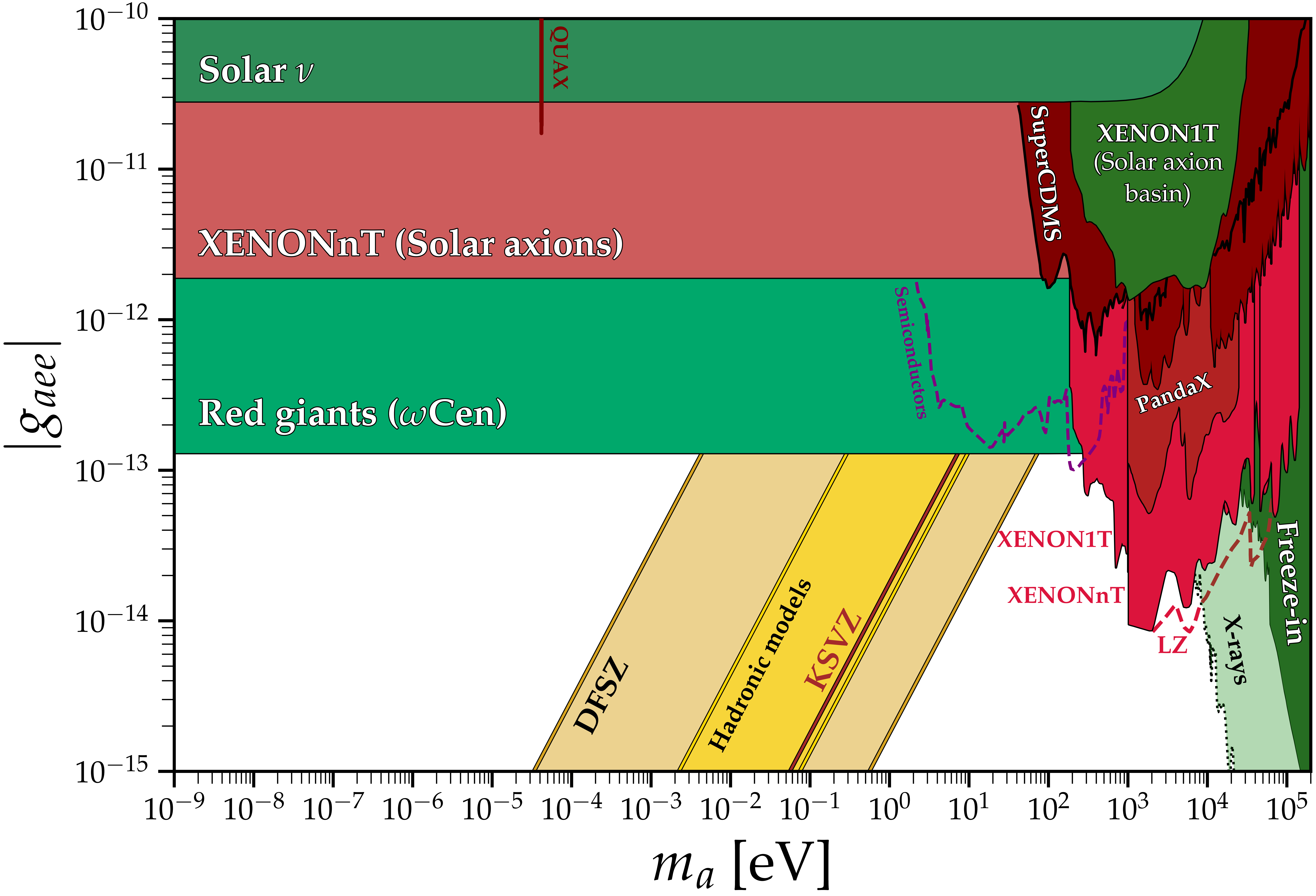

Solar ν
QUAX
XENONnT (Solar axions)
SuperCDMS
XENON1T (Solar axion basin)
Red giants (ωCen)
Semiconductors
PandaX
XENON1T
XENONnT
LZ
X-rays
Freeze-in
DFSZ
Hadronic models
KSVZ
$|g_{aee}|$
m_a [eV]
10^{-10}
10^{-11}
10^{-12}
10^{-13}
10^{-14}
10^{-15}
10^{-9} 10^{-8} 10^{-7} 10^{-6} 10^{-5} 10^{-4} 10^{-3} 10^{-2} 10^{-1} 10^{0} 10^{1} 10^{2} 10^{3} 10^{4} 10^{5}

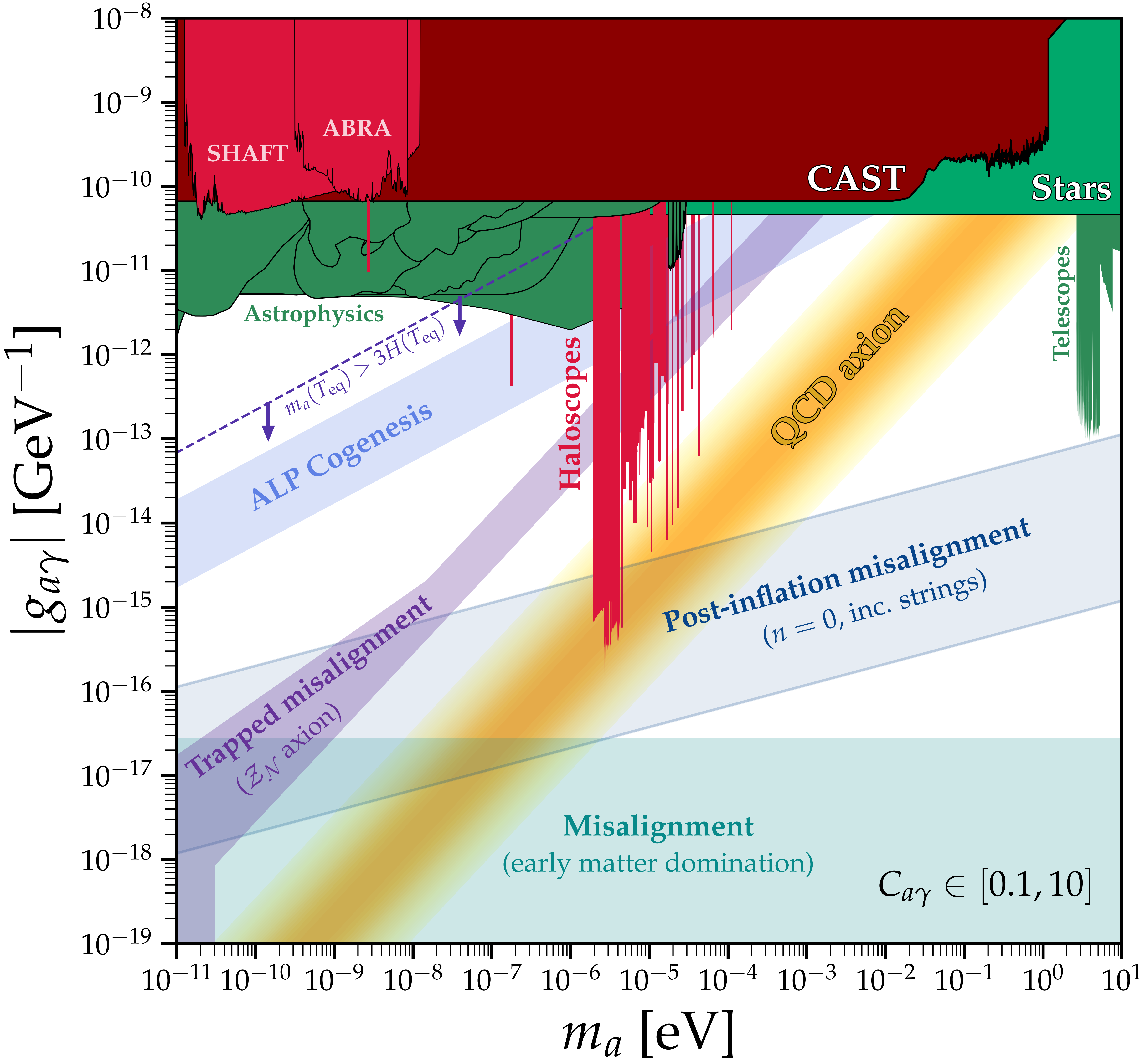
SHAFT
ABRA
CAST
Stars
Astrophysics
Telescopes
Haloscopes
QCD axion
ALP Cogenesis
$m_a(T_{eq}) > 3H(T_{eq})$
Post-inflation misalignment
($n = 0$, inc. strings)
Trapped misalignment
($\mathbb{Z}_N$ axion)
Misalignment
(early matter domination)
$C_{a\gamma} \in [0.1, 10]$
$|g_{a\gamma}|$ [GeV^{-1}]
m_a [eV]

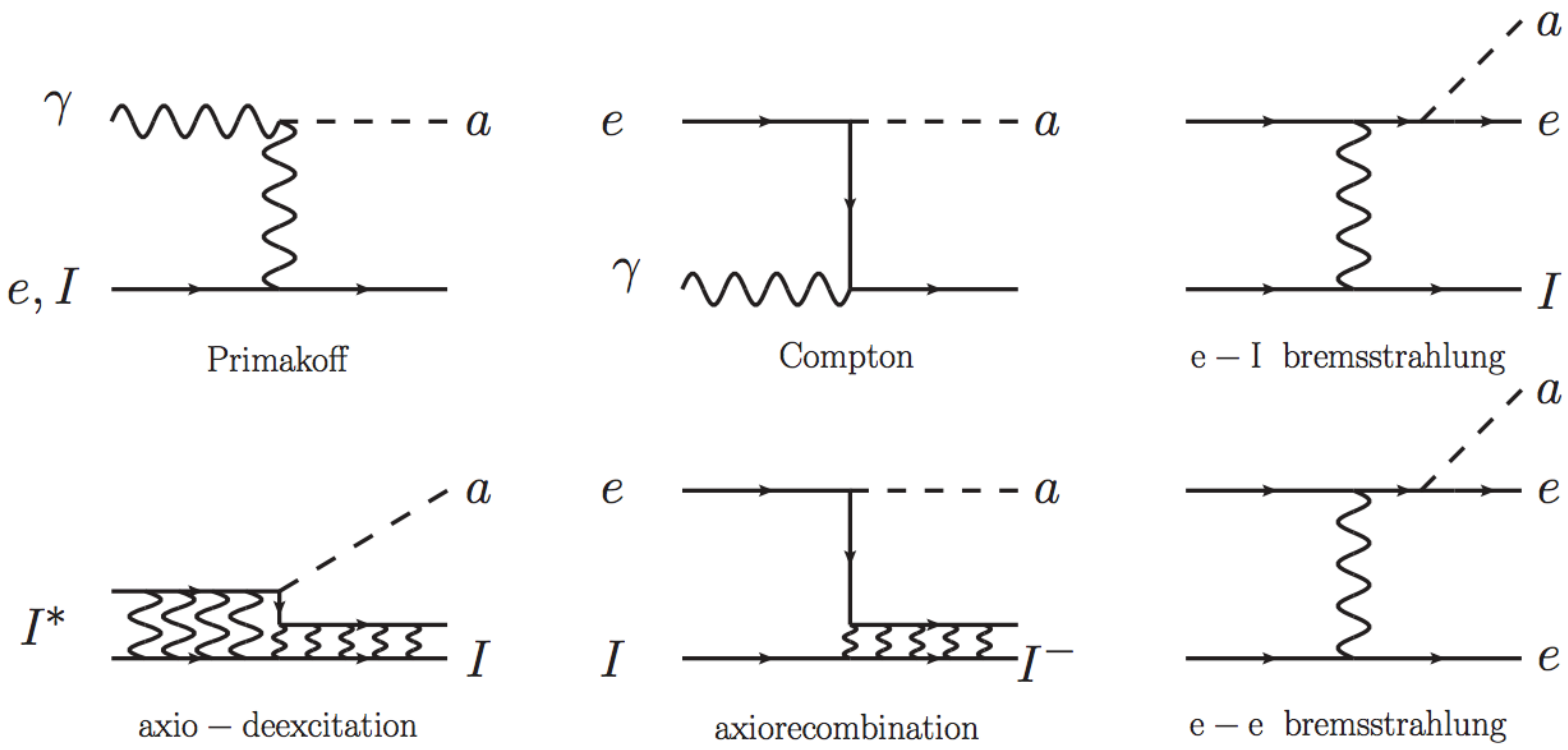

γ
a
e, I
Primakoff
e
a
γ
Compton
a
e
I
e − I bremsstrahlung
a
I*
I
axio − deexcitation
e
a
I
I⁻
axiorecombination
a
e
e
e − e bremsstrahlung

[1310.0823]

Pure laboratory tests of axion-fermion fifth forces

Key point: any SM or BSM CP-violation (could be e.g. size of Jarlskog invariant of CKM matrix) could shift axion vev and generate **CP-violating** axion-fermion couplings in addition to the **CP-conserving** ones

$$\mathcal{L} \supset -a \sum_{\psi} \underline{g_p^{\psi} \left(i\bar{\psi}\gamma^5\psi\right)} - a \sum_{\psi} \underline{g_s^{\psi} (\bar{\psi}\psi)}$$

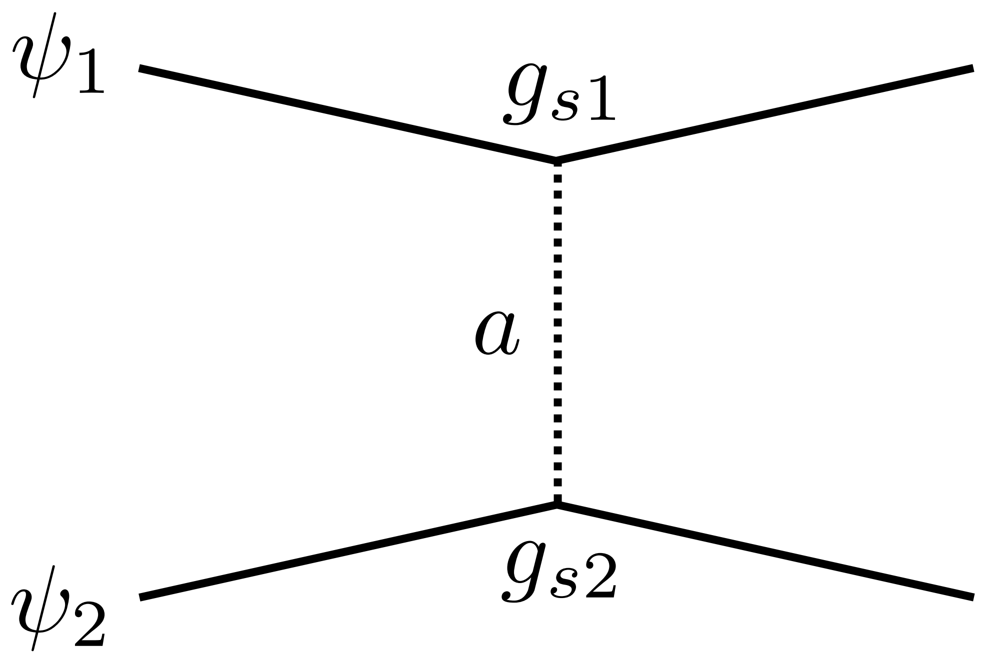

Monopole-monopole
(Spin independent)

→ e.g. tests of inverse square law/WEP

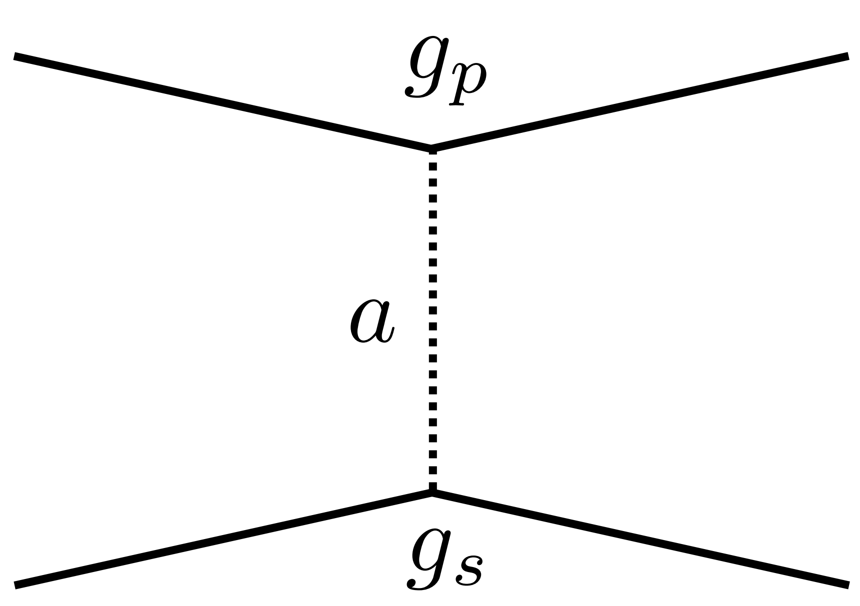

Monopole-dipole
(Spin dependent)

→ Spin-mass forces e.g. ARIADNE/QUAX

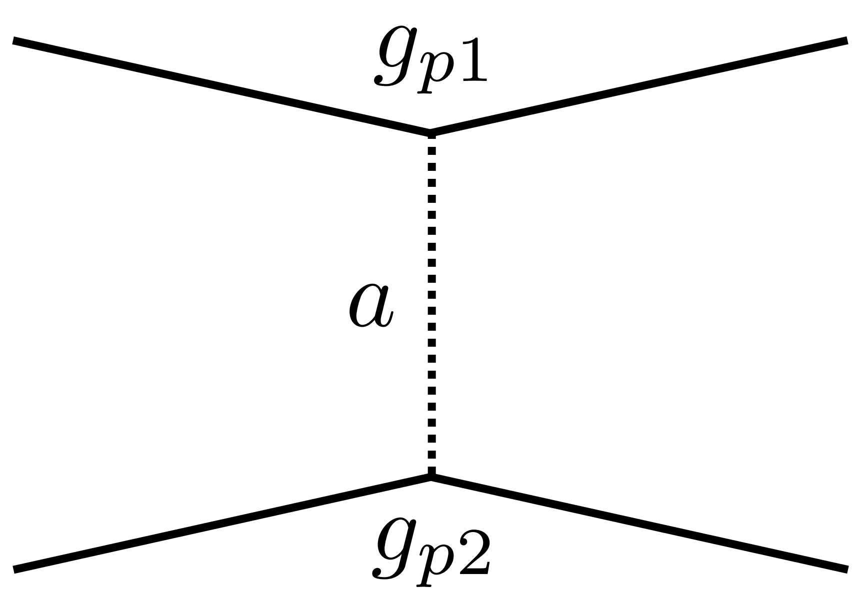

Dipole-dipole
(Spin dependent)

→ Forces between spin-polarised samples

Monopole-dipole searches

Conceptually similar, spin an unpolarised source mass near to a spin-polarised target

ARIADNE

Constrains: $g_p\ g_s$ (nucleon-nucleon)

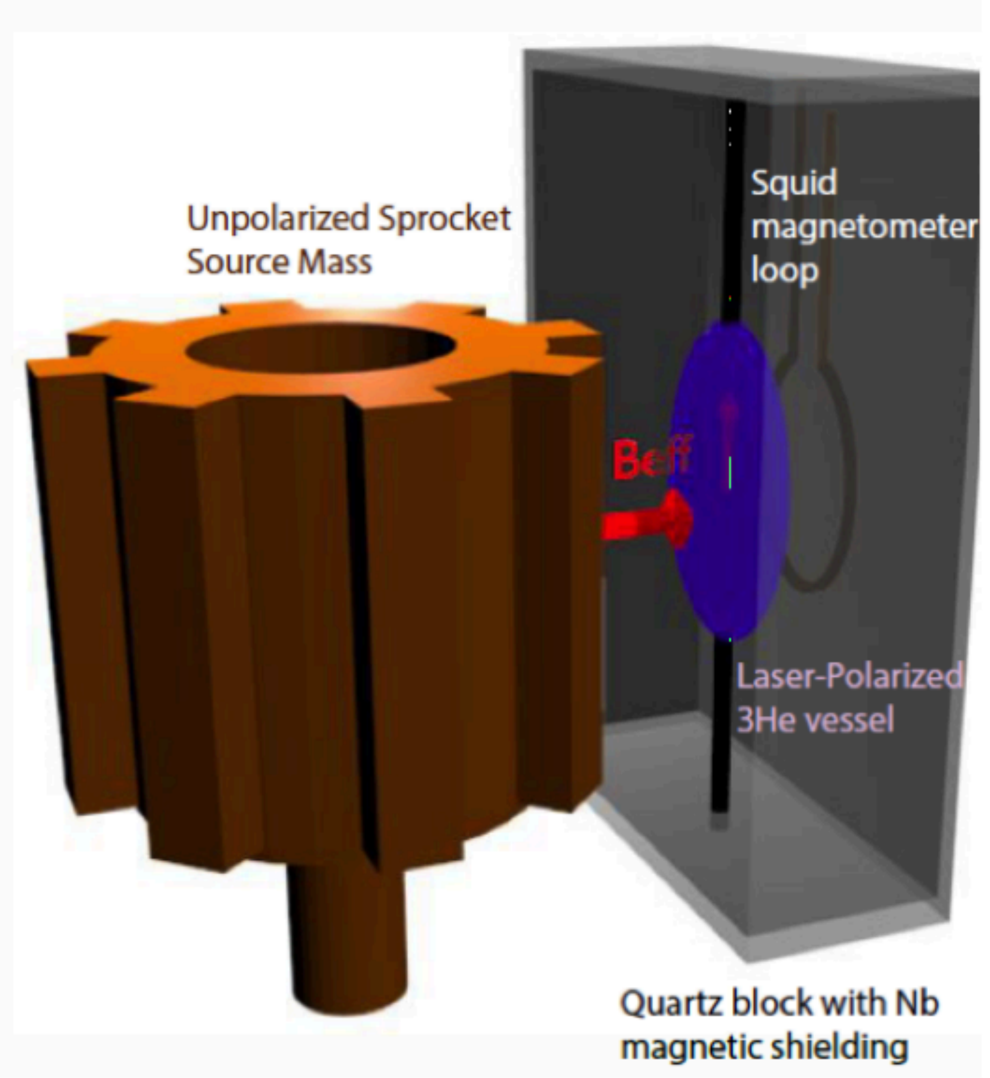

QUAX

Constrains: $g_p\ g_s$ (electron-nucleon)

(Latest QUAX result **2011.07100)**

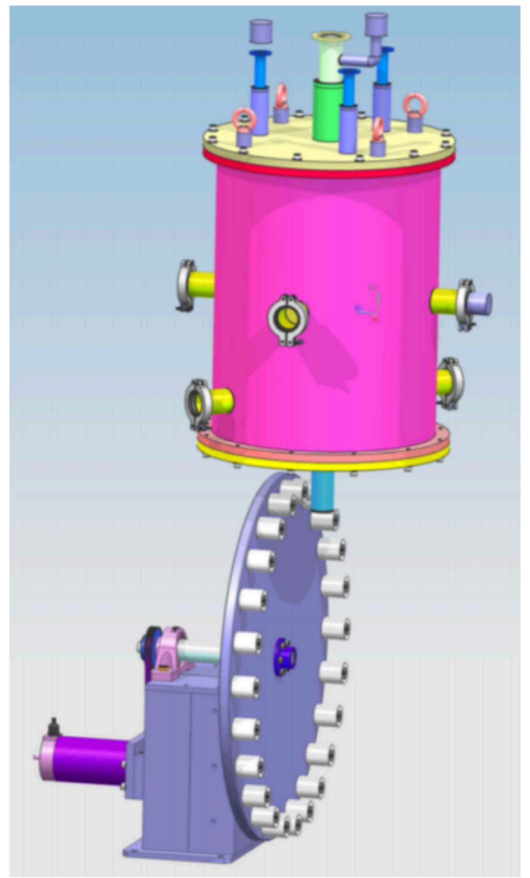

Challenge: stellar bounds tightly constrain g_p, and spin independent fifth force tests easily constrain g_s: so Astro x Lab bound on these coupling combos are very strong

Pure laboratory tests for monopole-dipole axion-mediated forces

Electron-nucleon coupling

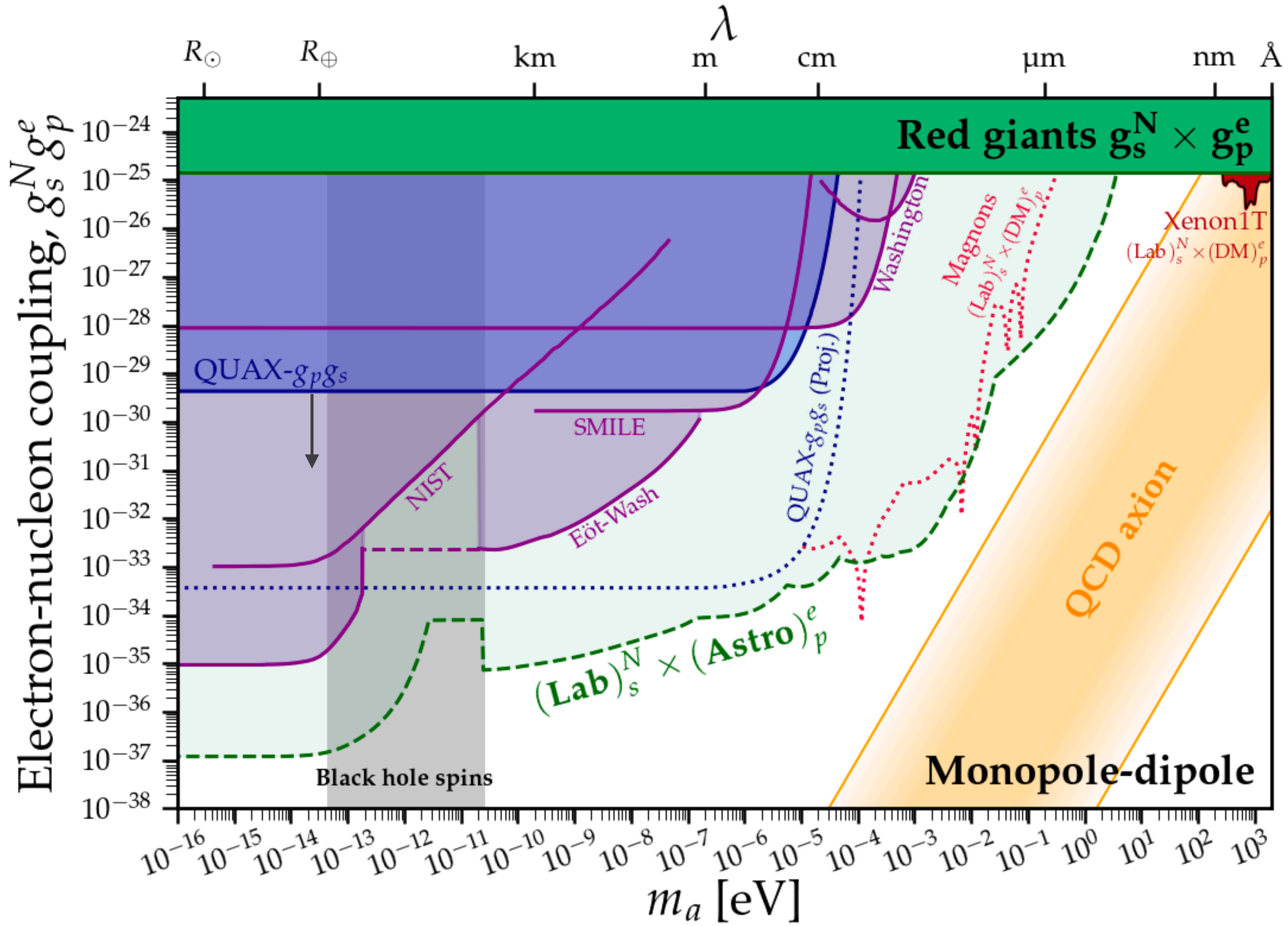

Nucleon-nucleon coupling

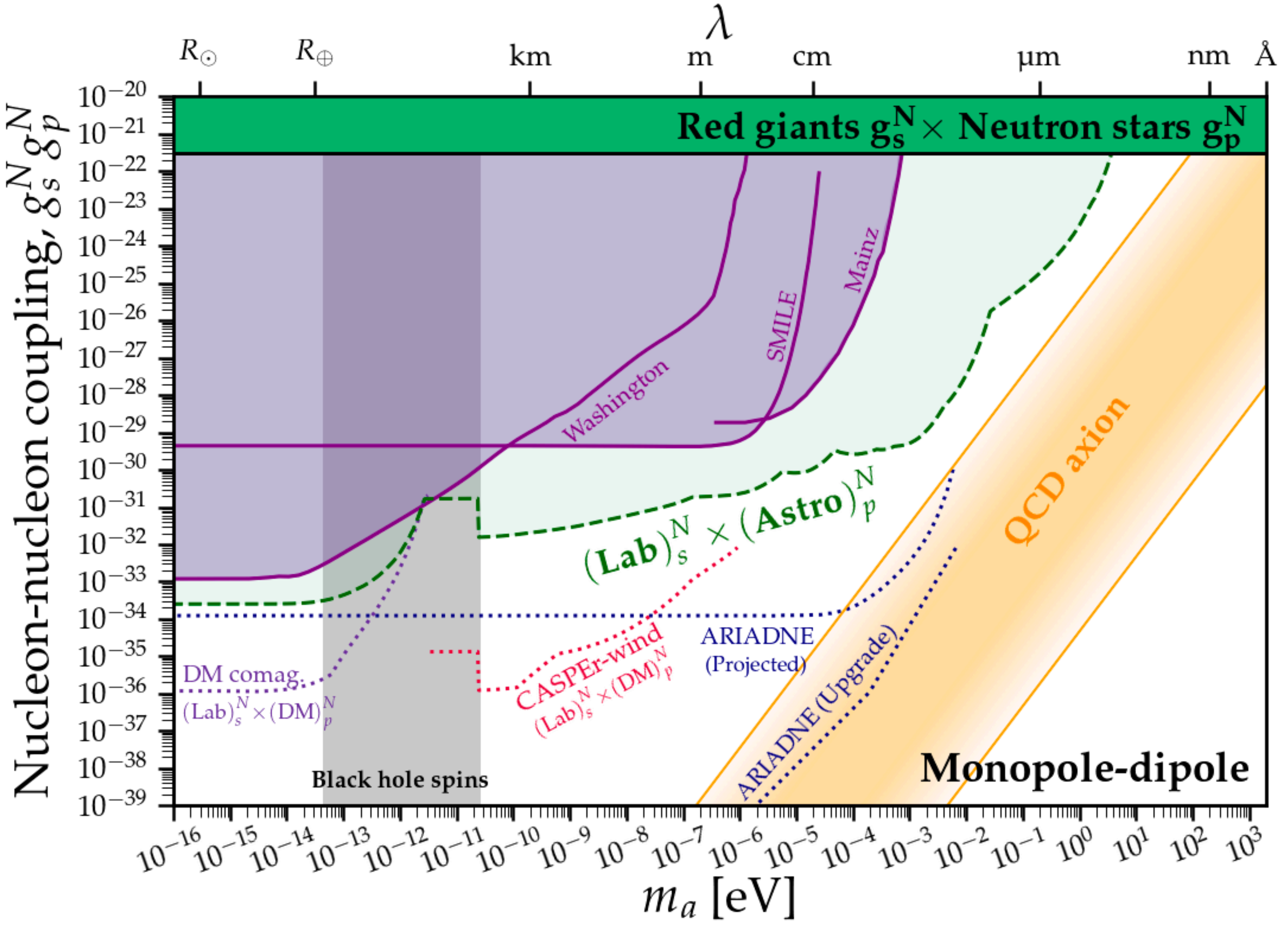

Hard to beat the astrophysical bounds, but **ARIADNE** projects that it will

O'Hare & Vitagliano [2010.03889]

Dark matter axions

behave like a classical field : $a(\mathbf{x}, t) \approx \frac{\sqrt{2\rho_a}}{m_a} \cos(\omega t - \mathbf{p} \cdot \mathbf{x} + \alpha)$

$\omega \approx m_a$

Oscillating at the axion mass

$$F_{\mu\nu} = \partial_\mu A_\nu - \partial_\nu A_\mu$$
$$\widetilde{F}^{\mu\nu} = \frac{1}{2}\epsilon^{\mu\nu\alpha\beta}F_{\alpha\beta}$$
$$\mathbf{E} = -\nabla A_0 - \dot{\mathbf{A}}$$
$$\mathbf{B} = \nabla \times \mathbf{A}$$

Axion electrodynamics

$$\mathcal{L} = -\frac{1}{4}F_{\mu\nu}F^{\mu\nu} - J^\mu A_\mu - \frac{g_{a\gamma}}{4}F_{\mu\nu}\widetilde{F}^{\mu\nu}a$$

- EL equation for photon shows we can interpret axion as the source of an effective current:

$$\partial_\mu F^{\mu\nu} = J^\nu \underbrace{- g_{a\gamma}\widetilde{F}_{\mu\nu}\partial_\mu a}$$

$$J_a^\mu = g_{a\gamma}(-\mathbf{B}\cdot\nabla a,\ -\mathbf{E}\times\nabla a + \partial_t a\mathbf{B})$$

- Rewrite Maxwell's equations with $J \to J + J_a$:

$$\nabla\cdot\mathbf{E} = \rho$$
$$\nabla\cdot\mathbf{B} = 0$$
$$\nabla\times\mathbf{E} = -\frac{\partial\mathbf{B}}{\partial t}$$
$$\nabla\times\mathbf{B} = \frac{\partial\mathbf{E}}{\partial t} + \mathbf{J}$$

Ampere's law

$$\nabla \times \mathbf{B} = \frac{\partial \mathbf{E}}{\partial t} + \cancel{\mathbf{J}} - g_{a\gamma}\left(\cancel{\mathbf{E} \times \nabla a} - \frac{\partial a}{\partial t}\mathbf{B}\right)$$

Usually not important unless experiment larger than

$\lambda_{dB} \sim (\nabla a)^{-1} \sim (m_a \mathbf{v})^{-1} \sim 10^3 \lambda_c$

(Most experiments are actually around $\lambda_c \sim 1/m_a$ or smaller)

Ampere's law

$$\nabla \times \mathbf{B} = \frac{\partial \mathbf{E}}{\partial t} + g_{a\gamma} \frac{\partial a}{\partial t} \mathbf{B}$$

Axion-induced magnetic field

Axion-induced electric field

Oscillating axion field

What kind of experiment do we need to measure this?

→ Depends on size of Compton wavelength ($1/m_a$) relative to the size of some instrument, say $\mathcal{O}$(metres)

Haloscope strategies

<μeV: Compton wavelength long relative to experiment. DC magnetic field induces oscillating magnetic field

$$\nabla \times \mathbf{B}_a = \frac{\partial \mathbf{E}_a}{\partial t} - g_{a\gamma}\mathbf{B}_0 \frac{\partial a}{\partial t}$$

~1-100 μeV: Compton wavelength similar scale to experiment. Axion sources oscillating E&M-fields → couple to an EM mode inside a cavity

$$\nabla \times \mathbf{B}_a = \frac{\partial \mathbf{E}_a}{\partial t} - g_{a\gamma}\mathbf{B}_0 \frac{\partial a}{\partial t}$$

$\gtrsim$ 100 μeV: Compton wavelength short relative to experiment. Axion generates radiation → arrange experiment to have constructive interference

$$\nabla \times \mathbf{B}_a = \frac{\partial \mathbf{E}_a}{\partial t} - g_{a\gamma}\mathbf{B}_0 \frac{\partial a}{\partial t}$$

$$\nabla \times \mathbf{B}_a = \frac{\partial \mathbf{E}_a}{\partial t} - g_{a\gamma}\mathbf{B}_0 \frac{\partial a}{\partial t}$$

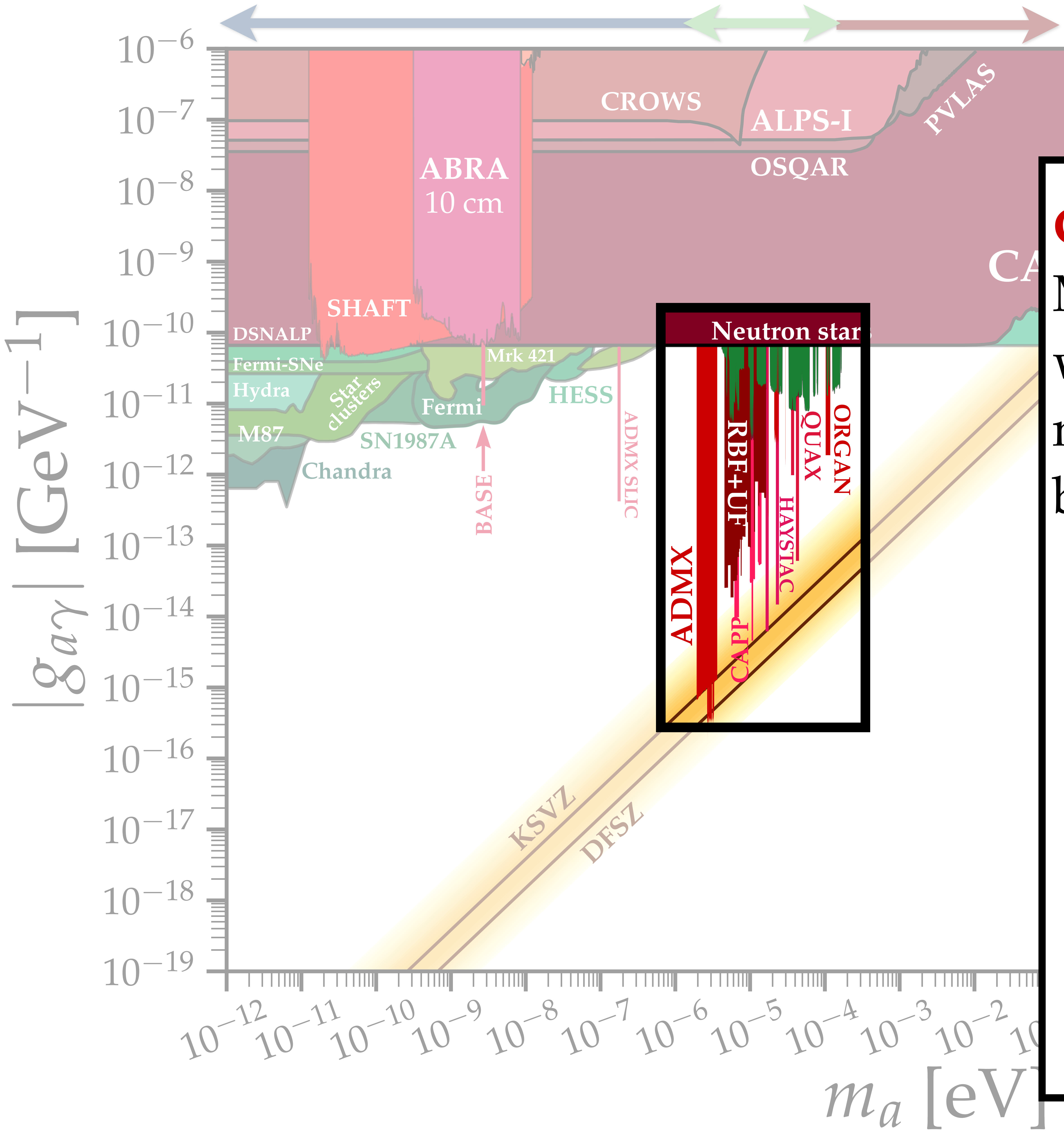

Cavity haloscopes

Most well-developed technique. High-Q cavity with modes that couple to the axion giving strong narrow-band signal, a range of axion masses can be scanned using tuning rods

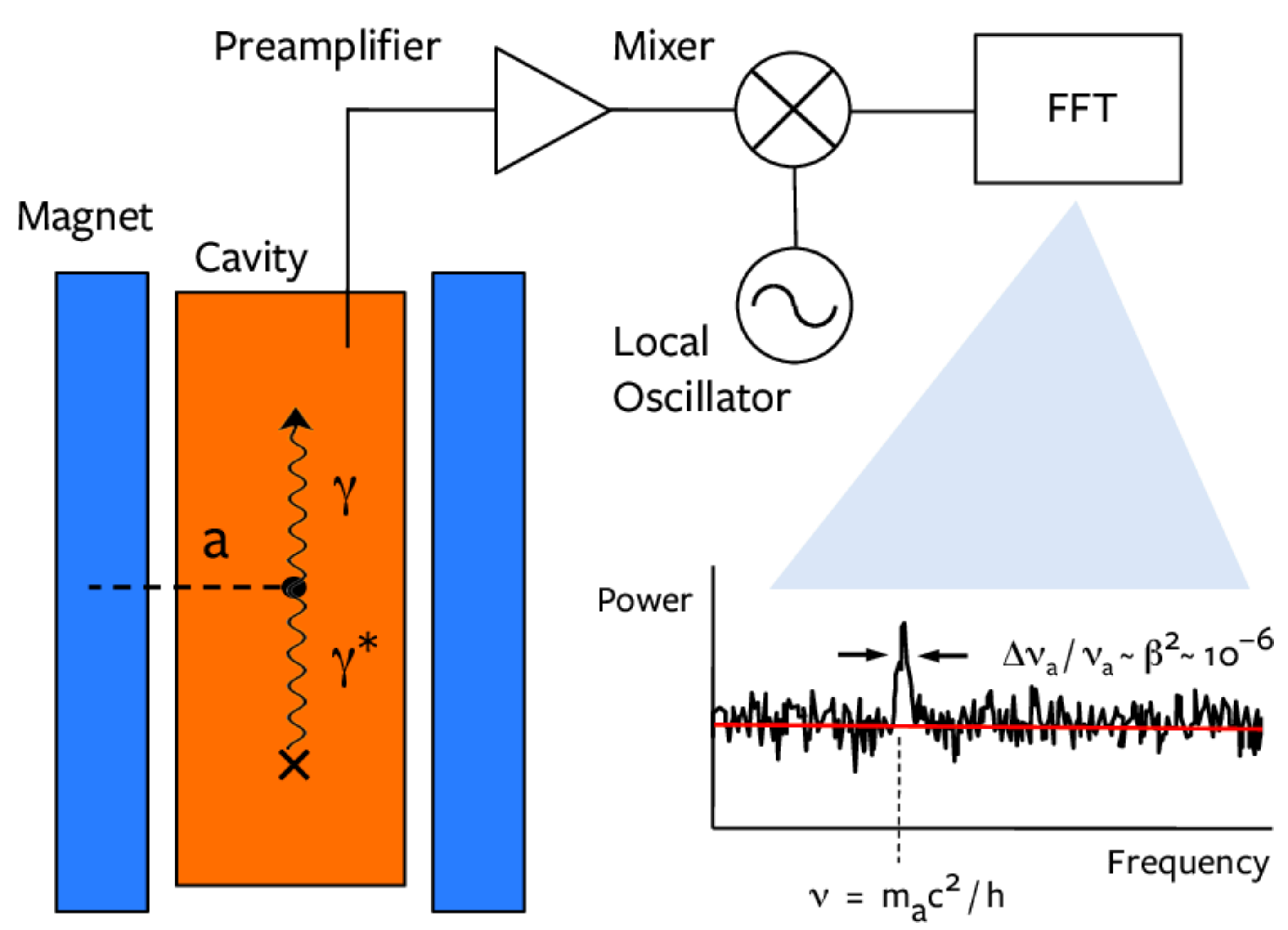

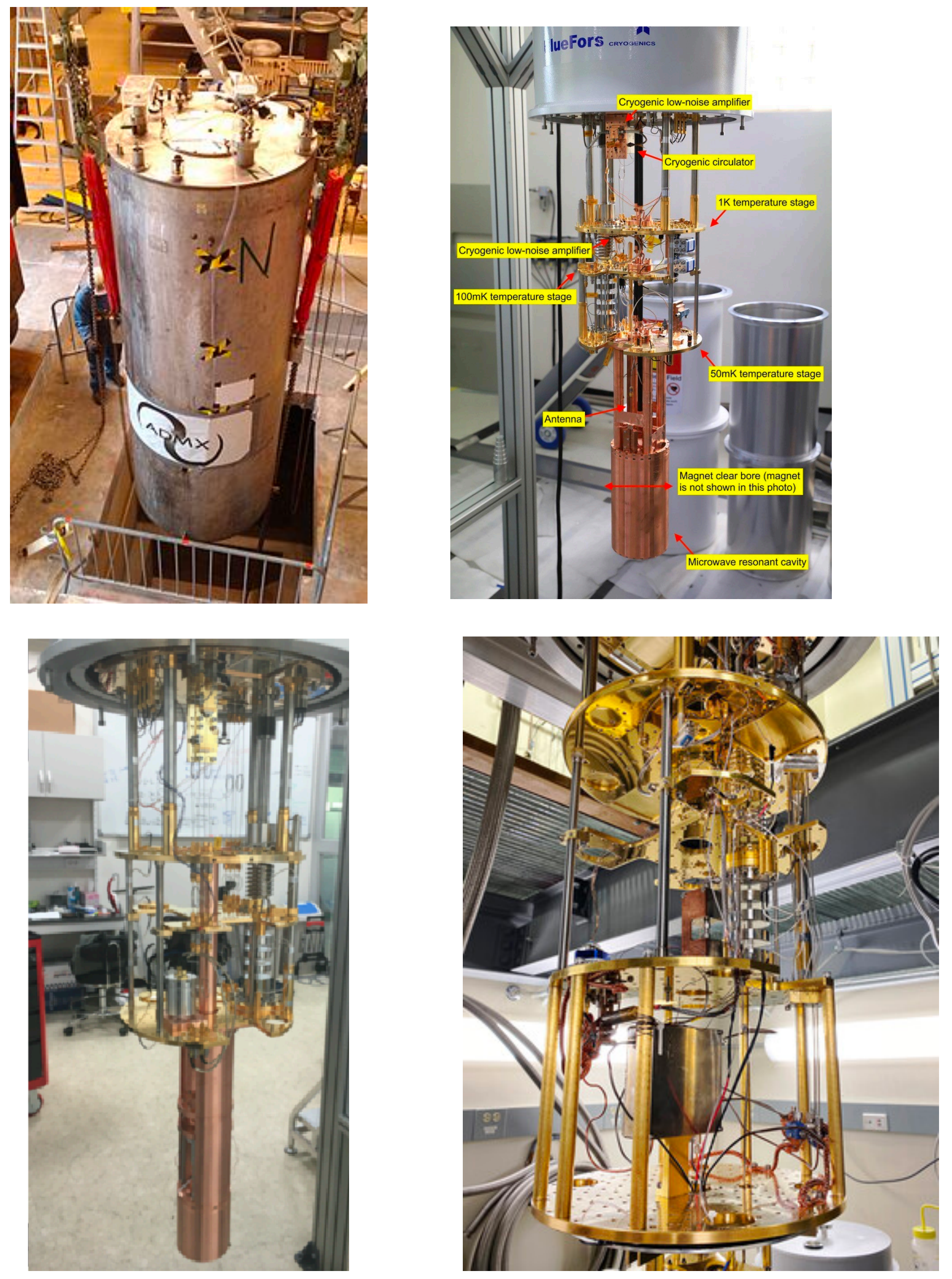

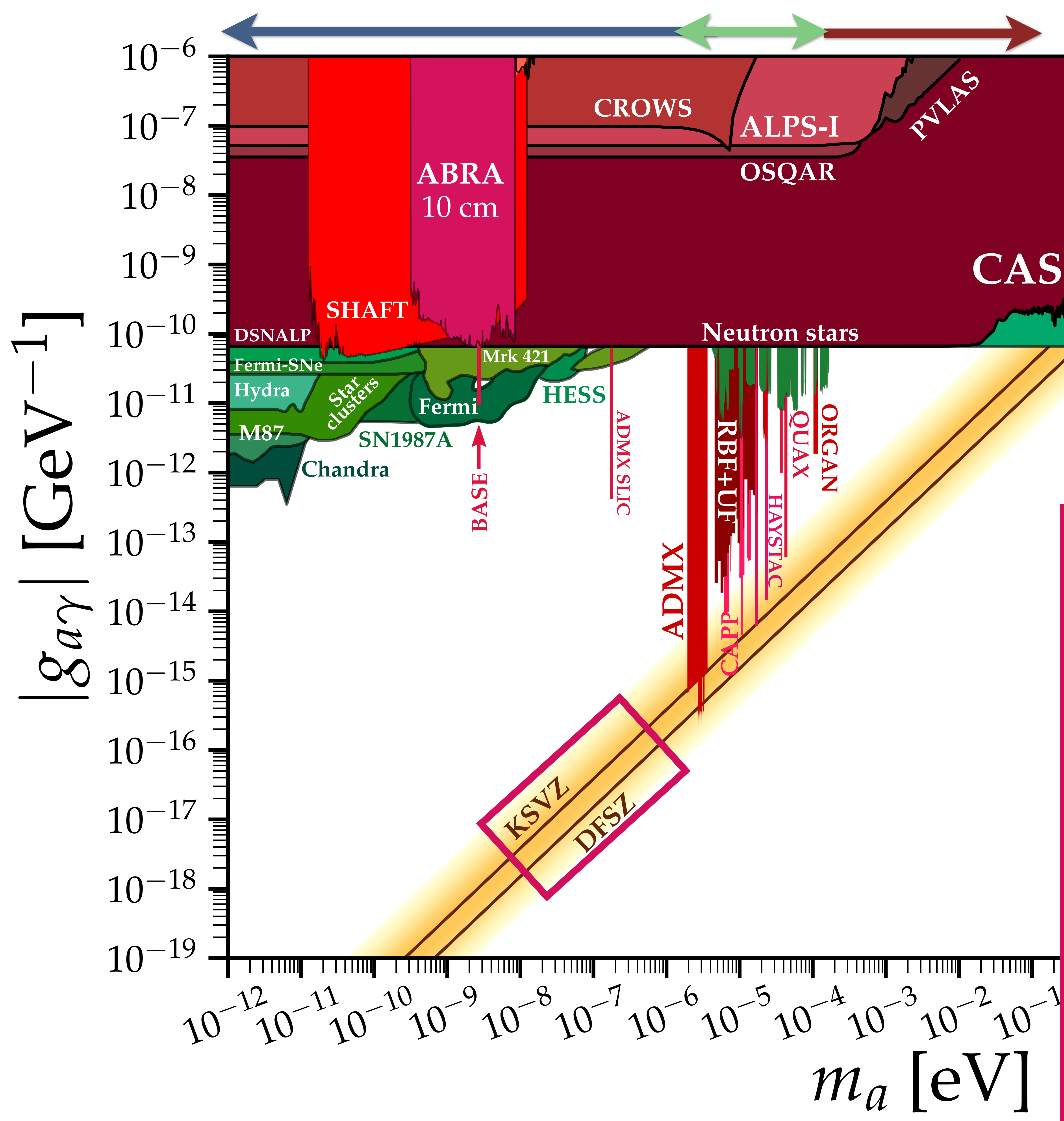

$$\nabla \times \mathbf{B}_a = \frac{\partial \mathbf{E}_a}{\partial t} - g_{a\gamma}\mathbf{B}_0 \frac{\partial a}{\partial t}$$

ABRACADABRA/DMRadio [2102.06722]

→ essentially an LC-circuit. Axion effective current sources a B-field inside a pickup loop. Broadband and resonant capabilities

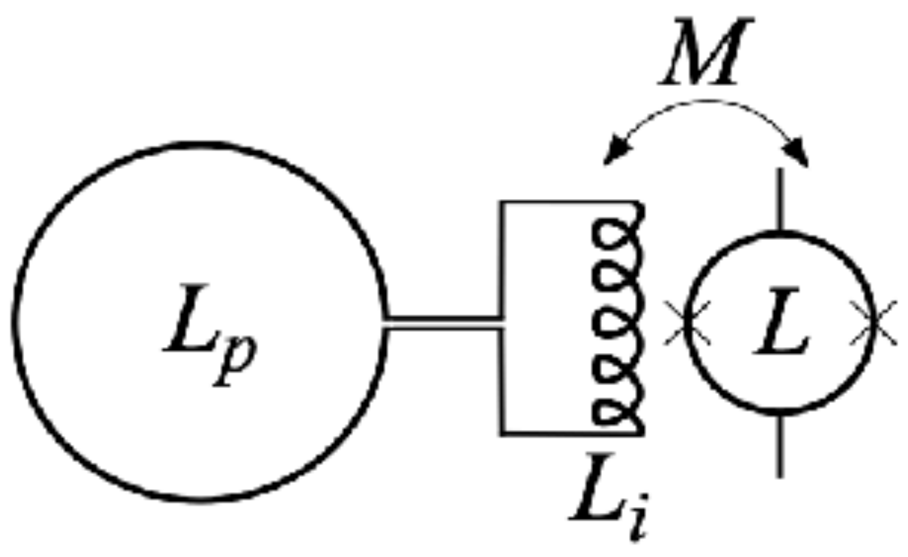

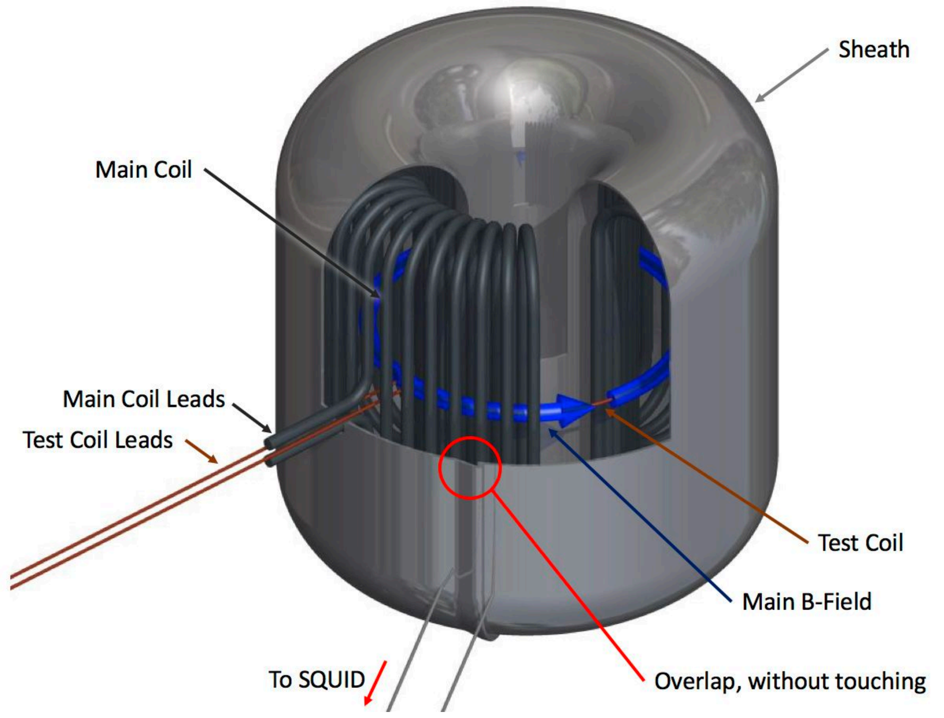

$$\nabla \times \mathbf{B}_a = \frac{\partial \mathbf{E}_a}{\partial t} - g_{a\gamma}\mathbf{B}_0\frac{\partial a}{\partial t}$$

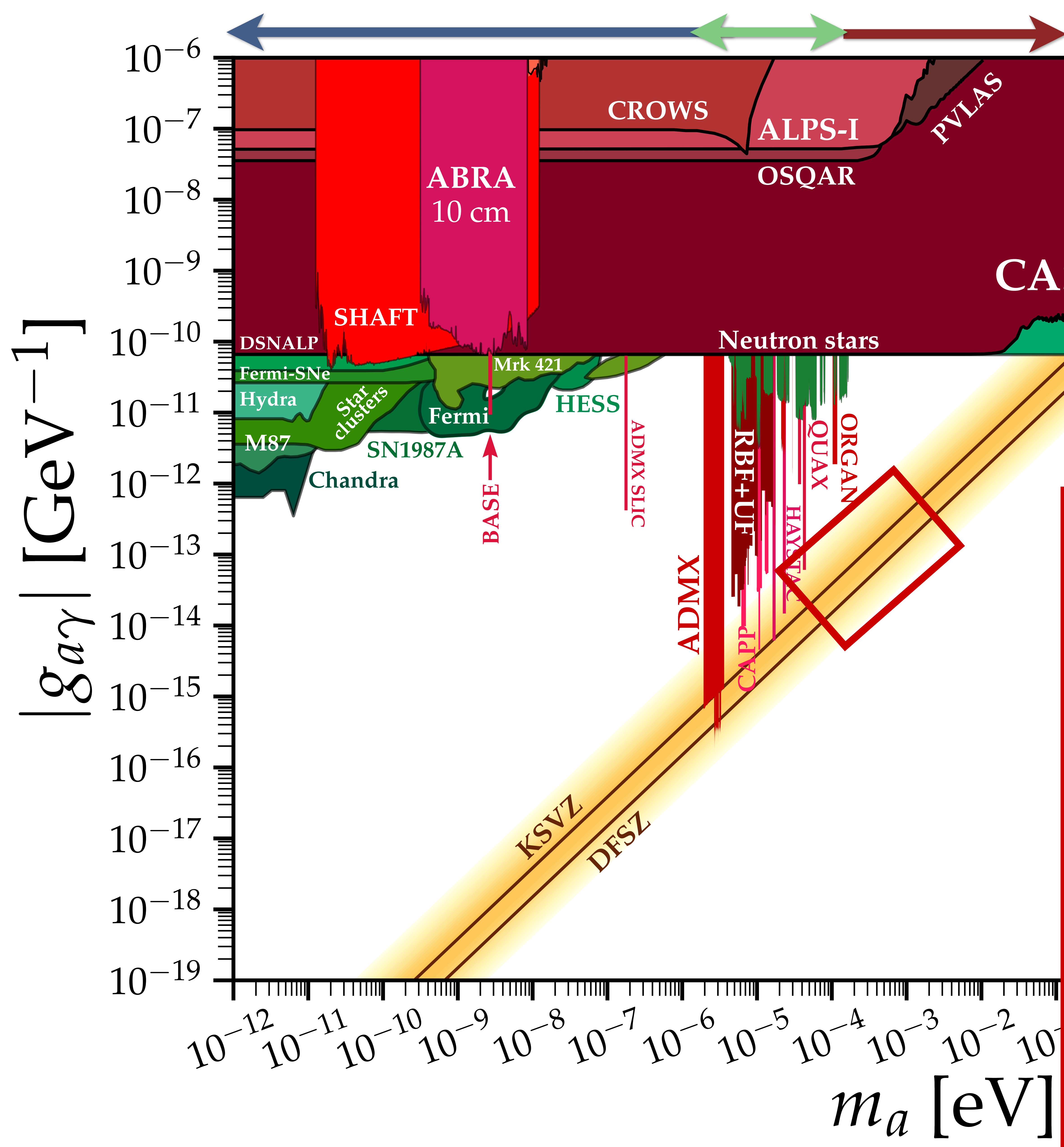

MADMAX "Dielectric haloscope" [2003.10894]

Constructively add axion-induced radiation emitted by a series of dielectric surfaces.

Tuneable via disk-spacing

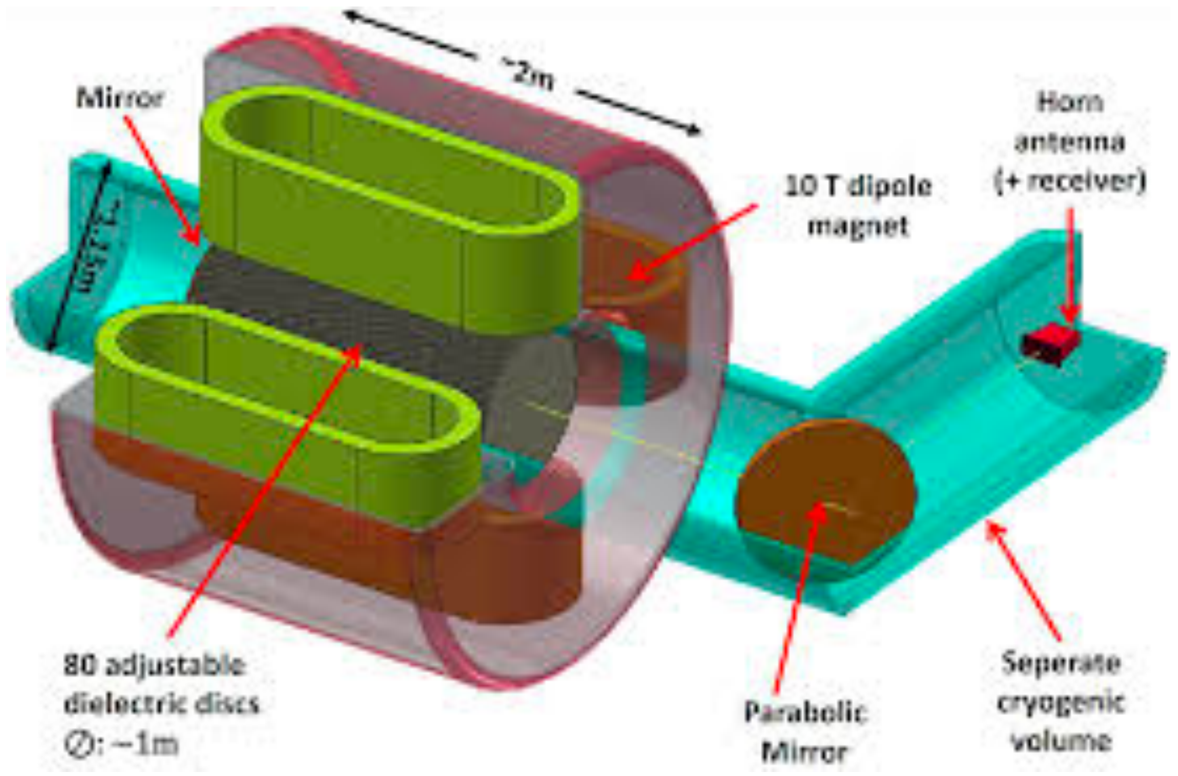

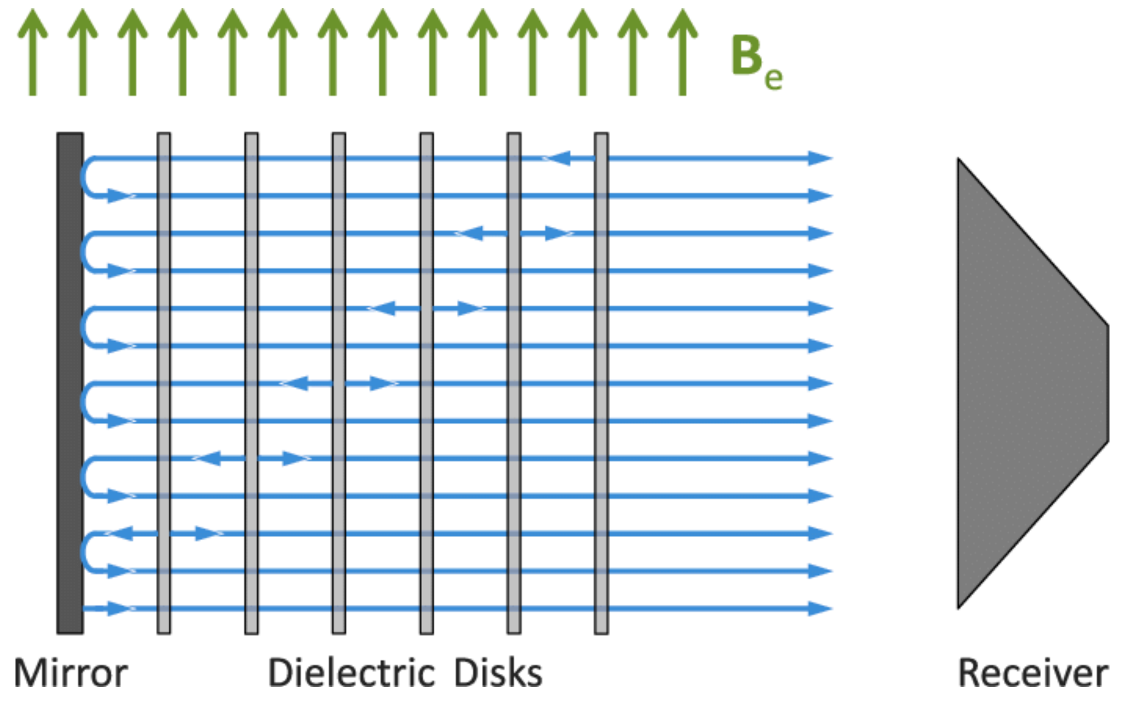

But there's a complication: what about $\nabla\theta$?

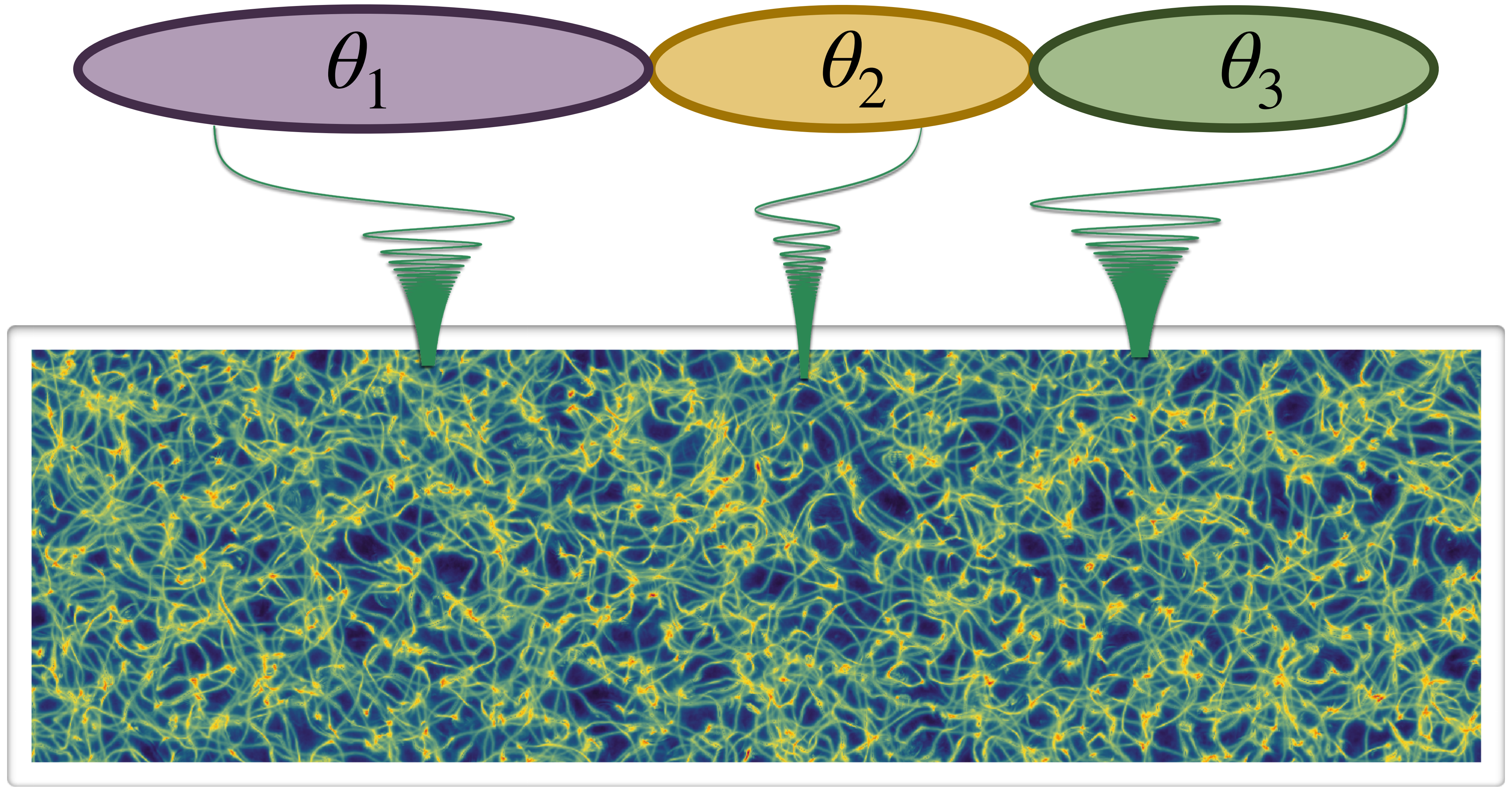

Different causal patches take on different initial angles
→ Field gradients!

$$\ddot{\theta} + 3H\dot{\theta} \boxed{- \frac{1}{R^2}\nabla^2\theta} + m_a^2\theta = 0$$

⇒ <u>**Cosmic strings**</u> from axion field winding around 2π

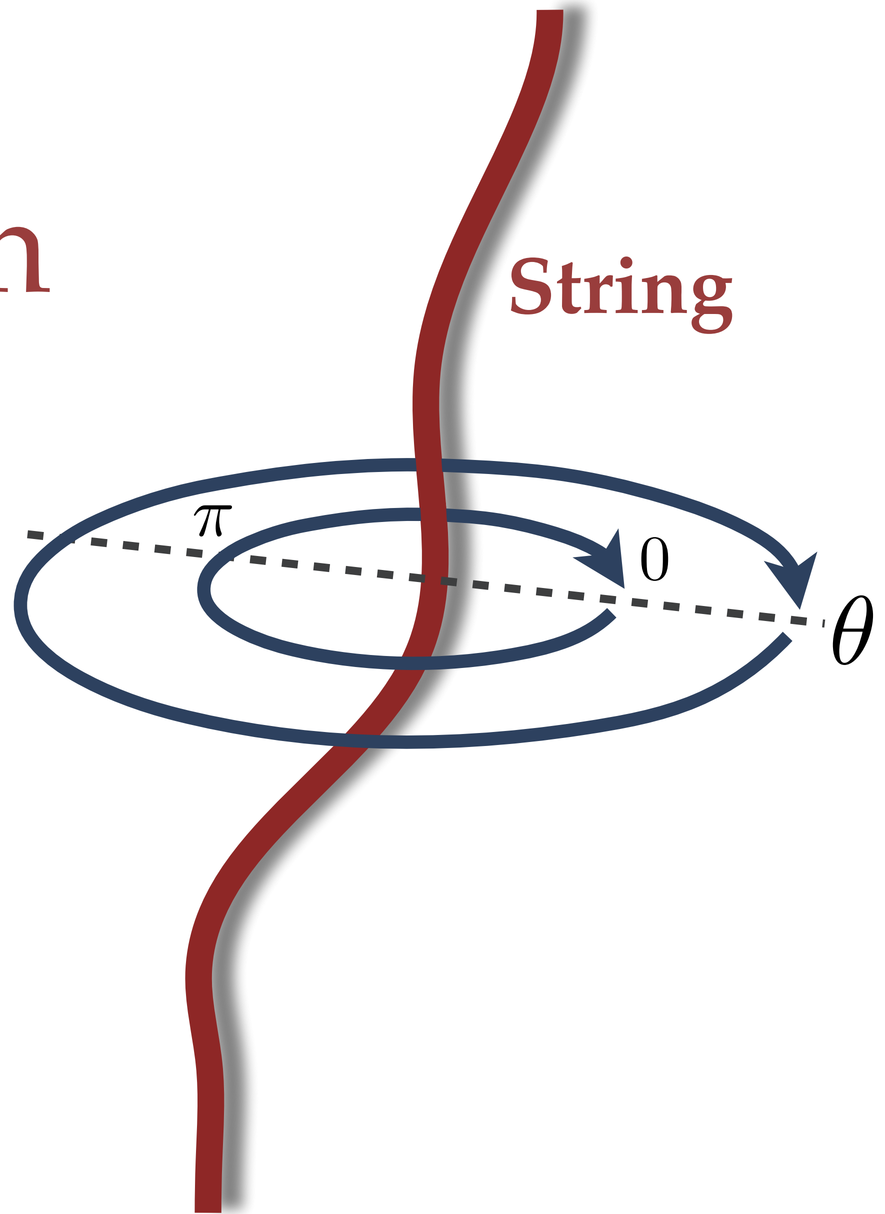

⇒ <u>**Domain walls**</u> between true/false vacuum (0 and π)

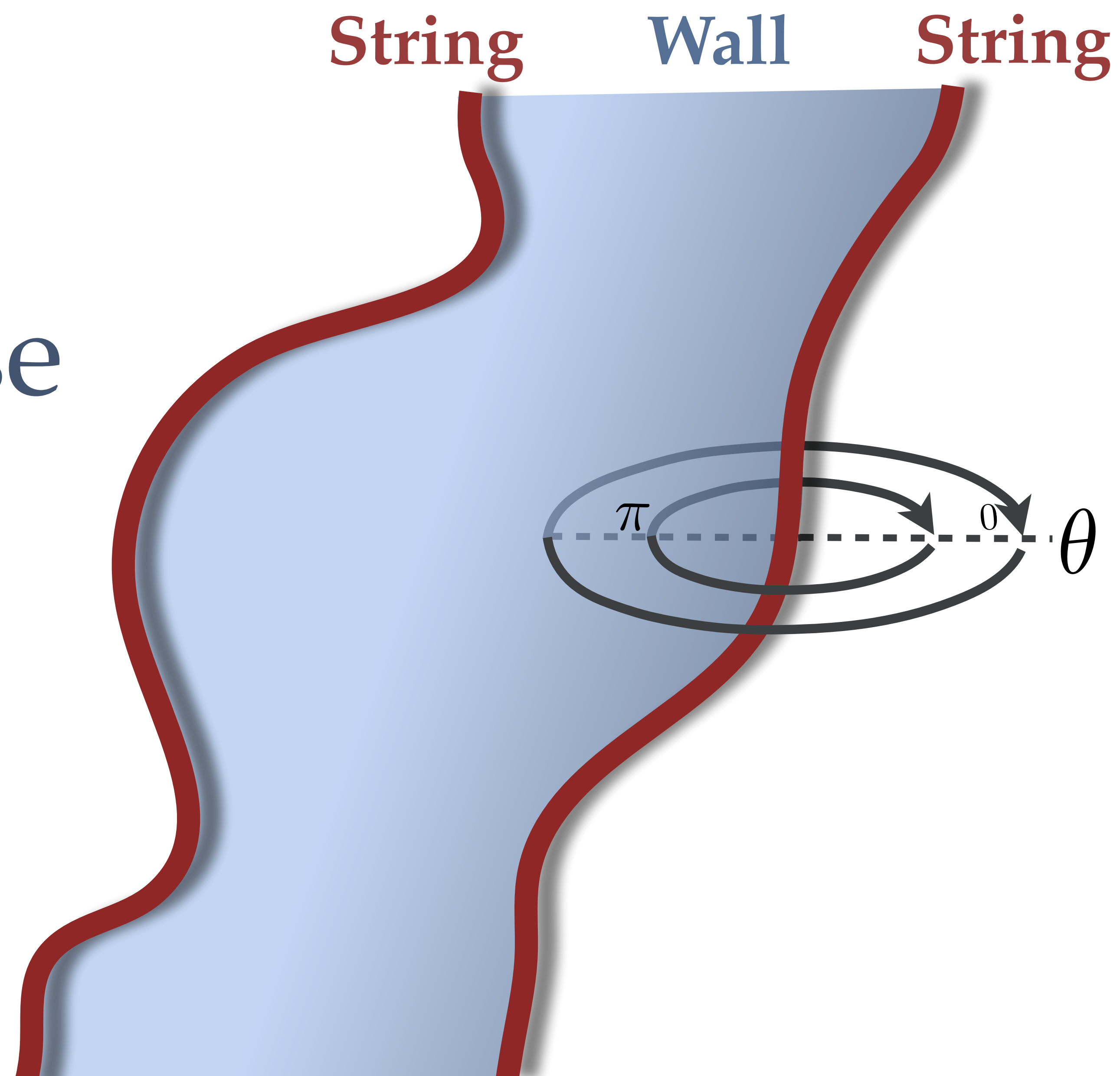

What do we need to do?
→ simulate

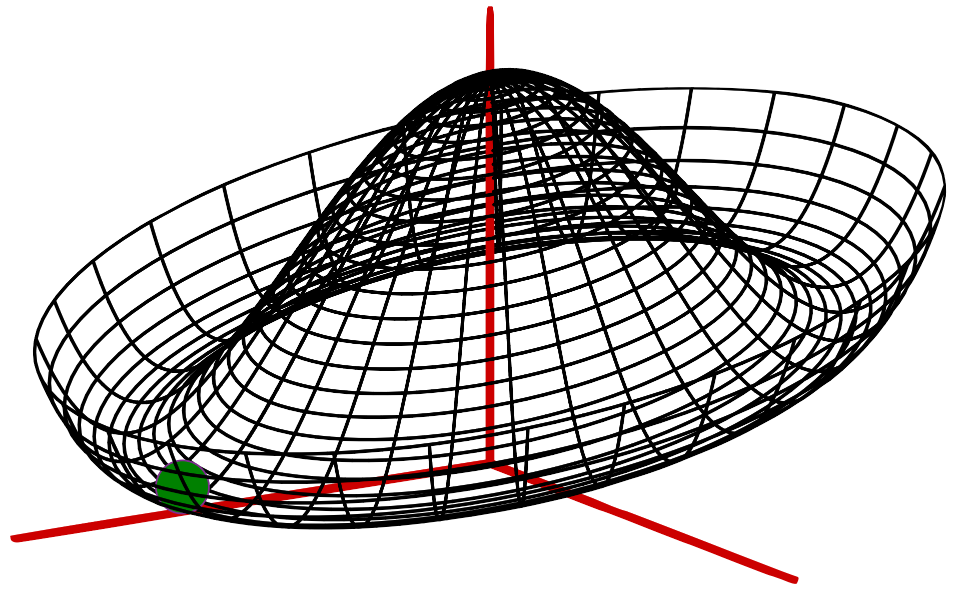

Evolve the axion field…

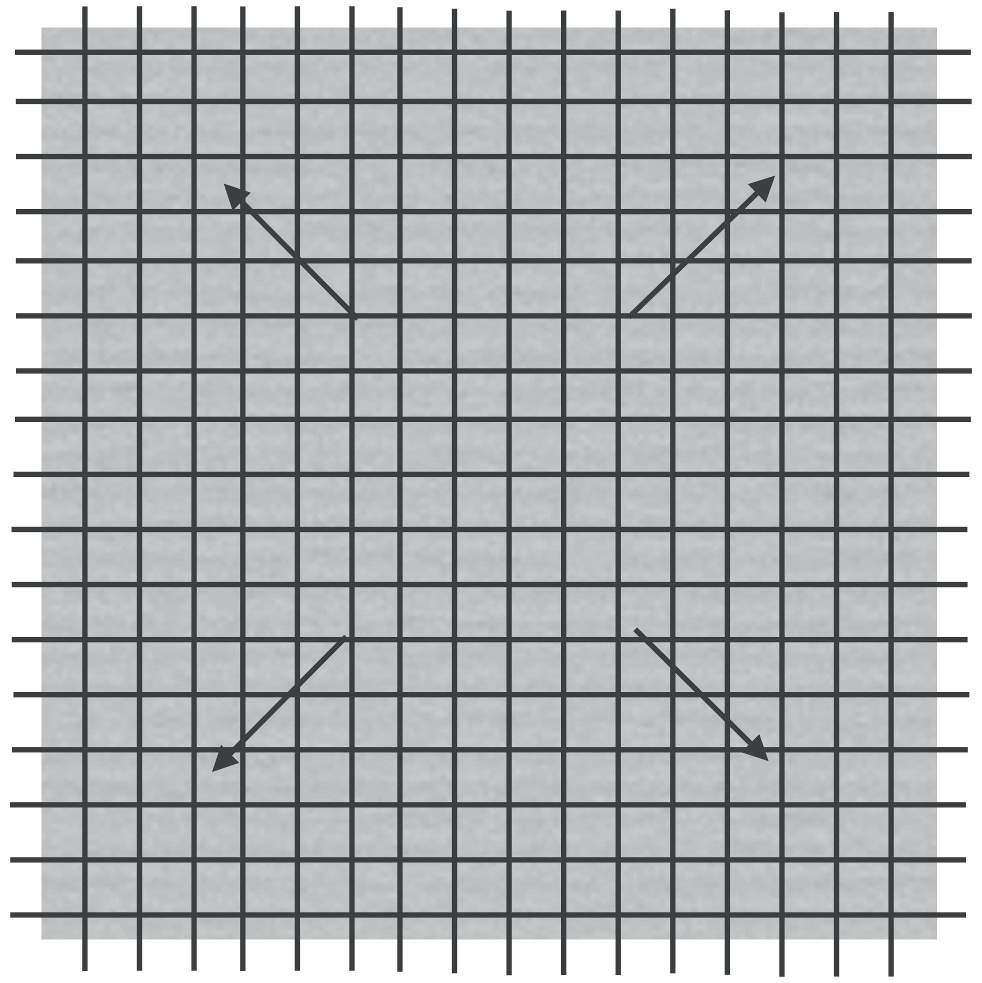

…on an expanding lattice…

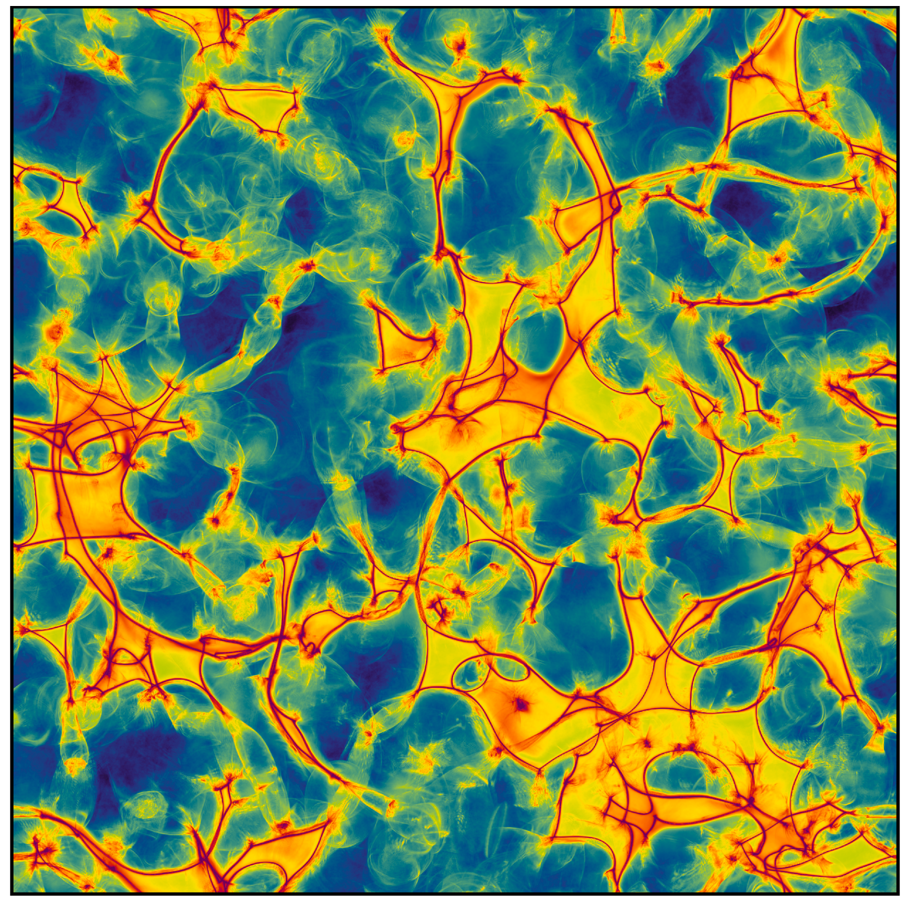

…to measure the relic abundance of axions…

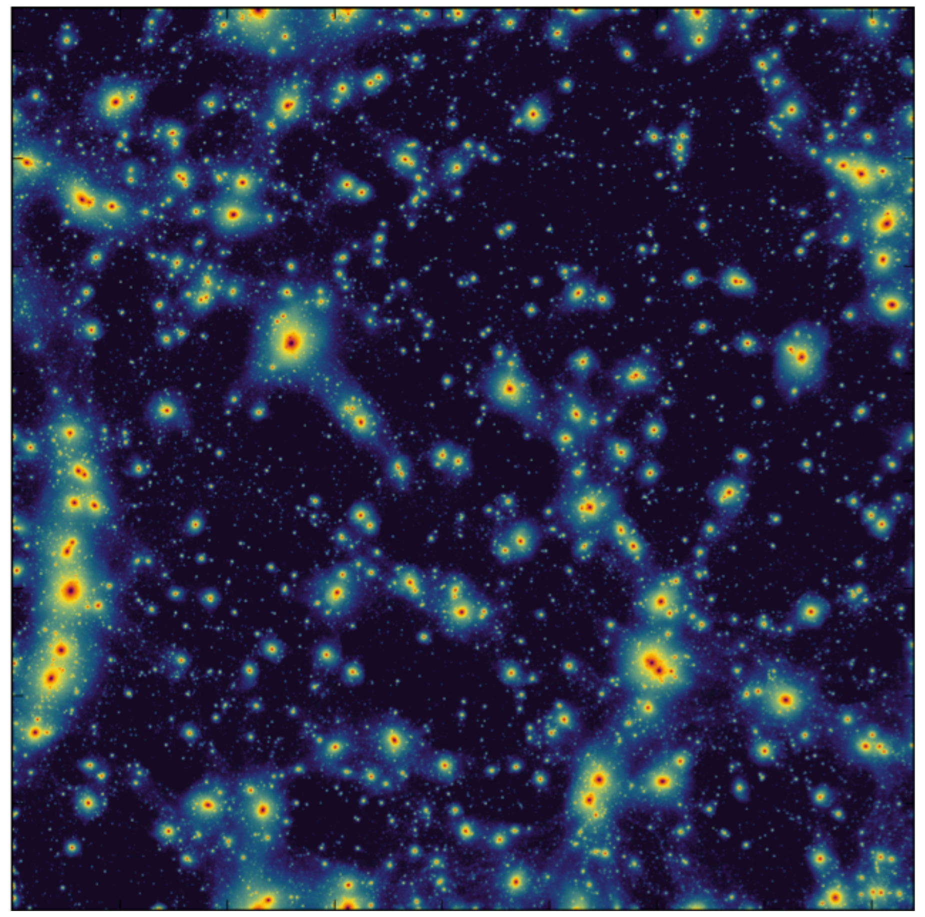

…and predict its present day distribution

The axion potential

$$V(\phi) = \frac{\lambda_\phi}{8}\left(|\phi|^2 - f_a^2\right)^2 + \chi(T)(1 - \cos\arg\phi)$$

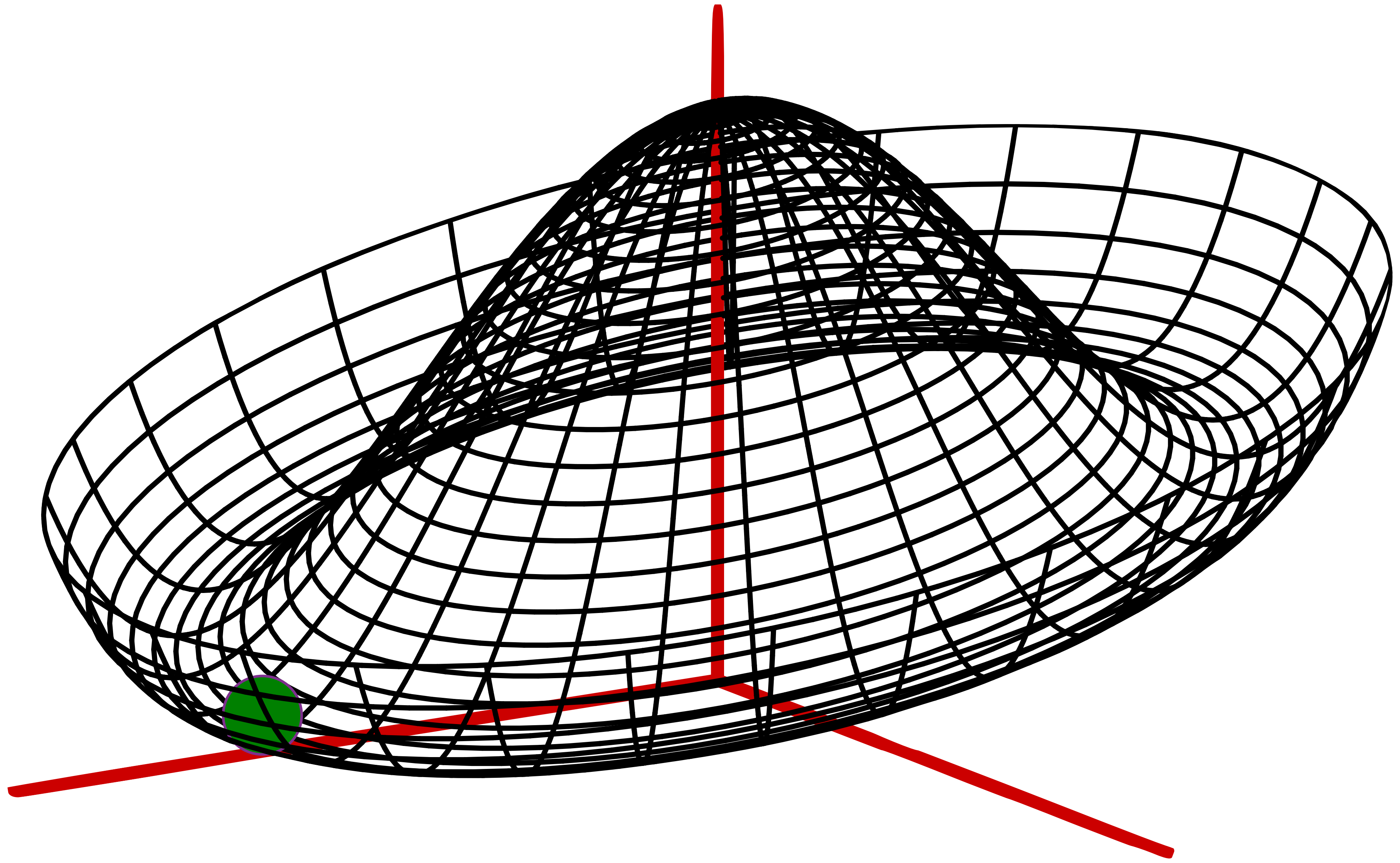

$$\phi(\mathbf{x}) \sim |\phi(\mathbf{x})| e^{i\theta(\mathbf{x})}$$

Wine bottle

Governs

$$|\phi(\mathbf{x})|$$

Radial dof: "saxion"

Sets string width

Tilt

Governs

$$\theta(\mathbf{x}) = a(\mathbf{x})/f_a$$

Angular dof: "axion"

Sets domain wall width

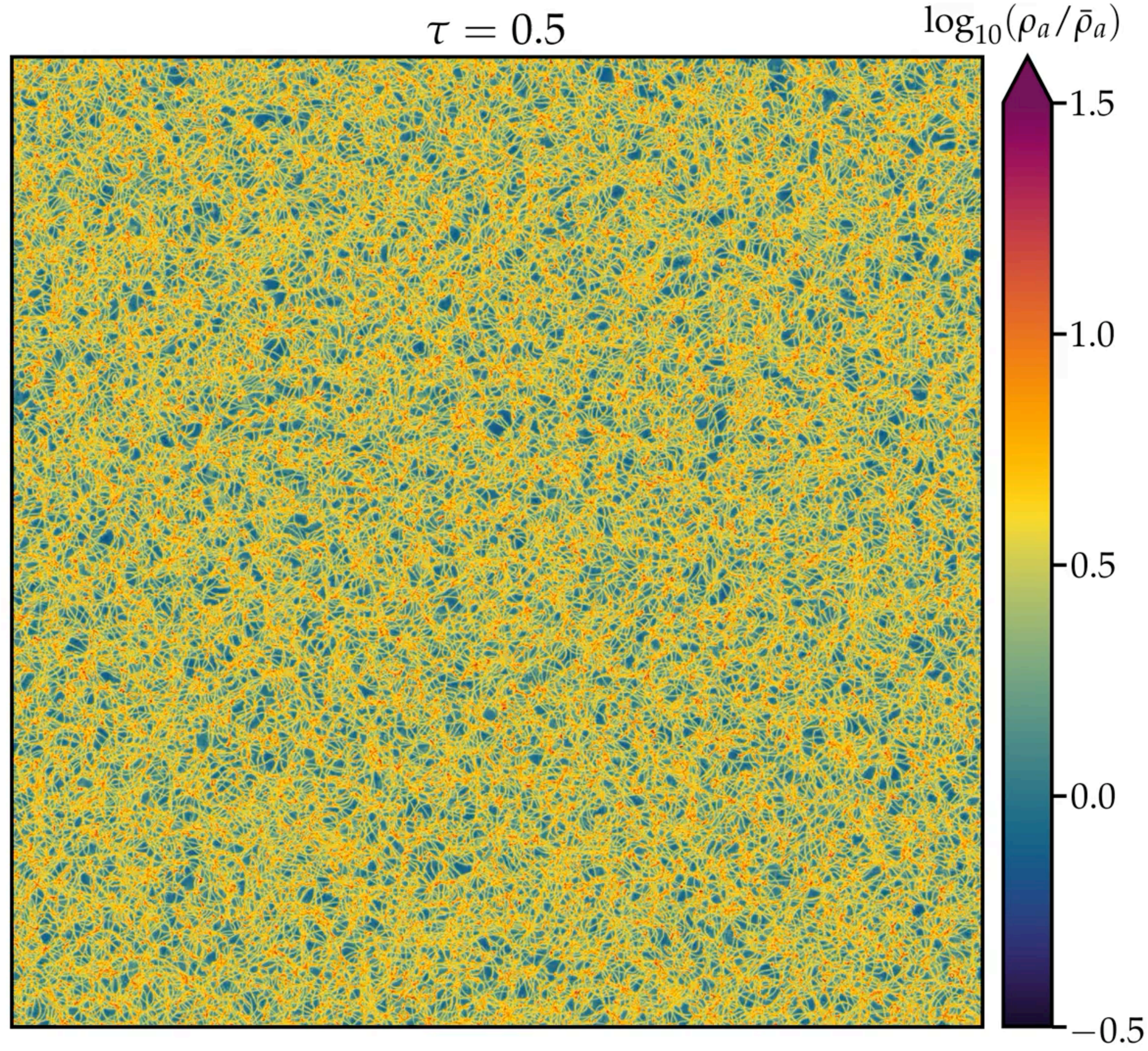

$\tau = 0.5$
$\log_{10}(\rho_a/\bar{\rho}_a)$
1.5
1.0
0.5
0.0
−0.5

Evolution of the axion field in the post-inflationary scenario

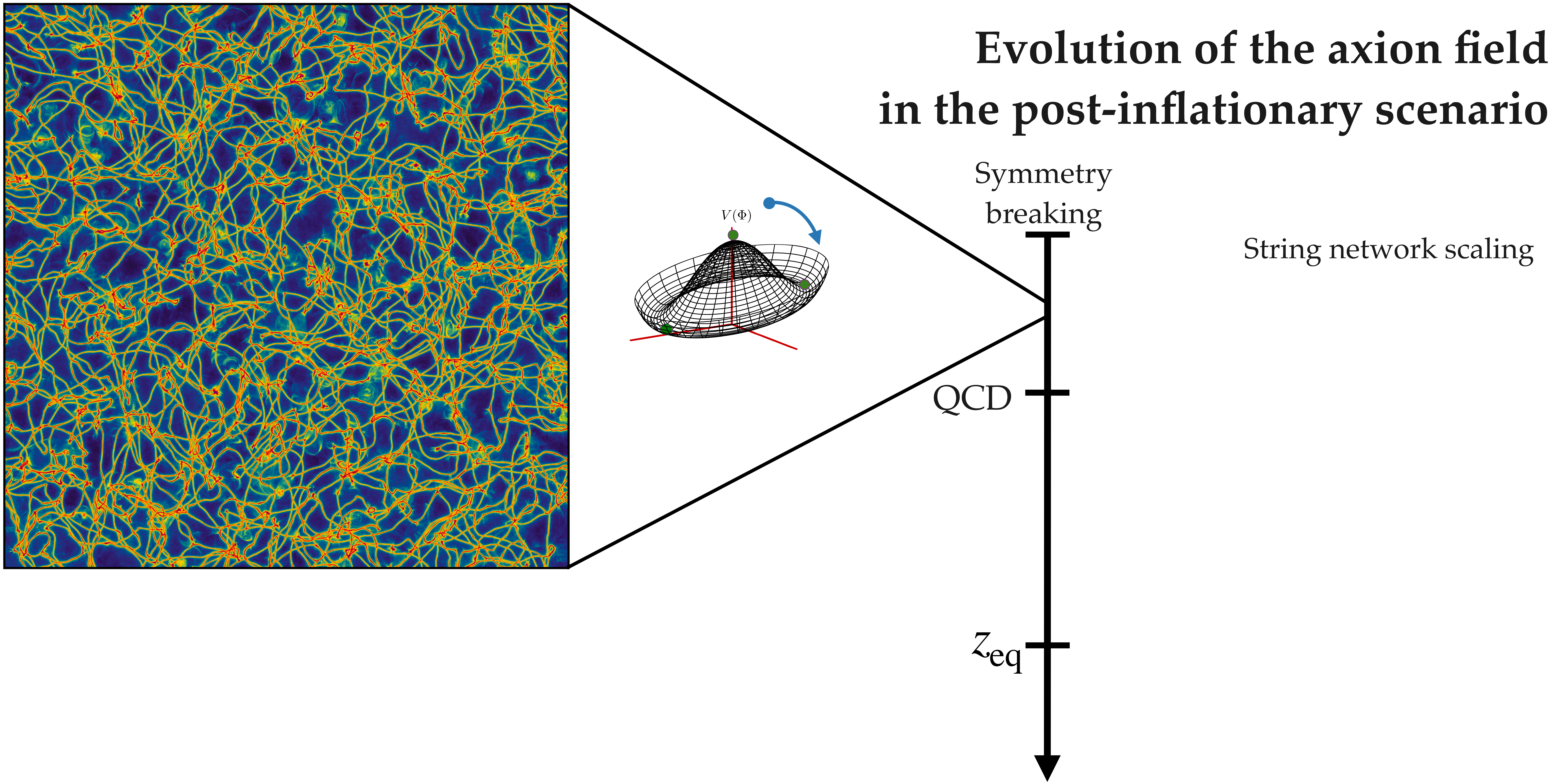

Evolution of the axion field in the post-inflationary scenario

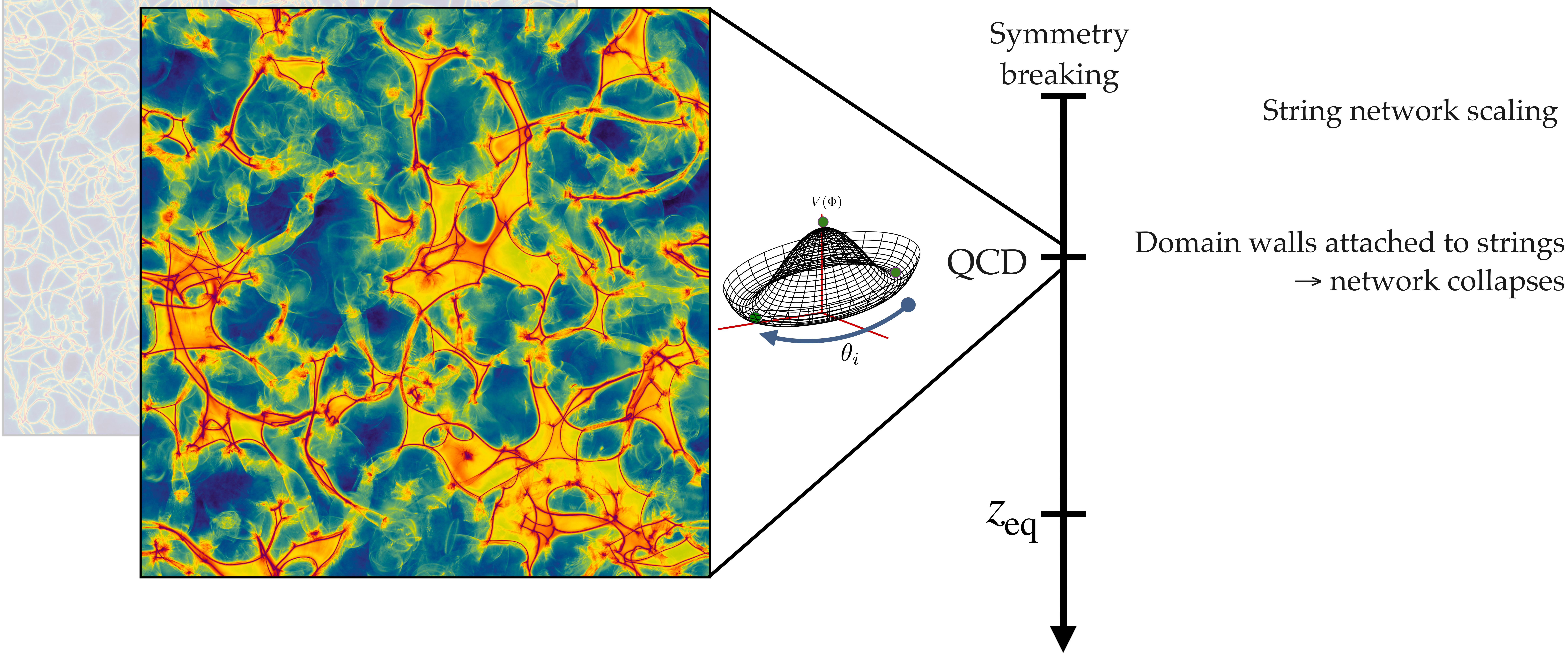

Evolution of the axion field in the post-inflationary scenario

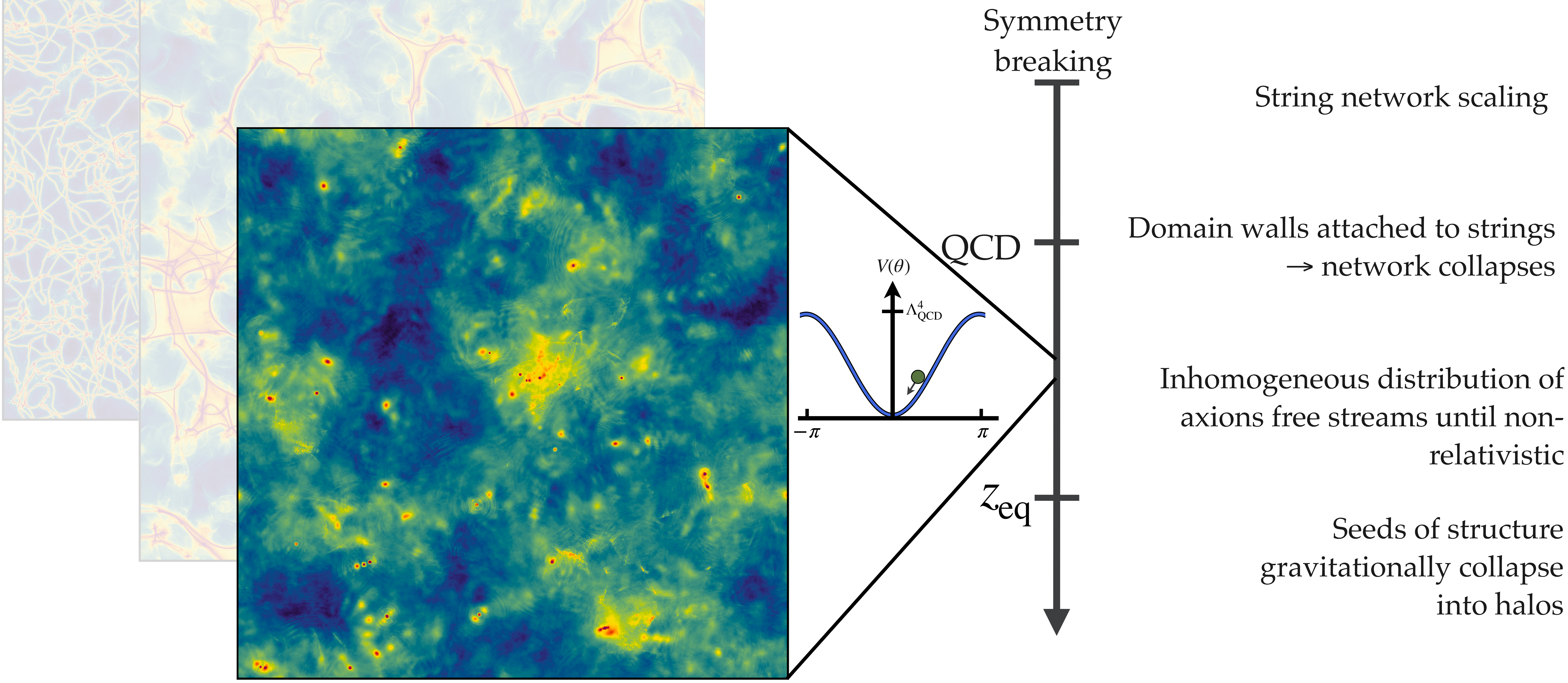

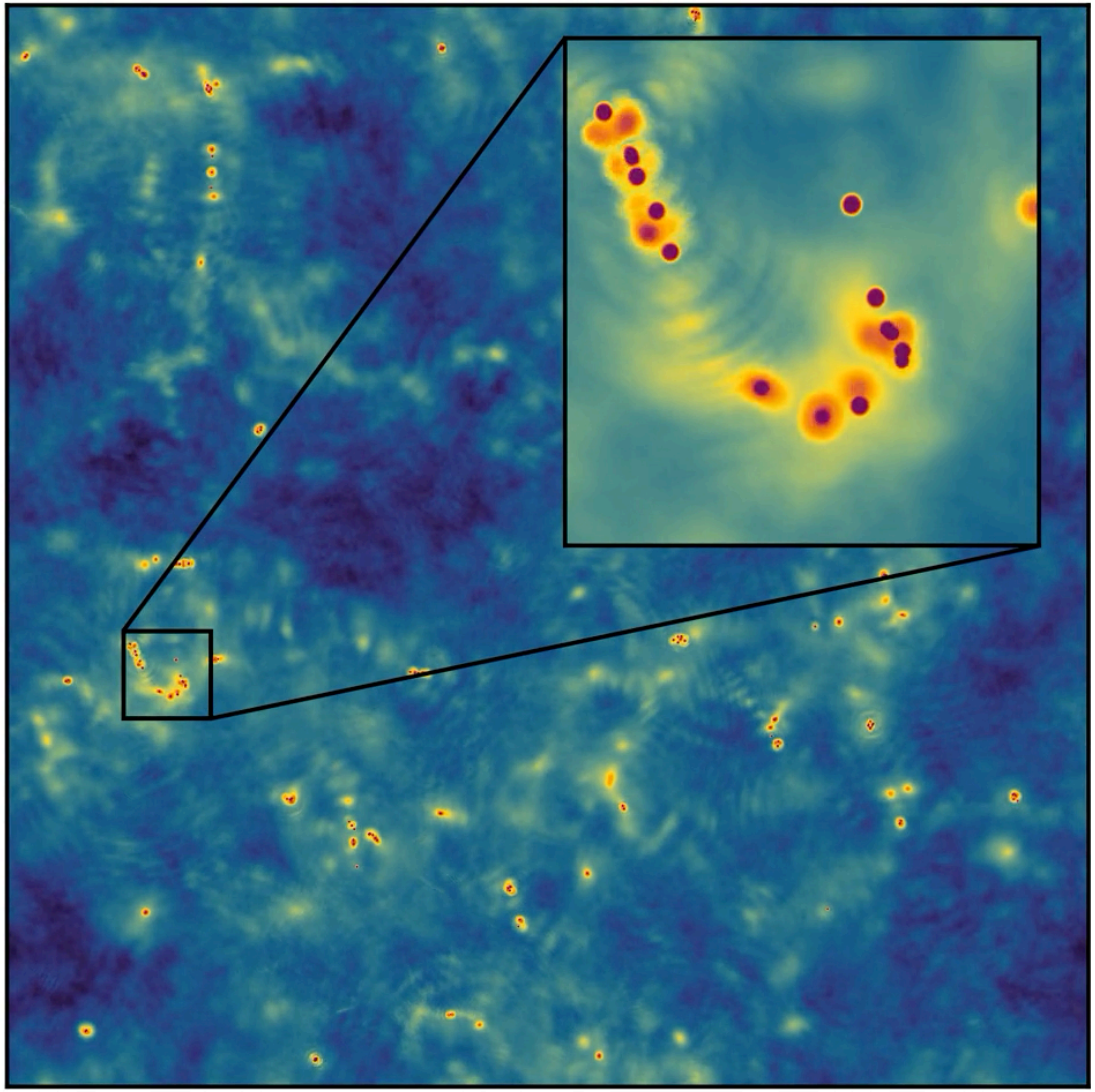

Large numbers of high-density oscillating lumps are seeded towards the end of the simulation

"Axitons"

Axitons (aka oscillons)

- Quasi-stable solutions of the Sine-Gordon equation with a growing mass $m_a^2(T) \propto T^{-n}$
- Can also be thought of as the unstable transition between dilute and dense axion stars
- Size = $1/m_a(T)$
- Eventually dissipate once the axion mass stops growing as $T \to 0$

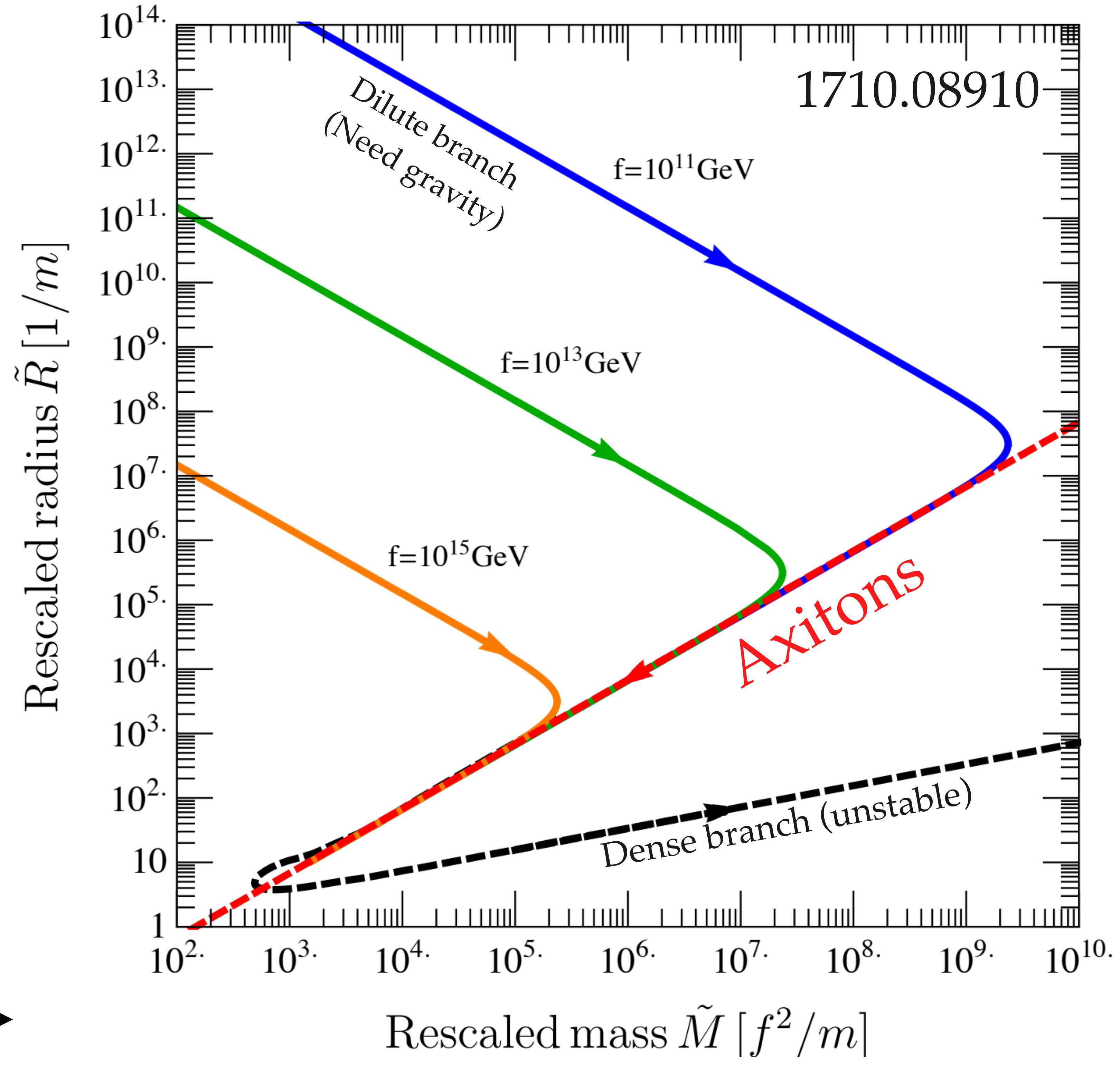

Axion mass increasing with time ⟶

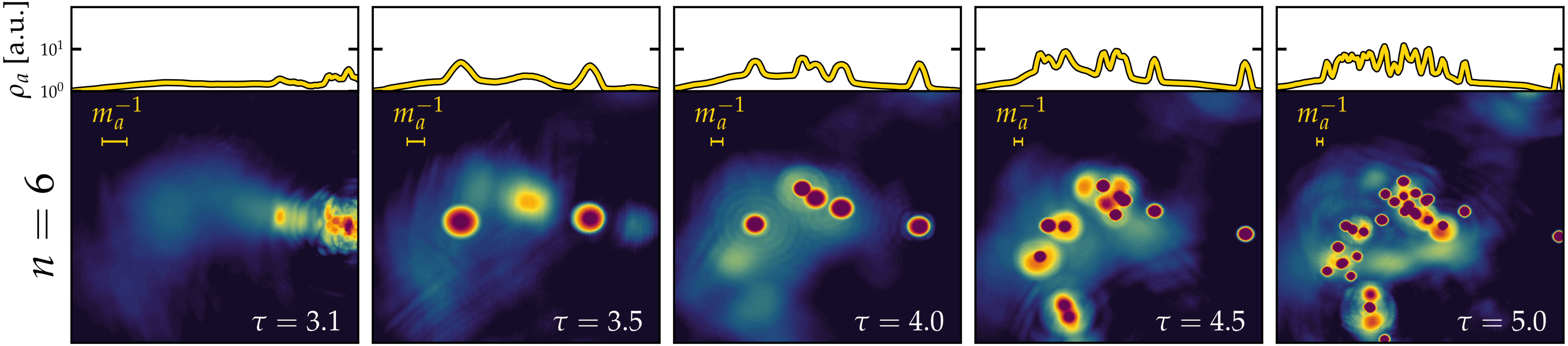

Gravitational collapse

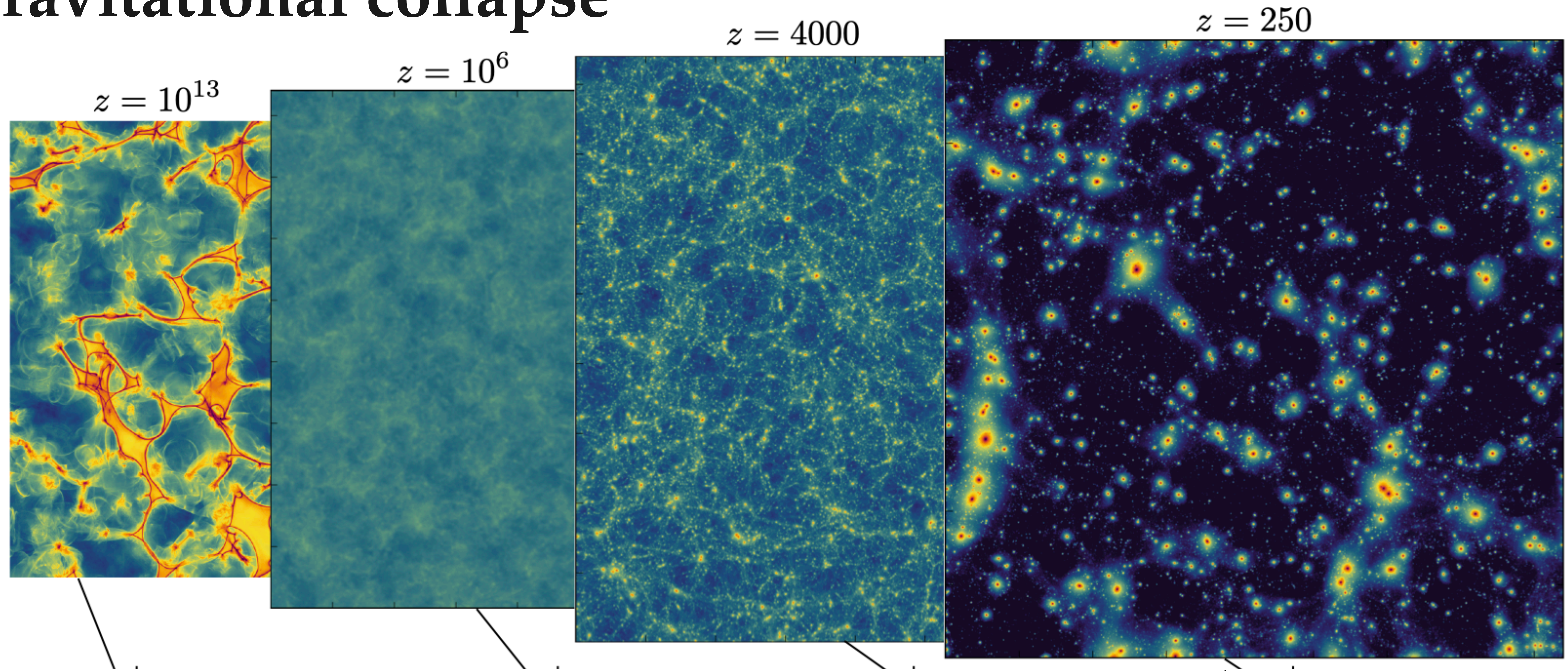

Initial conditions from field simulation

WKB approx. + Schrodinger-Poisson system for linear growth

N-body methods for non-linear gravitational collapse

Gravitational collapse of seeds left over by the axitons leads to the formation of ~AU sized clumps of axions with masses $M \in [10^{-15}, 10^{-9}]\ M_\odot$

→ **axion miniclusters**

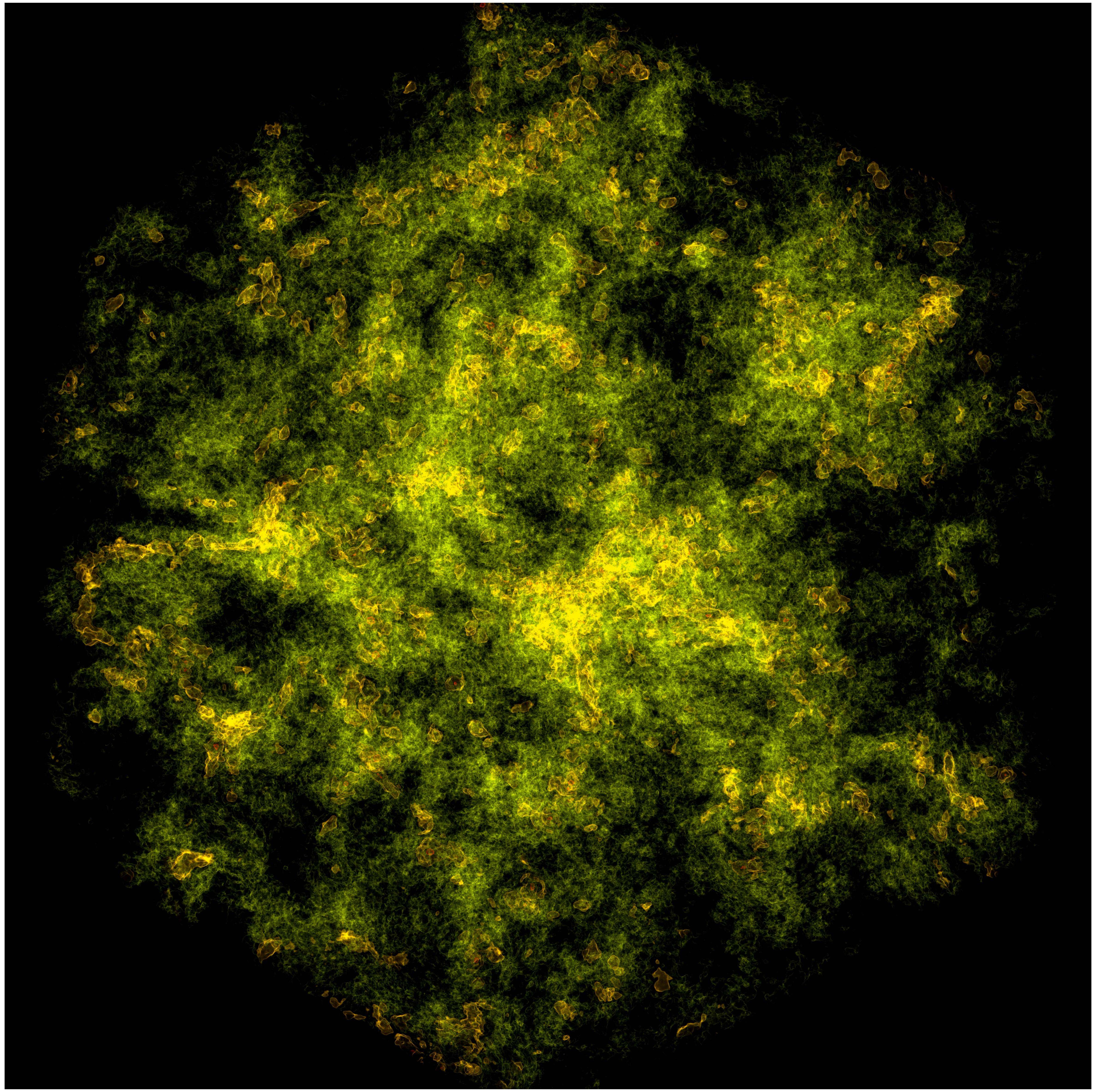

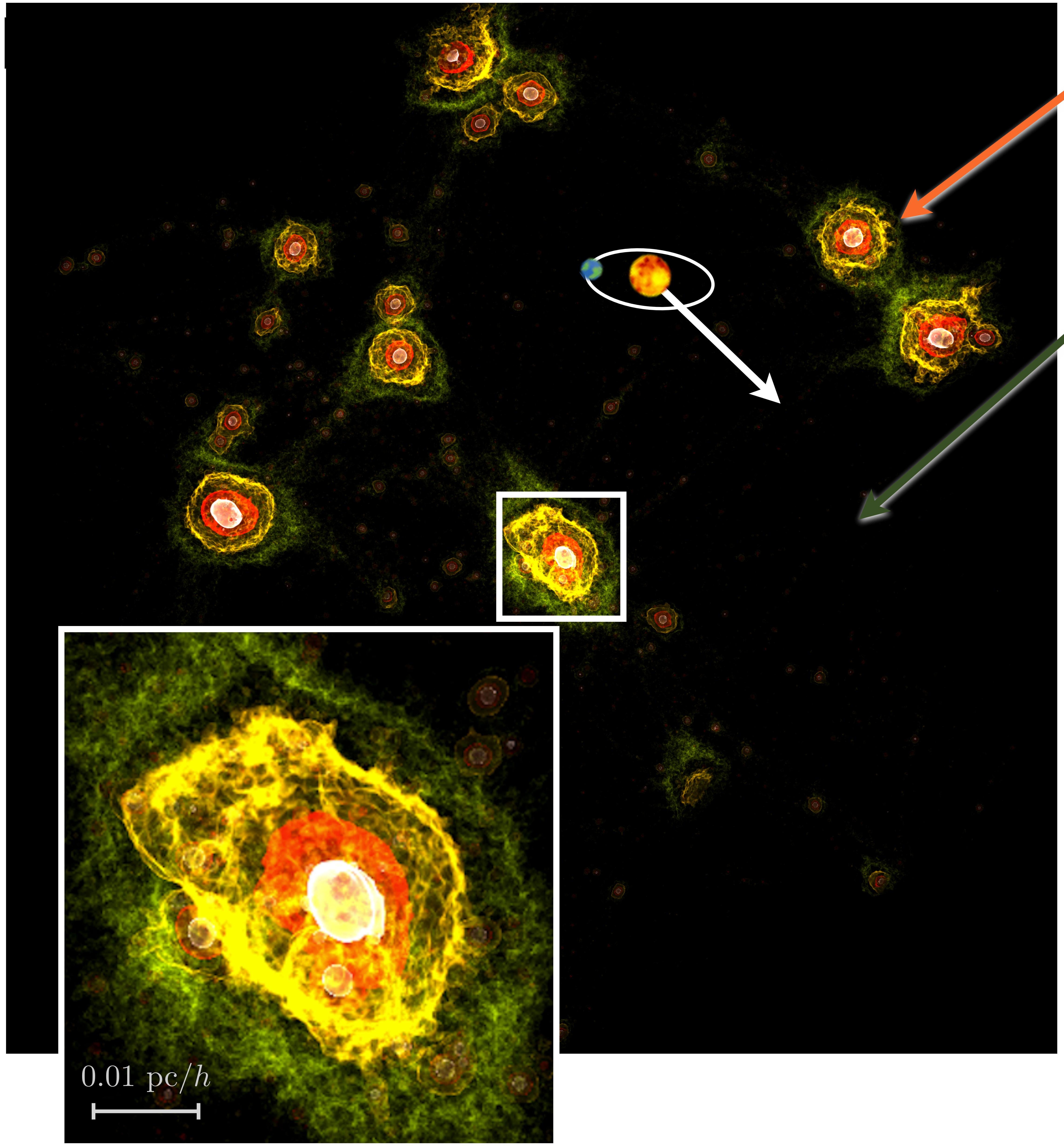

Miniclusters

Minivoids

Miniclusters contain >80% of the axions but make up <1% of the volume

Experiments travel about 0.2 mpc per year so are much more likely to sample the minivoids than the miniclusters

Implications for haloscopes

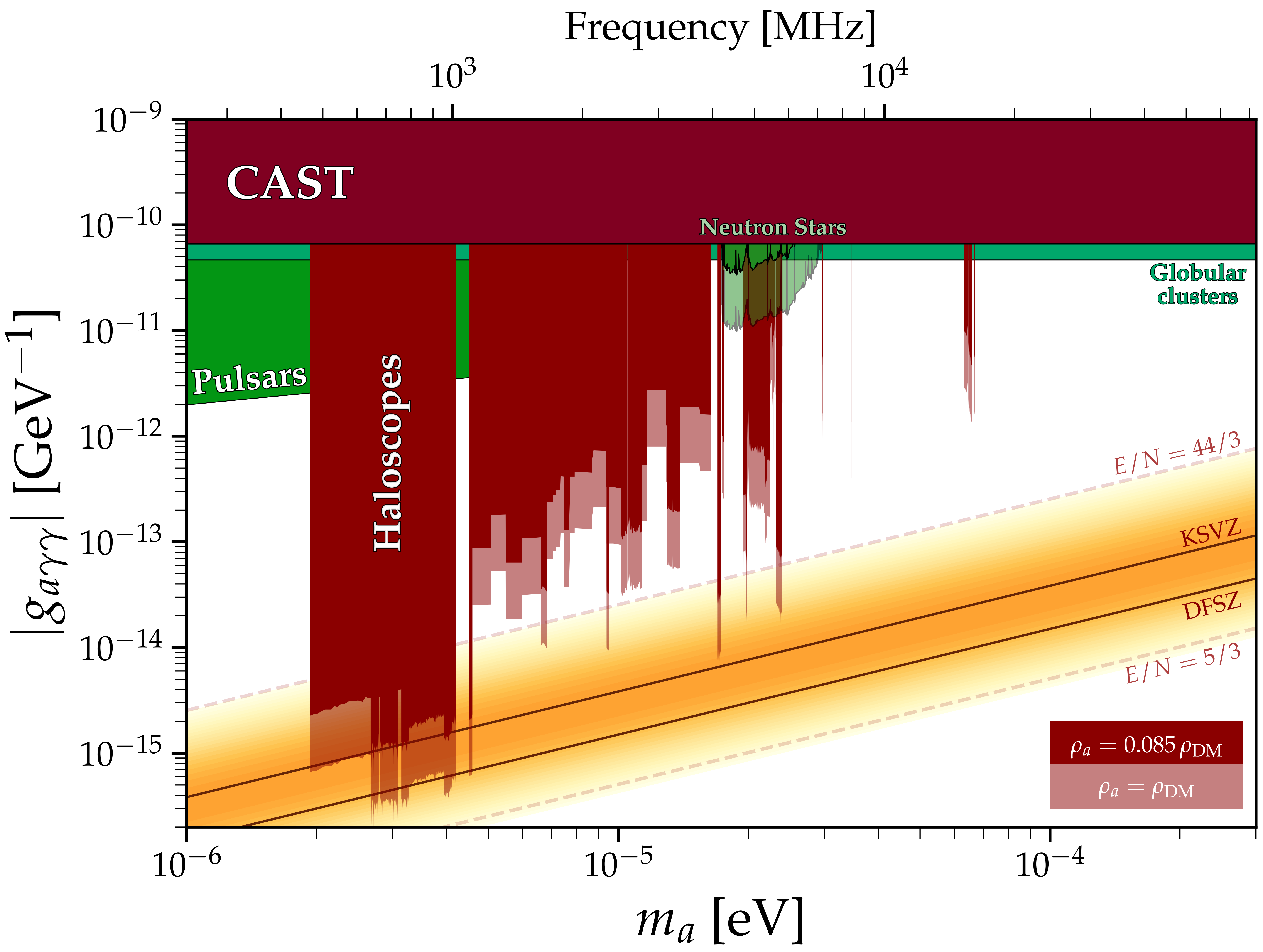

Typical density in the minivoids is ~0.085 of the mean density of dark matter

→ the miniclusters are no longer growing at the final redshift of the simulation, therefore this places a **lower bound** on the density of axions

→ Not a nice conclusion, but it could have been much worse!

Problem 2: String radiation and the dynamical range

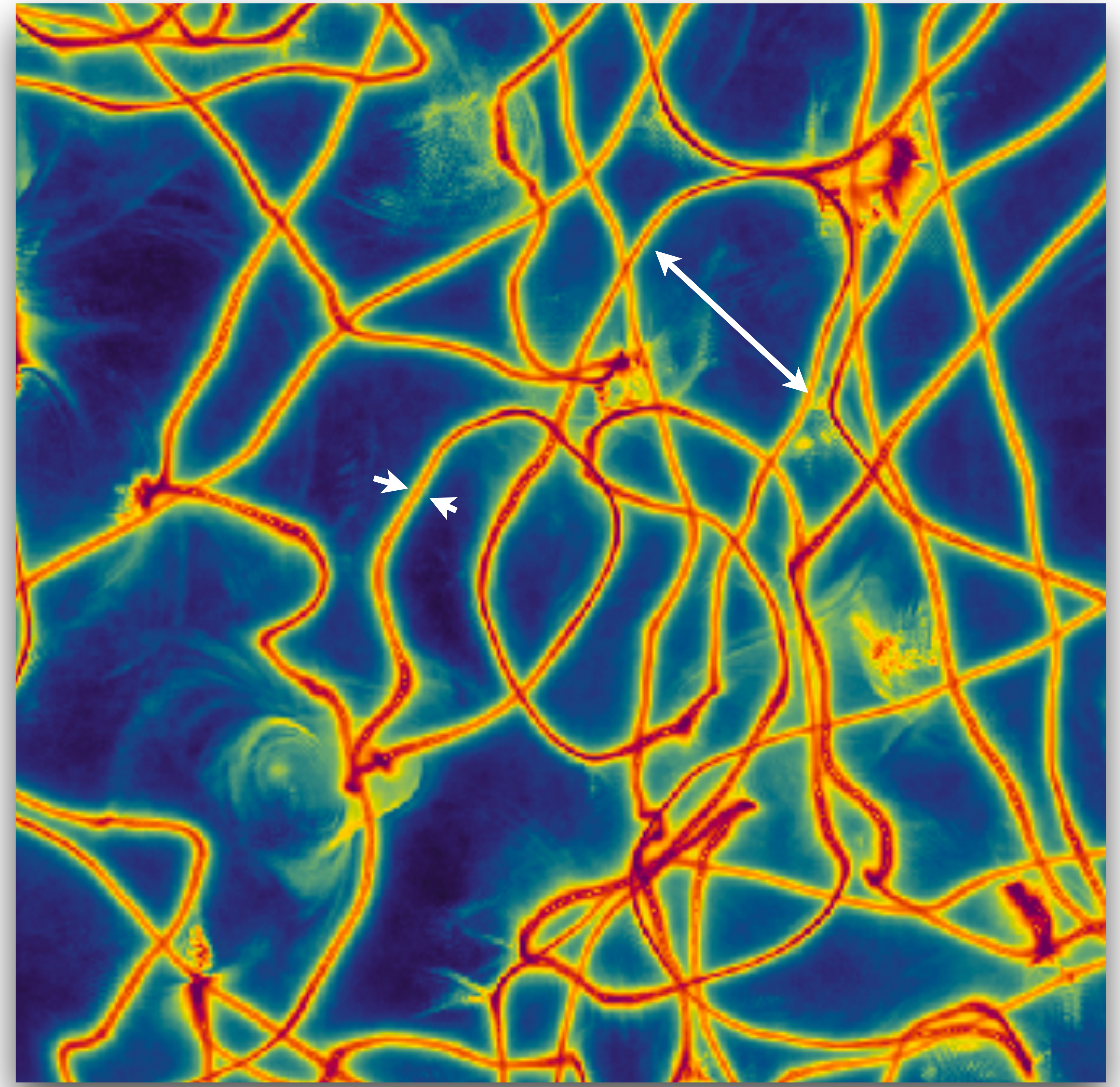

- Want to simulate larger than the causal horizon $L \sim 1/H$

- Whilst also resolving string cores $\Delta x \sim 1/m_s = (\sqrt{\lambda} f_a)^{-1}$

- For a realistic model e.g. $f_a = 10^{11}$ GeV $\rightarrow m_s/H \sim 10^{28}$

- With current resources $\lesssim 8192^3$ grid points, can only simulate $m_s/H \sim 10^{3-4}$

- Might be okay since this parameter enters as $\log m_s/H$ in the string tension but still needs to be checked, e.g. with AMR [2108.05368]

Key issues to be resolved

Axion dark matter abundance/axion mass

→ Current simulations cannot study the string scaling regime in full due to high required dynamical range, see e.g. [2007.04990]

→ Not clear if the spectrum is dominated by IR modes (meaning large overproduction) or UV modes (Important for predicting the axion mass, see [2108.05368] for recent work with AMR)

Implications of an inhomogeneous axion distribution

→ Formation of gravitationally bound structures "axion miniclusters"

→ Do miniclusters survive to present day? Could be important for direct and indirect searches

→ Can stable axion stars form inside miniclusters? Could there be signals of these e.g. fast radio bursts? May need to solve full SP system to understand this. [1804.05857]

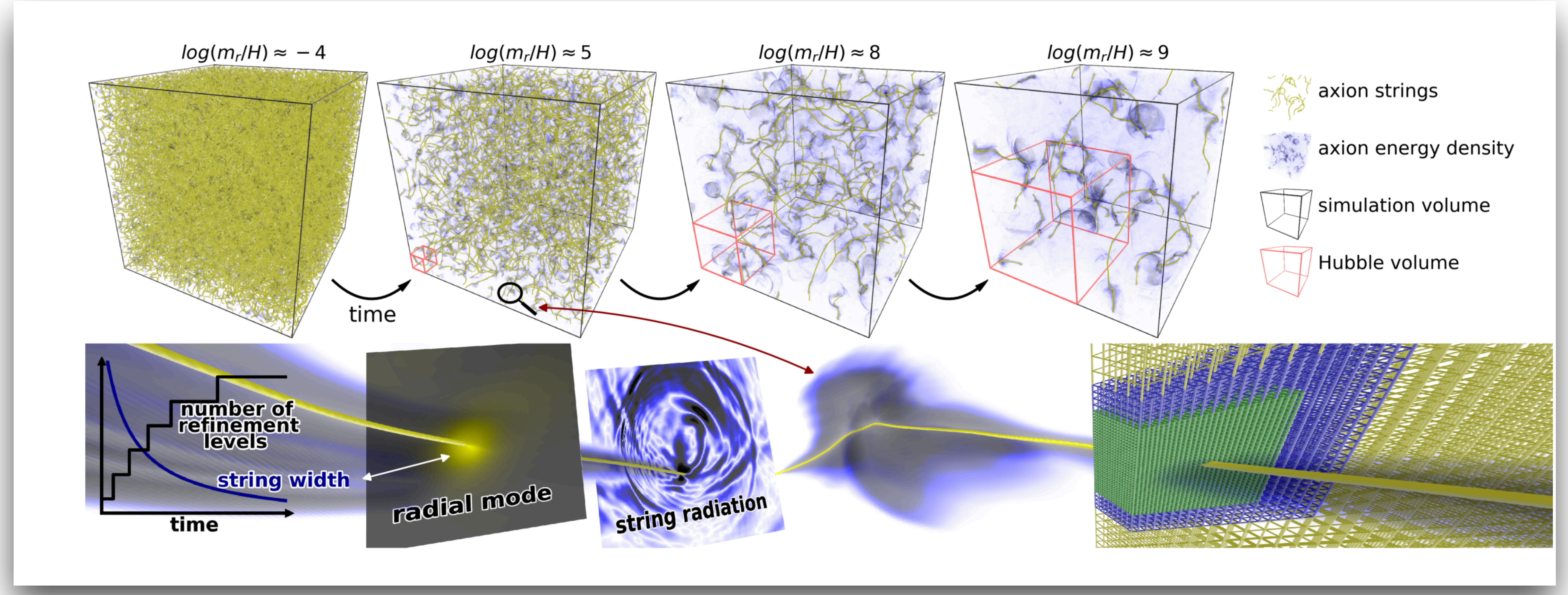

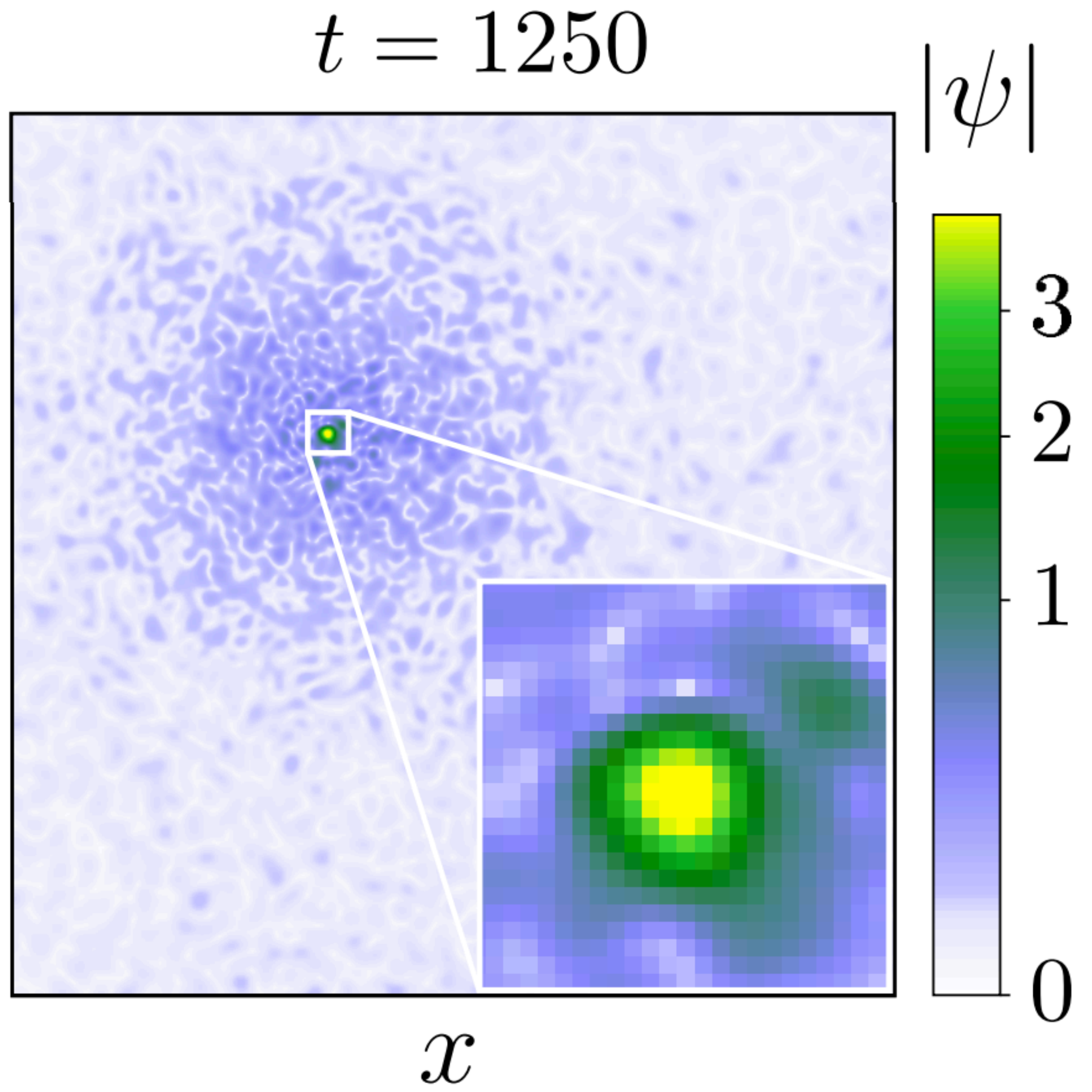

Schematic of a parameter space for an ultralight boson

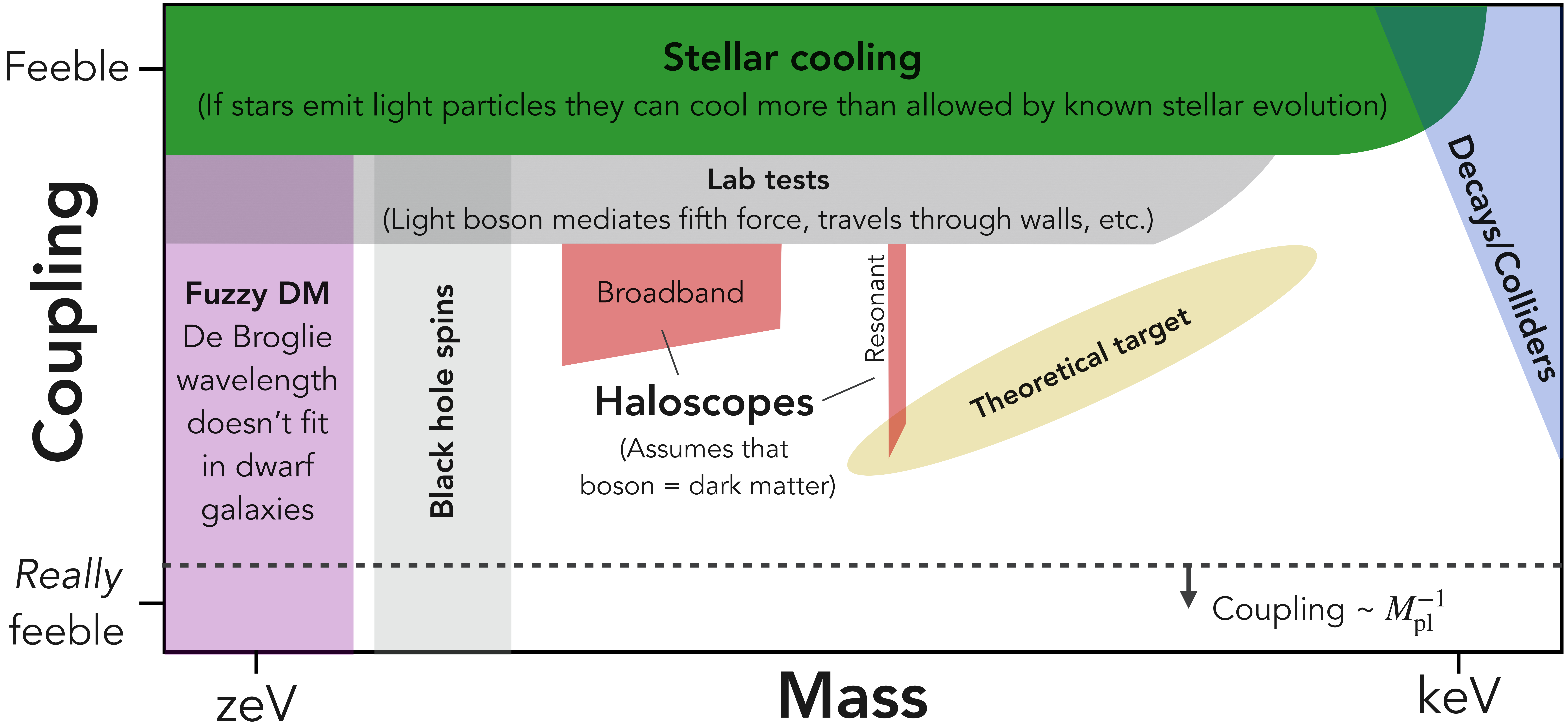

Wave-like dark matter experiments

How light can dark matter be if it is made of fermions?

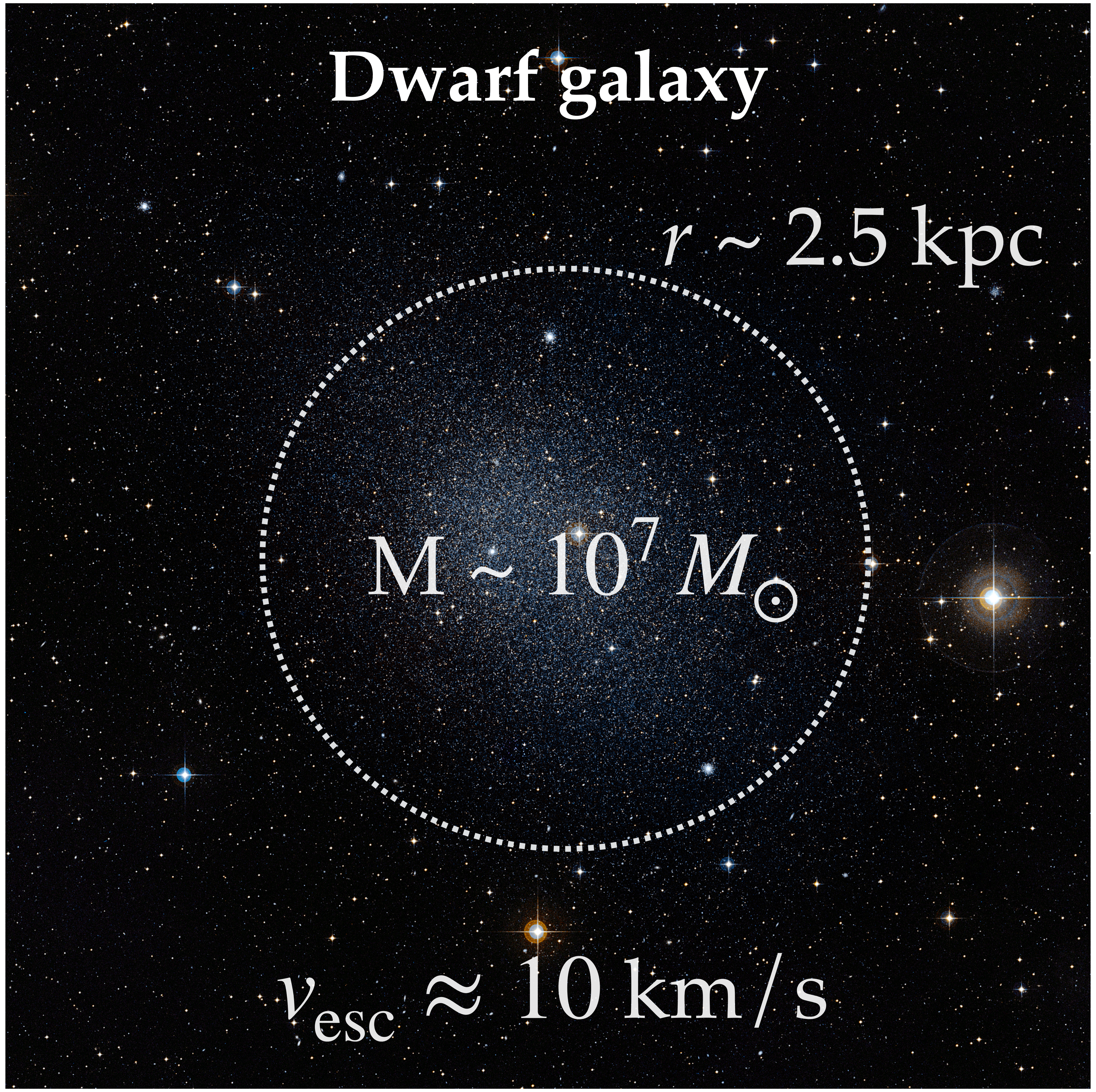

Sphere of degenerate fermions

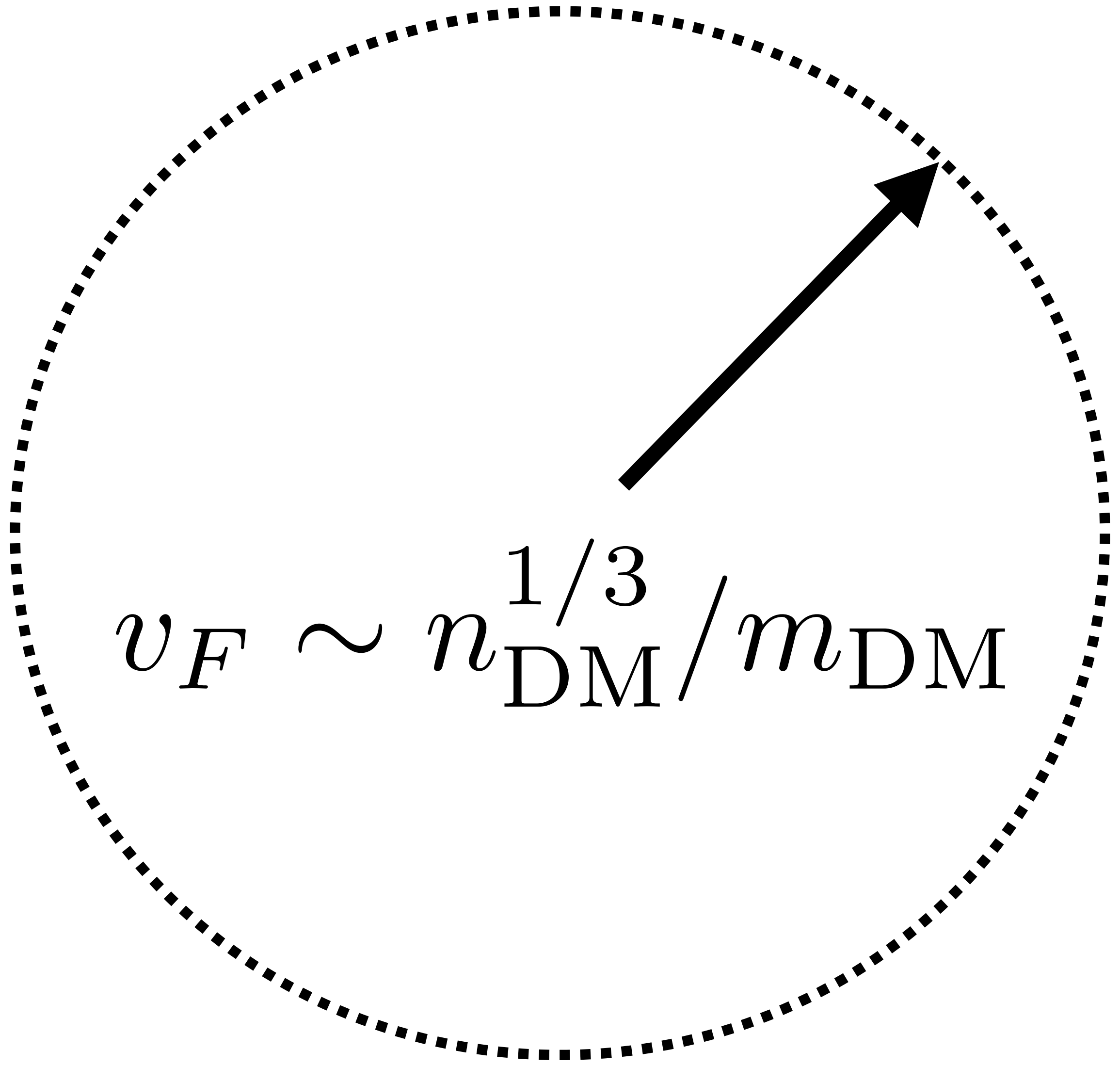

$$v_F < v_{esc}$$

$$\Rightarrow m_\chi \gtrsim 100 \text{ eV}$$

"Tremaine-Gunn bound": Pauli exclusion principle prevents you from cramming fermions lighter than ~100 eV into dark matter halos

Bosonic “wave-like” dark matter

<u>Occupation number:</u>

$$\mathcal{N} \approx (\rho_{\rm DM}/m) \times \lambda_{\rm dB}^3$$

$m = 1\,\mu$eV ⟶ $\mathcal{N} \approx 10^{32}$ ⟶ Macroscopically occupied ground state ⟶ Classical field

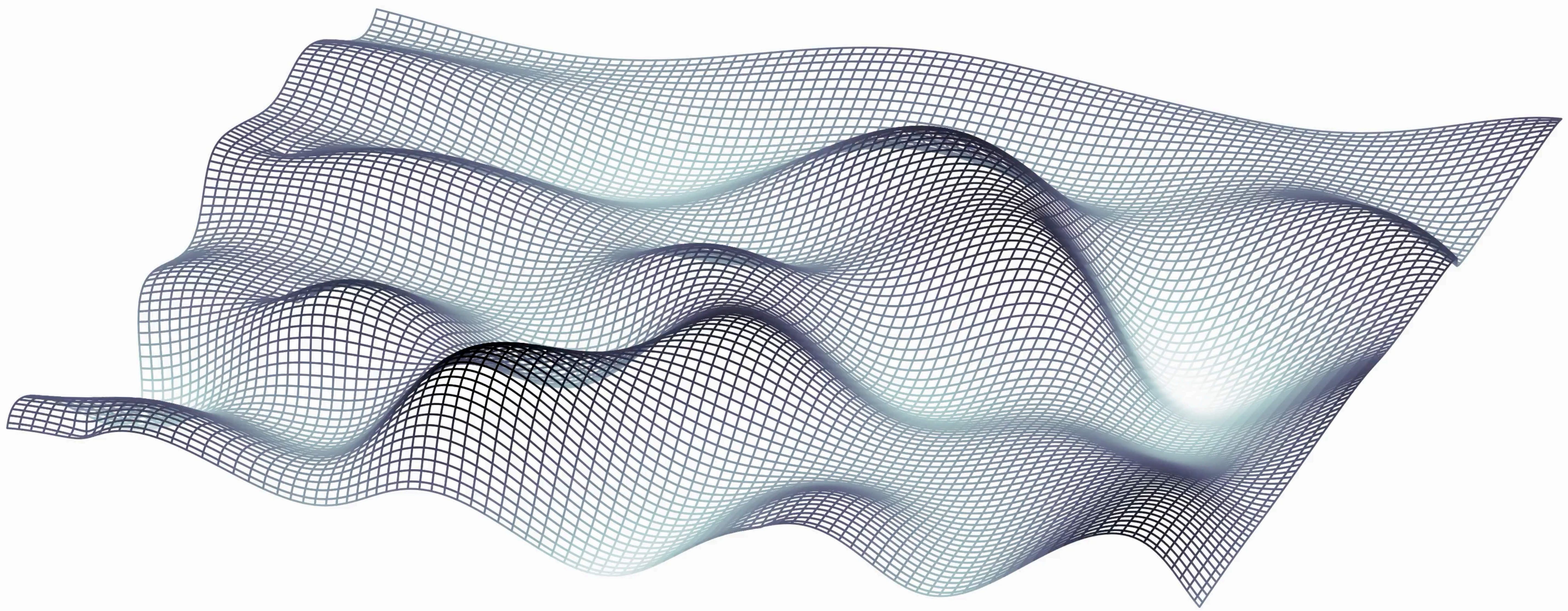

Wave-like dark matter mass range

yeV zeV aeV feV peV neV μeV meV eV

Particle DM →

"Fuzzy dark matter"
Wave-like effects on scales $\lambda_{dB} \gtrsim$ pc

"Black hole superradiance"
Build up of boson cloud around BHs sucks their spins away

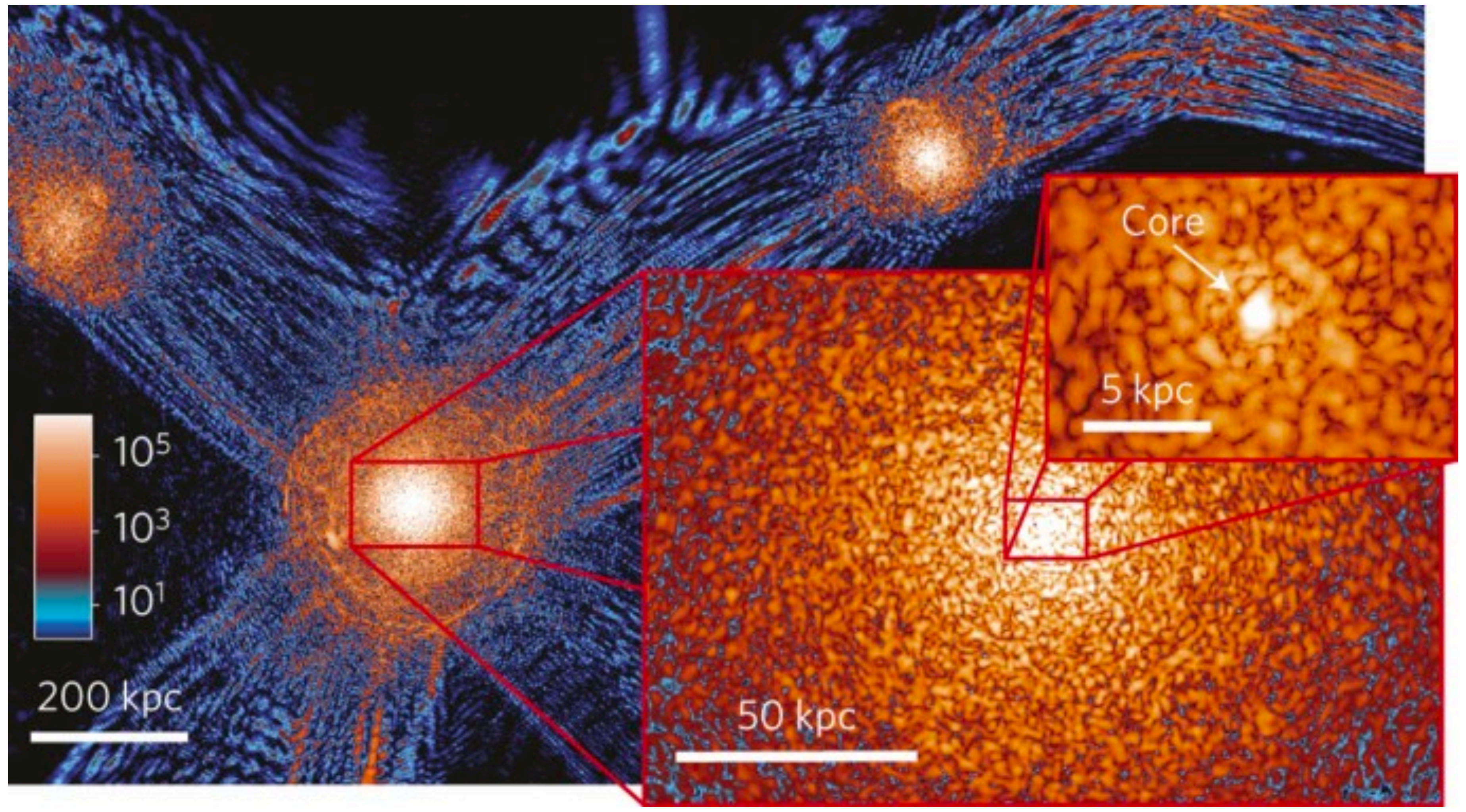

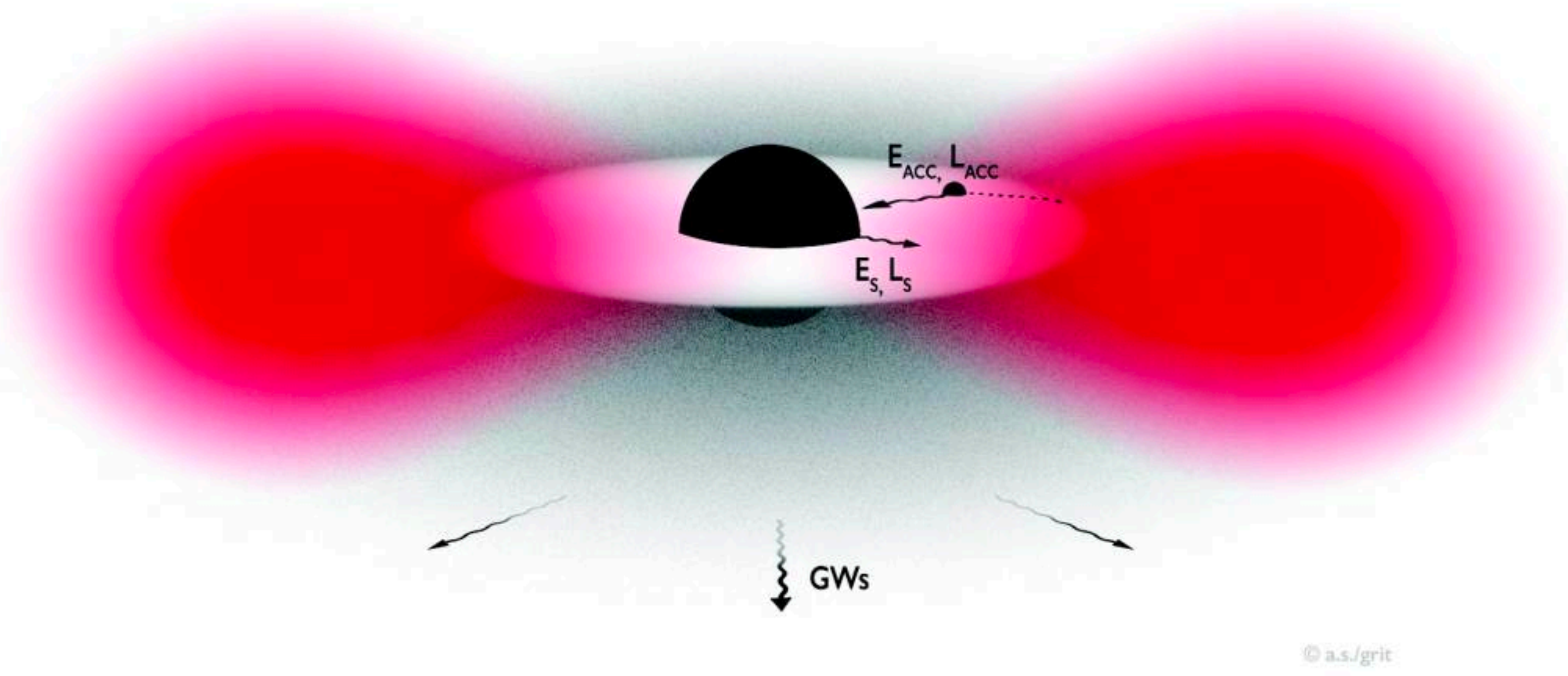

Direct detection

To calculate *any* experimental signal of dark matter we need to know

1. How much dark matter there is around the Earth, ρ
2. How fast it's moving, v

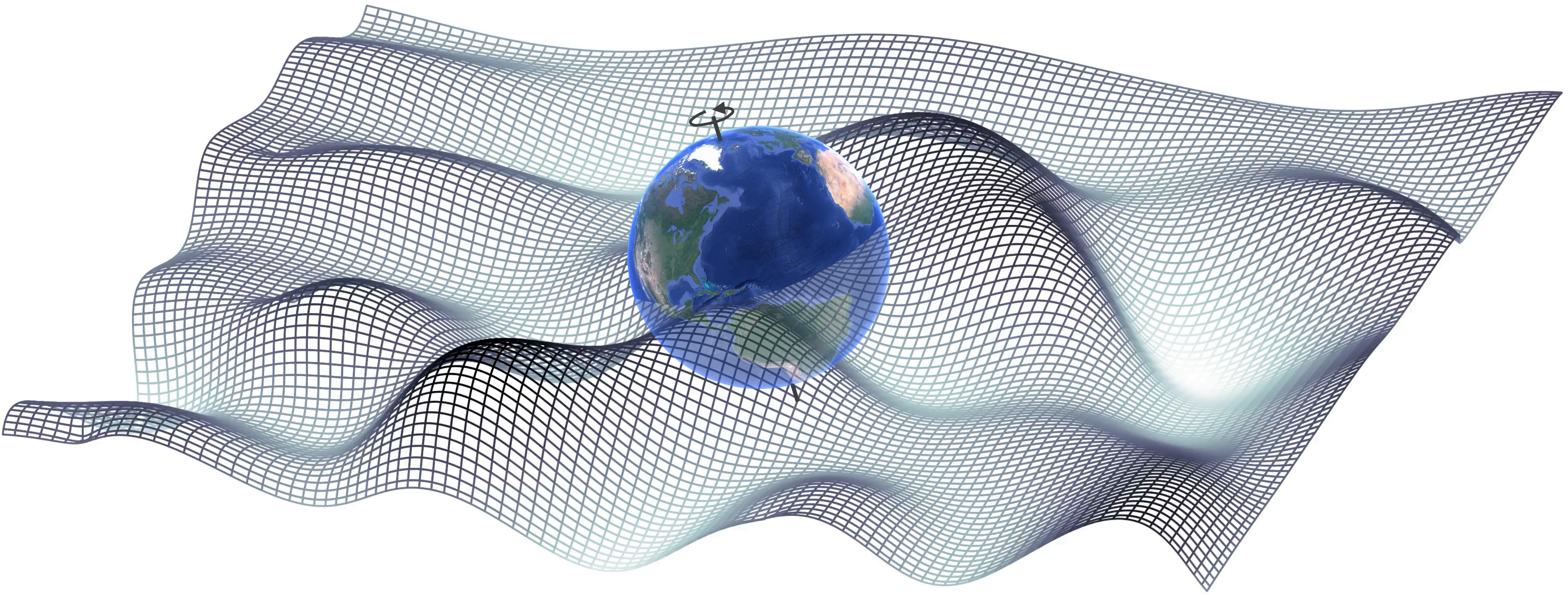

For wave-like dark matter these correspond to:

Amplitude: $A = \frac{\sqrt{2\rho_a}}{m_a}$

Frequency: $\omega = m_a + \frac{1}{2} m_a v^2$

$$\approx m_a(1 + 10^{-6})$$

Photon-axion mixing in a B-field

Raffelt & Stodolsky 1988
(https://inspirehep.net/literature/253874)

$$\mathcal{L}_{a\gamma} = \frac{1}{2}\partial_\mu a \partial^\mu a - \frac{1}{2}m_a^2 a^2 - \frac{1}{4}F_{\mu\nu}F^{\mu\nu} + g_{a\gamma} a \mathbf{E}\cdot\mathbf{B}$$

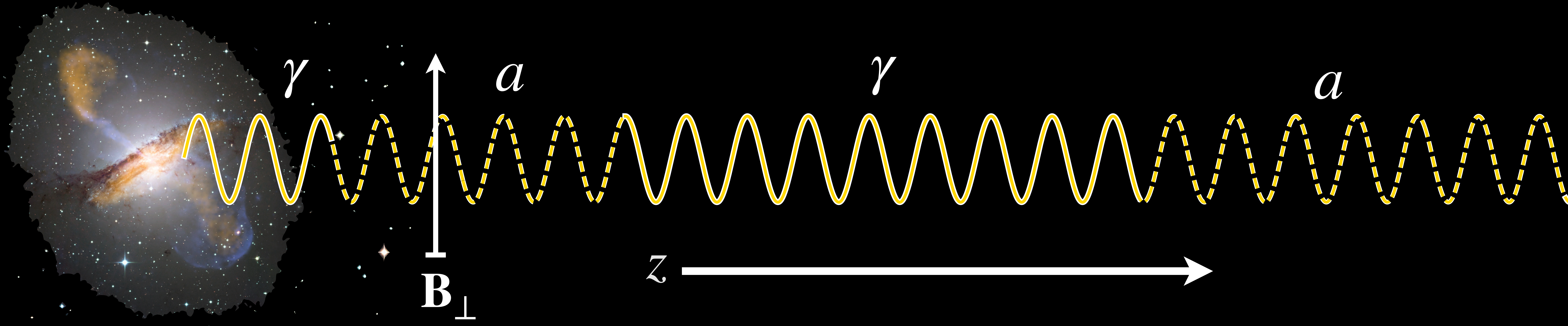

Linearised wave equation for photon-axion mixing

$$\left(\omega + \begin{pmatrix} \Delta_{\rm pl} & 0 & 0 \\ 0 & \Delta_{\rm pl} & \Delta_{\gamma a} \\ 0 & \Delta_{\gamma a} & \Delta_a \end{pmatrix} - i\partial_z\right)\begin{pmatrix} |A_\perp\rangle \\ |A_\parallel\rangle \\ |a\rangle \end{pmatrix} = 0$$

$$\Delta_{\gamma a} = \frac{g_{a\gamma}B_\perp}{2} \qquad \Delta_a = -\frac{m_a^2}{2\omega} \qquad \Delta_{\rm pl} = -\frac{\omega_{\rm pl}^2}{2\omega}$$

Mixing element | Axion mass element | Photon mass element

Axion only mixes with $A_{\parallel}$ so rotate into new basis and solve like neutrino oscillations:

$$\begin{pmatrix} \left|A'_{\parallel}\right\rangle \\ |a'\rangle \end{pmatrix} = \begin{pmatrix} \cos\theta & \sin\theta \\ -\sin\theta & \cos\theta \end{pmatrix} \begin{pmatrix} \left|A_{\parallel}\right\rangle \\ |a\rangle \end{pmatrix}$$

Probability for photon to convert to axion after travelling distance *z:*

$$|\langle\gamma(0) \mid a(L)\rangle|^2 = P_{a\to\gamma} = \sin^2(2\theta)\sin^2\left(\frac{\Delta}{\cos(2\theta)}\right)$$

Where,

$$\theta = \frac{1}{2}\arctan\left(\frac{2\Delta_{\gamma a}}{\Delta_{\rm pl} - \Delta_a}\right) \qquad \Delta = \frac{|m_a^2 - \omega_{\rm pl}^2|L}{4\omega}$$

Photon-axion conversion probability

For very light axions, m_a is negligible compared to $\omega_{\rm pl}$

$\rightarrow$ $m_a \lesssim 10^{-12}$ eV for typical astrophysical plasmas $n_e = 10^{-3}$ cm^{-3}

$$\theta \sim g_{a\gamma} \frac{B_\perp \omega}{n_e} \qquad \Delta \sim \frac{n_e L}{\omega}$$